HIGH PERFORMANCE AXIALLY LAMINATED ANISOTROPIC SELF EXCITED THREE PHASE SYNCHRONOUS RELUCTANCE GENERATOR

Thesis

Submitted to the

G.B. Pant University of Agriculture & Technology,

PANTNAGAR–263145 (Udham Singh Nagar), Uttaranchal, INDIA

By

Ajay Srivastava

IN PARTIAL FULFILMENT OF THE REQUIREMENTS FOR THE DEGREE OF

Doctor of Philosophy
in
Electrical Engineering

July, 2006

ACKNOWLEDGEMENT

Had it been easy to express the feelings, the emotions, in words, I would have to reveal my thoughts, my gratitude, my thanks, my love to every soul who helped me and supported me through the meticulous task of thesis writing. I offer my truest love and affection to all who pray for my thesis submission.

I would like to give my first thanks to the almighty God, as without His mercy accomplishment of my work and preparation of this manuscript would have not been possible.

The author is at loss of words to express his deep sense of gratitude and indebtedness to his advisor and chairman of Advisory Committee, Dr. Subir Ray, Professor, Department of Electrical Engineering, for his insightfulness and patience in guidance, constant encouragement and abundance benevolence throughout the period of investigation and preparation of this manuscript.

Indeed, the words at my command are inadequate to deem my immense pleasure and deep seated obligations in expressing my heartfelt regards and profound sense of gratitude to my esteemed members of Advisory Committee, Dr. G.K. Banerjee, Professor, Department of Electrical Engineering, Dr R.P.S. Gangwar, Professor & Head, Department of Electronics and Communication Engineering, and Dr Manoj Kumar, Professor, Department of Mathematics, Statistics and Computer Science.

Extreme honour and heartfelt feelings are due to Late Dr. K.N. Shukla, Ex. Dean, College of Technology, Dr D. K. Gupta, Dean, College of Technology and Dr. J.P. Tiwari, Dean, College of Post Graduate Studies, G.B. Pant University of Agriculture and Technology, Pantnagar, Uttaranchal for furnishing necessary aids to achieve this endeavor.

The author proudly expresses his utmost gratitude and cordial thanks to Dr. A.K. Swami, Professor, Prof. & Head, Department of Electrical engineering and Dr. R.C.S. Mehta Head, Department of Production engineering for their evincing keen interest, sustained support, and encouragement in absence of which the work would not have seen the light of the day.

The author can offer here only an inadequate acknowledgement of his appreciation to Dr. S.R. Singh, Prfessor, Banaras Hindu University, Dr. Rakesh Saxena, Associate Professor, Department of Mechanical engineering and Sri Abhishek Yadav, Assistant Professor, Department of Electrical Engineering, for their valuable suggestions and help.

The author is highly obliged and thankful Dr Avinash Kumar, Ex. Professor & Head, and Sri Sanjay Mathur, Associate Professor, Department of Electronics and Communication Engineering.

With a sense of gratitude and great pleasure, the author acknowledges the whole hearted cooperation extended by Sri Ajay Kumar, Shri D.D Pant, Sri D.D Mishra, Sri Ashok Arya, and all other staff members of Electrical Engineering Department.

The author acknowledges the assistance of Sri A.K. Agarwal, Assistance Director, Electric Division, G.B.P.U.A&T Pantnagar, and Sri P.C. Sati, M/s Allied Electro Services, Haldwani.

I express my heartfelt thanks to my friends Dr. S. K. Goel, Dr. M. C. Joshi, Prof. K. K. Sharma, and my student Mr. H.S. Rawat.

I wish to express my heart felt gratitude to my parents, mother in-law, my wife Anju, son Aman and daughter Aishwarya for their support and patience throughout this period.

In the end with full regards I thank all those persons who directly or indirectly helped me.

Pantnagar
July, 2006

Ajay Srvastava
Author

CERTIFICATE

This is to certify that the thesis entitled "***HIGH PERFORMANCE AXIALLY LAMINATED ANISOTROPIC SELF EXCITED THREE PHASE SYNCHRONOUS RELUCTANCE GENERATOR***" submitted in partial fulfillment of the requirements for the degree of **Doctor of Philosophy** with major in **Electrical Engineering** of the College of Post-Graduate Studies, G.B. Pant University of Agriculture and Technology, Pantnagar, is a record of *bona fide* research carried out by **Mr. Ajay Srivastava, Id.No. 23026,** under my supervision, and no part of the thesis has been submitted for any other degree or diploma.

The assistance and help received during the course of this investigation and source of literature have been acknowledged.

Subir Ray

(Dr. Subir Ray)
Chairman
Advisory Committee

Pantnagar
29 July, 2006

CERTIFICATE

We, the undersigned, members of the Advisory Committee of **Mr. Ajay Srivastava, Id.No. 23026,** a candidate for the degree of **Doctor of Philosophy** with major in **Electrical Engineering,** agree that the thesis entitled ***"HIGH PERFORMANCE AXIALLY LAMINATED ANISOTROPIC SELF EXCITED THREE PHASE SYNCHRONOUS RELUCTANCE GENERATOR"*** may be submitted in partial fulfillment of the requirements for the degree.

(Dr. Subir Ray)
Chairman

Dr. R.P.S. Gangwar
(Member)

Dr. G.K. Banerjee
(Member)

Dr. Manoj Kumar
(Member)

CONTENTS

LIST OF FIGURES

LIST OF SYMBOLS

Symbol	Description
μ_r	Relative permeability
ξ	Saliency ratio
δ	Torque angle
ω_r	Rotor angular speed
λ	Flux linkage
emf	Electromotive force
I_d	Direct axis current
I_q	Quadrature axis current
I_{nl}	No load current
I_a	Armature current
L_q	Quadrature axis inductance
L_l	Leakage inductances
L_{s0}	Amplitude of constant magnetizing inductance
L_{s2}	Amplitude of the sinusoidally varying magnetizing inductance
mmf	Magnetomotive force
r_s	Stator resistance per phase
V	Voltage
X_{md}	Direct axis magnetizing reactance

X_{mq}	Quadrature axis magnetizing reactance
X_d	Direct axis reactance
X_q	Quadrature axis reactance
T_i	Instantaneous torque
C	Connecting matrix in Park transformation
C_t	Transpose of connecting matrix in Park transformation
I	Identity matrix
L_A	Constant magnetizing inductance
L_B	Sinusoidal varying magnetizing inductance
T_e	Electromagnetic torque developed by SRM
SRM	Synchronous reluctance machine
SERG	Self excited reluctance generator
ALA	Axially laminated anisotropic rotor
DCM	Direct current motor
C_{sh}	Excitation capacitance connected in shunt
C_{se}	Capacitance connected in series with load for voltage regulation improvement
P_{SRM}	Power developed by synchronous reluctance machine
t	Average ratio of flux barrier thickness to combined thickness of lamination and flux barrier

g	Length of airgap
ε	Rotor position in mechanical radians
β	Rotor angle in mechanical radians
B_d	Flux density in direct axis
B_q	Flux density in quadrature axis
p	No. of pole pairs
L	Stack length of SRM
r	Airgap radius
D	Bore diameter of SRM
B_m	Peak value of magnetic loading
ac_m	Peak value of electrical loading
P_{max}	Optimum power developed by an electrical machine
L_r	Rotor leakage inductance of induction machine
L_m	Magnetizing inductance of induction machine
K	Ratio of magnetizing current to load current
P_{in}	Power developed by induction machine

INTRODUCTION

Chapter -1

INTRODUCTION

The whole essence of human civilization is the way natural energy has been harnessed to meet the requirements of human race without causing ecological imbalance. Electrical Energy has been found to be the most efficient, clean, and easy to use form of energy. Modern civilization can not be even perceived in the absence of electrical energy. In fact, per capita consumption of electrical energy is the index of development and progress of a country. With ever growing population, improvement in the living standard of the humanity, industrialization of developing countries, the global demand of energy is increasing at a rate hither to unthinkable. Fossil fuels are the main source of conventional energy. Hydro power and nuclear power also fall under the same category. Modern power systems use all these power sources for generation and transmit power via interconnected grid system. While use of conventional sources of energy for supplying interconnected system can not be substituted as of today, one must not loose sight of the following point facts:

(i) That fossil fuels are depleting at a rate enormously larger than the rates at which these are replenished by nature;

(ii) That fossil fuels, large hydro power sources, and nuclear fuels cause ecological imbalance of one or the other type;

(iii) That remote and undeveloped areas of large countries can not

be fed electrical energy with proper quality at a cheap cost due to the non-availability of the grid system and scattered local distribution ;

This calls for a serious attention to non conventional and renewable sources of energy - like solar energy, wind energy, small and very small (micro) hydro potential sources etc.

In India solar and wind power are available in abundance at the remote costal regions and small hydro potential sources are plenty at remote hilly regions. The estimated potential of small hydro power in India is about 15000 MW.

In the newly formed state of Uttaranchal, the quantity and quality of energy services required in remote and hilly areas is quite low due to the scattered settlement pattern, lack of infrastructural development, and diversification of economies. At the same time, the extension of grid electricity in the mountain areas is not economically feasible. Taking into account of above factors, the micro/small hydro potential for rural electrification in this mountainous region is well accepted. A number of micro and small size hydro-sites have already been identified to be developed in the private sector or in public-private partnership. Thus the Government of Uttarnchal is committed for assured supply of quality power to its far flung areas at the end of this decade. This goal can be achieved by fully harnessing its immense hydro potential by developing micro /small hydro power projects as isolated power sources. Quantitatively small volume of water with large heads (hills) and too large volume of water with small heads

(such that canals) can be tapped. The force of the flowing and falling water is used to run water turbine to generate electricity.

Most of the micro hydro projects are used for stand alone power generation application and cater to domestic uses and rural entrepreneurs. Traditional synchronous generator used for an isolated power supply using non conventional energy sources is uneconomical as it has many demerits, i.e., need of separate source of excitation, rotor with slipring and brushes, and high maintenance cost. The objective of harnessing of such non conventional energy sources as an isolated power source could be achieved in big way by the development of the suitable low cost generating system. The ability of induction generators to convert mechanical power to electrical power over a wide range of speed has made them good candidates to replace synchronous machines in such applications. Their other merits are low unit price, brushless rotor, no separate source for excitation, robustness in operation and low maintenance cost etc. These features of induction machine are particularly suitable for generating electricity from tidal, wind, solar, micro and small hydro potential. In recent years, induction motors have been installed as generators on micro hydro schemes.

An induction machine can be used as an induction generator in two ways, namely, in the externally excited mode and in the self excitation mode. The frequency and voltage of the externally excited induction generator is governed by the frequency and voltage of the power source to which it is connected. However, if an appropriate

capacitor bank is connected across the terminals of rotating induction machine, a voltage is developed across the machine terminals without external excitation. In this mode the machine is known to be working as a Self Excited Induction Generator (SEIG). The squirrel cage induction generators have been preferred in comparison to the synchronous generators for small scale power generation due to their low cost, robust construction and ease of maintenance. The protection of the machine is simple and cheap because the fault current level of the machine collapse to zero as the capacitor excitation falls with collapse of terminal voltage. In case of the short circuit across the machine terminals, the sustained transients are not generated due to the absence of field.

However, in spite of the several advantages, the conventional induction motor used as the self excited induction generator(SEIG), has various disadvantage such as poor voltage regulation and frequency regulation with changes in load. This is because of the operating condition of the machine in the motoring and the generating modes are different. Induction machine basically being singly excited requires reactive power for its operation. If connected to grid it draws necessary VAR from the lines. But in case of its operation as SEIG, a VAR generating unit should be connected across its terminals, which is generally realized in the form of capacitor banks. When the load connected across the terminals is varied. The terminal voltage and its frequency reduce considerably with the load implying inherent poor voltage and frequency regulation. A complex control mechanism is

therefore needed to overcome this inherent problem in induction generator which will increase its cost. Reluctance machine while retaining almost all the positive aspects of induction machines, offers answers to the problems faced by the latter.

Reluctance machines have been known as early as induction machines but they have not been developed and exploited until the early sixties. The reason for lack of attention in the early days had been due to their poor overall performance compared with well developed squirrel-cage induction machines. But reluctance machines have attracted considerable attention during the last two decades or so, resulting in much improved performance. The early reluctance machines were mostly salient pole in construction giving poor performance. Reluctance power is produced due to the variation in air gap between the stator and rotor over a complete mechanical cycle. Salient pole synchronous machines also produce reluctance power due to this reason. The power developed by a salient pole alternator is given by the following expression:

$$P_{syn} = \frac{E.V}{x_d}\sin\delta + V^2\frac{x_d - x_q}{2x_d x_q}\sin 2\delta$$

In the above expression, first component represents the electromagnetic power because it depends on the existence of both, the armature winding and the field winding. The second component represents reluctance power which dependent on the degree of saliency. Reluctance power is very small in comparison to

electromagnetic power in such a machine. However, it enhances the synchronizing power coefficient. The rate at which synchronous power P varies with δ is called the synchronizing power coefficient. It is a measure of the stiffness of electromagnetic coupling between stator and rotor fields. The second part exists even when the field current is zero, i.e., E is zero. Under such operational constraint, the machine is known as synchronous reluctance machine (SRM). Without field excitation above equation of power developed by machine reduces to following expression:

$$P_{SRM} = V^2 \frac{x_d - x_q}{2 x_d x_q} \sin 2\delta$$

This is the power developed by synchronous reluctance machine. It is obvious that for a given torque angle δ, power developed by reluctance machine depends upon difference between direct axis reactance and quadrature axis reactance. The ratio of the direct axis and quadrature axis reactance is known as saliency ratio. Almost all important performance parameters of the synchronous reluctance machine depend on its saliency ratio. The saliency ratio of a conventional salient pole rotor is of the order of two, and the reluctance power is very small. Therefore, no serious attention had been given to reluctance motor with conventional salient pole rotor. Various rotor configurations other than salient pole structure were thought over to improve the performance of reluctance machine by increasing the reluctance power. Several key papers examining the

performance of reluctance motor, published in the 1960s and 1970s, provide reviews of early work and discuss the geometry needed to achieve a high saliency ratio [45, 47]. Few early scientists recognized the ultimate potential of the reluctance machine, but they could not achieve it in practice.

A typical rotor punching, identical to many induction motor punching excepting that a few teeth being cut out, was utilized during the fifties of the last century. A high saliency ratio could not be expected for this rotor configuration. These machines were generally characterized by very low power factors or efficiency or both. As a result reluctance machines were larger than induction machines of corresponding rating. Their low efficiency and poor performance were inadmissible in motors of large output and seemed to justify the general opinion that the synchronous reluctance motor was inherently inferior to the other type of motors.

Saliency ratio of two or more than two is obtained by utilizing segmental rotor construction in synchronous reluctance motor to secure optimum performance. Cost was a problem since the rotor segments were constructed either with solid pole or with many small laminations. However, poor power factor and efficiency have continued to plague the widespread use of such machines.

Saliency ratios of four or more have been achieved by using flux guided/axially laminated anisotropic rotor. Reluctance machine fitted with this type of rotor competes with an induction motor. The cost of

such rotors will be drastically reduced when mass production takes place. In flux guided rotor, the flux guides should ideally have the shape of the flux path. This will maximize the d-axis flux linkage and thus, the value of x_d will be large. On the other hand, the flux barrier should be ideally perpendicular to the flux lines. This will ensure minimum q-axis flux linkage resulting in low value of x_q. Thus the saliency ratio will be large. These requirements lead to multiple barrier rotors. By using higher number of barriers, a large saliency ratio is achievable which can give sufficiently large operational power factor. Owing to difficulty of constructing the multiple-barrier from a unitary lamination, attention was given to replace the usual radial lamination by axial lamination of anisotropic material whose permeability is not only directional but which also follows a pattern corresponding to the natural shape of the flux lines. Conventional radial laminations are replaced by axial lamination of anisotropic material with planes parallel to the axis of rotation, using essentially the technique of cut C cores.

To improve the performance of synchronous reluctance machine (SRM), essentially four types of rotor core designs have been used and are listed in their chronological order:

- Conventional salient pole rotor
- Segmented rotor
- Rotor with multiple flux barriers
- Axially laminated anisotropic (ALA) rotor

The design, analysis, and construction based on these rotor core developments have taken place centering around a reluctance motor. At a later stage, attention has been given to use reluctance motor as a Self Exited Reluctance Generator (SERG). This has been necessitated to overcome the problems faced by self excited induction generator. Needless to mention, the SERG was conceived as a stand-alone generator to exploit nonconventional energy sources to supply electricity to remote hilly areas and sparsely populated regions.

1.1 SELF EXCITED RELUCTANCE GENERATOR:

Reluctance generator acts as a parametric oscillator through the pumping action of its variable reluctance [3] utilizing the self excitation process. The phenomena of self excitation in an isolated induction machine by means of a terminal capacitor have been known since the early of the last century [46]. Similarly self excitation in isolated reluctance generator is achieved when the rotor is driven by an external prime mover and its terminals are connected to a suitable three phase capacitor bank. The process of voltage build up is initiated by a small amount of EMF induced in the stator by the action of residual flux. This EMF is sufficient to cause a current to circulate in the stator winding. If the proper amount of capacitance has been connected to the machine, the subsequent stator MMF will produce flux in the direction of the residual magnetism thus causing more voltage buildup and a greater current flow. As in all self excited

machines, buildup of induced EMF and current will continue until equilibrium is attained by the action of magnetic saturation. This is determined by the balance of real and reactive power flow between the machine, the excitation capacitance and the connected load.

Self excited synchronous reluctance generator can be contemplated as an alternative choice to the induction generator if a high x_d/x_q ratio were realized. A high x_d/x_q ratio can be realized by axially laminated anisotropic (ALA) rotor. Axially laminated anisotropic rotor uses axial laminations of cold rolled grain oriented material in place of normal radial laminations, an attempt to confer polar properties of the rotor by controlling both the external and internal anisotropy, whose permeability is not only direction dependent but also followes a pattern corresponding to the natural shape of the flux lines.

Fitted with axially laminated anisotropic rotor, a detailed study of SERG is essential to make a practical choice for self excited generator as a suitable alternative for self excited induction generator. Its steady state and transient state performances must be investigated through simulation as well as by experimental verification.

Development of a machine model of reluctance machine is required to investigate steady state and transient state performance. The model employed for self excited reluctance generator (SERG) is based on d-q axis steady state model of a synchronous machine. This model is inadequate to predict the complete performance considering the saturation of magnetic core. The models used so far are unable to

predict the phenomena of voltage build up. To overcome these problems the space vector approach is adopted to analyze the SERG in rotor reference frame. They do not contain the time varying terms with the electrical angular frequency of the rotor. Furthermore, their steady state values are constant values, and so simple algebraic equations can be used to compute the steady state values of the generator variables. The digital computer simulation of transient behavior the self excited reluctance generator can be performed faster in rotor reference frame.

1.2 SCOPE OF THE PRESENT RESEARCH WORK:

The main objective of this research is to develop a mathematical model of three phase synchronous reluctance generator using Park's transformation and based on space vector approach. This model is utilized to evaluate the dynamic as well as steady state performance of axially laminated anisotropic rotor SRM.

Another objective is to design and fabricate the axially laminated anisotropic rotor to obtain a high performance self excited synchronous reluctance generator. ALA rotor has been used for the given frame and rating of a three phase induction machine so that a comparison can be made between three phase self excited induction generator and reluctance generator. This machine has been tested in the laboratory by performing the various experiments to verify the results obtained by simulation. A self regulating feature in axially

laminated anisotropic rotor SERG has been carried out by using suitable short shunt compensation. To the best of the knowledge of the author the following, therefore, are his original contribution as brought out in the present thesis:

(i) A mathematical model of a synchronous reluctance machine with axially laminated anisotropic rotor based on space vector approach to predict its performance has been suggested,

(ii) An axially laminated anisotropic rotor has been designed and fabricated in the laboratory, and

(iii) The test results of a self excited reluctance generator with such a rotor have been compared with predicted results given by the model.

1.3 ORGANISATION OF THE WORK

Chapter two of the thesis details historical development in the area of SRM operation and optimization of rotor geometry. The use of synchronous reluctance machine as an isolated power source utilizing self excitation has been highlighted.

Chapter three deals with theory and operation of synchronous reluctance machine, maximization of saliency ratio, SRM as a self excited generator, development of machine model and self regulating feature of SERG by using suitable short shunt capacitor.

Chapter four presents simple mathematical expression for the estimation of saliency ratio of axially laminated anisotropic (ALA) rotor

as well as an analytical method for the design of ALA rotor. A brief discussion has been made to evaluate the parameters of synchronous reluctance machine and its experimental set-up.

In chapter five, effect of saturation on its parameters and self excitation process has also been investigated in this section. Various experimental and simulated test results with self regulating feature of SERG has also been presented in this chapter.

Chapter six presents the summary and conclusion of the entire thesis along with the proposal for future work.

LITERATURE REVIEW

LITERATURE REVIEW

The literature survey is the important part of the research activity on any subject and need to be carried out extensively. This will avoid wastage of effort by researchers working in the same field and will help in supplementing and complementing the research work carried out by each one of them. The main purpose of this chapter is to discuss the origin and historical development of synchronous reluctance machine. The treatment is intended to provide a brief background of advances gained in rotor of synchronous reluctance machine (SRM) over the years that led to a thought of using this machine as self excited reluctance generator (SERG).

2.1 HISTORICAL DEVELOPMENTS OF THE SRM:

The principles for the design and operation of ac motors were patented by Nicola Tesla on May 1, 1888. Details were announced on May 16 of the same year. Tesla's paper described three forms of his invention. The common factor between the three forms was the ring-wound stator with four salient poles. The first form had wound rotor and ran at slightly less than synchronous speed, forming an induction motor. The second form was a synchronous motor, as dc was supplied to the rotor windings. The third form had rotor with four

salient poles, forming a reluctance motor that ran at synchronous speed. This form was not self starting.

Gorge Westinghouse bought Tesla's patents and employed him to develop them. Today, almost 80% of electric drives in domestic and industrial application utilize induction motor, i.e., Tesla's first patent. The second patent of Tesla, synchronous machine is primarily used for conversion of conventional energy to electrical energy. Tesla's third patent; the reluctance motor got no serious attention due to its very poor performance. Its poor performance was attributed to its small saliency ratio. Almost all important performance parameters of the synchronous reluctance machine depend on its saliency ratio. Various rotor configurations other than salient pole structure were thought over to improve the performance of reluctance machine by increasing the reluctance power. Several key papers examining the performance of reluctance motor and published in the 1960s and 1970s provide reviews of early work and discuss the geometry needed to achieve a high saliency ratio. Few early scientists [47,44] recognized the ultimate potential of the reluctance machine, but they could not achieve it in practice.

In **1923, Kostko** proposed the adoption of a cylindrical rotor with multiple slits along the lines of direct-axis flux shown in Fig. 2.1(a). His work was substantially the basis for the design of a rotor with reluctance slots, flux guides and segments. The author pointed out the essential limitation of the salient pole design that widening of

the interpolar cutout to decrease the q-axis inductance, the pole arc being thereby narrowed, results in an unwanted reduction in L_d. So the multiple barrier or segmented arrangement is the natural way to make a synchronous reluctance machine because it involves no sacrifice of pole arc in d-axis. Subsequent workers, generally aware of **Kostko's** work, developed the geometry along two main lines: the segmented geometry and the axially laminated geometry.

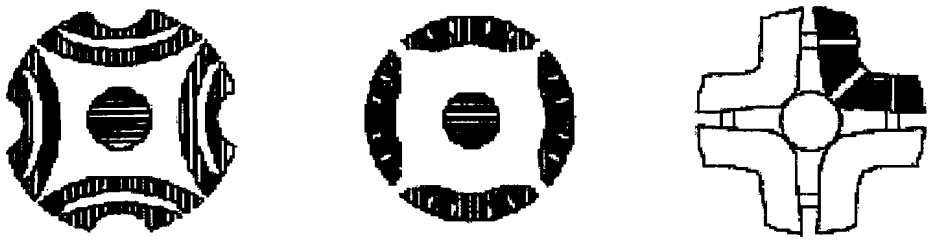

(a) (b) (c)

Fig. 2.1 (a) Kostkos rotor in 1923; (b) Lawrenson isolated segmental rotor; (c) General construction of axially laminated anisotropic rotor synchronous reluctance motor

In 1930s, a typical rotor punching identical to many induction motor punching excepting that a few teeth being cut out, was utilized. A high saliency ratio could not be expected for this rotor configuration. These machines were generally characterized by very low power factors or efficiency or both. As a result reluctance machines were larger than induction machines of corresponding rating. Its low efficiency and poor performance were inadmissible in motors of large output and seemed to justify the general opinion that the

synchronous reluctance motor was inherently inferior to the other type of motors.

The rotor of second generation of synchronous reluctance motor appeared some what later as shown in Fig.2.1 (b). This utilized a segmental rotor construction. **Lawrenson *et al* (1964)** presented a paper regarding the theory and performance of polyphase reluctance machines for two types of rotor structure e.g. conventional two pole salient rotor and new form of segmental rotor which consists of a number of circumferentially extending pole segments. Starting from the flux distribution in the airgap the general equations for the synchronous performance of reluctance machine was developed by the authors showing the superiority of new machine over the conventional one. A method based upon the theory of the impedance and current circle diagram was utilized for the determination of the axis reactances. **Gupta *et al* (1967)** presented improvements in reluctance motors experimentally and theoretically with purely segmental rotors. These improvements resulted from incorporating a shallow axial channel in the center of the air-gap face of each segment, filling of this channel with conducting material, shaping of the ends of segments and optimization of the significant design parameters.

Few researchers also worked to evaluate the performance synchronous reluctance motor as it differed with others types of conventional motor during the same period. **V.B. Honsinger (1971)** obtained steady state performance of reluctance machine by direct-

and quadrature-axis components using circle diagram and by machine admittance. The author had deduced specific equations for pull-out torque, maximum power factor, no load current and pull-out current. No reference to machine geometrical configuration upon which these parameters depend had been made. The poor power factor and efficiency have continued to plague the widespread use of such machines.

Recent designs abandoned the traditional salient pole and segmental rotor. A modern third generation type of rotor design is shown in Fig. 2.1©. In this the rotor is provided with flux guides and flux barriers. The Saliency ratio of four or more has been reported with this type of structure, which typically results in a machine which competes with an induction motor. The problem of high manufacturing cost of the rotor with such a machine can be sorted out with its mass production. Two types of rotor have been reported in this generation to improve the performance of synchronous reluctance machine i.e. flux guided rotor and axially laminated anisotropic rotor. In flux guided rotor, to maximize d-axis flux linkage, the flux guides should ideally have the same shape as the flux path and to minimize the q-axis flux linkage, the flux barrier should be perpendicular to the flux lines. The proposal of axially laminated anisotropic rotor was made by **Menzies *et al* (1971)** and **Cruickshank (1971)** and was considerably different from previous developments, namely to replace the usual radial laminations by axial lamination of anisotropic

material with planes parallel to the axis of rotation, using essentially the technique of cut C cores. The axially laminated anisotropic rotor had the reluctance features of segmented rotor as well as of the flux barrier rotor. A single speed motor was designed to operate from a normal rated mains frequency of 50 or 60 Hz. Good synchronous performance is indicated by high efficiency, power density and power factor, together with its ability to sustain load with permissible reduction in supply voltage and to withstand transient loads. The maximum synchronous output can be increased by high reactance ratios. But very high value will lead to instability i.e. rotor oscillation about synchronous speed. This was demonstrated by **Lipo and Krause (1967)** with respect to certain motor parameters in stability analysis of reluctance motors. **Rao (1976)** analyzed dynamic performance of reluctance motors with axially laminated magnetically anisotropic rotors. Superior performance of these motors over conventional reluctance and segmental motors in performance has been predicted. **Klingshirn (1978)** developed an experimental method for measuring the quadrature axis inductance of polyphase synchronous machine. It is based on a measurement of the torque developed by the machine at standstill with direct current in its stator winding and without any excitation to its field winding. The method applicable to all synchronous machines is well suited to reluctance motors due to easy measurement of torque. Special techniques were used to minimize the measurement error due to hysteresis and due to

air gap permeance harmonics. Detailed results were presented for one reluctance motor with a highly variable quadrature axis inductance including the effect of saturation. **Boldea *et al.* (1991)** presented a review paper on emerging electric machines with axially laminated anisotropic rotor. The reluctance variation in axially laminated anisotropic rotor was computed for a wide range of air gaps and pole pitches. **Don Platt (1992)** presented a reluctance machine with a new rotor design, common with the segmented and axially laminated rotor. The new rotor achieves strong anisotropy by interleaving magnetic iron lamination with non magnetic spacers of approximately equal thickness. It is shown that the magnetizing inductance is very much lower in the quadrature axis than the direct axis and this has the potential to develop more power than the earlier machines. **Staton *et al* (1993)** analyzed the various known forms of the synchronous reluctance motor to maximize saliency ratio and identified the parameters on which it depends. It has been shown that the single barrier construction is not capable of achieving a saliency ratio large enough to make the motor competitive with induction machine in terms of power factor and KVA requirement. The single barrier motor also possesses a large component of torque ripple owing to combination of rotor saliency and stator slotting. The limitation on L_d, L_q and saliency ratio have been predicted by using an idealized model in which a solid rotor and airgap are used in the d-axis, and a non-magnetic rotor is used in the q-axis, corresponding to an ideal

anisotropic material. While multiple barriers produce significant improvement in saliency ratio over single barrier design but it is far behind the axially laminated anisotropic rotor. Therefore attention has been concentrated on axially laminated construction by the authors. **I.Boldea, Z.X.Fu, S.A.Nasar (1994)** proposed certain topological adaptations of the axially laminated anisotropic (ALA) rotor structure. In contrast to most existing ALA rotors, the ALA rotor topology presented here consists of single (thin) transformer laminations (66%) interleaved with thin insulation layers (33%) producing a uniform distribution of anisotropy. In this paper, authors presented an approach to obtain the performance analysis of synchronous reluctance machine (SRM) and the test results on a prototype ALA-rotor SRM. **M. Hippner and R.G. Harley (1996)** proposed a paper on the design of two axially laminated synchronous reluctance motors. Both motors were designed using standard, 3-phase, 1.5 KW induction motor stators. A finite element analysis of magnetic field was used to calculate the performance. Effect of different stator current and the effect of on saturation was investigated. It was found that the best remedy to achieve high saliency ratio is a proper selection of air gap length. Increased air gap can lead to a higher saliency ratio at typical operating values of current.

2.2 SRM AS A SELF EXCITED GENERATOR:

The depletion of conventional energy sources has brought great interest in other sources of energy e.g. wind, tidal and small hydro

potential. Power from these sources looks promising but one of the main difficulties of recovering is the varying speed of the prime mover. The conversion of the mechanical power available in the shaft to electrical power can not be performed satisfactorily using synchronous machine. The conventional synchronous generator requires dc supply for excitation, usually non-existent in rural and remote areas. Considering these factors, self excited induction generator got more attention as an alternative source to supply the far flung areas using the non conventional energy sources. The phenomenon of self excitation in an isolated induction machine, by means of a terminal capacitor goes back to early years of last centaury. The prediction of performance of the three phase self excited induction generator (SEIG) under no load and load conditions had been given by **Wagner (1939)**. It was realized that a rotating induction machine may remain excited if line voltage was removed and sufficient amount of capacitance was connected at the machine terminals while the rotation of machine was maintained by an external mechanical primemover. This phenomenon of the voltage buildup with capacitance is known as self excitation and was investigated by **Basset and Potter (1945)**. **Barkle and Ferguson (1954)** had derived the relation between the output power and the VAR for an induction generator from the circle diagram of the machine. At that time the phenomenon of self excitation was considered to be undesirable as it caused severe over voltage and could be dangerous to the machine winding and the capacitors. Due

to increasing cost of conventional energy and the need for pollution free and environmental friendly energy, the research in the field of harnessing non conventional energy sources i.e. tidal, solar, wind, small/ micro hydro potential has been intensified in recent past. This situation has led to revaluation of known sources of energy for commercial exploitation. As a result, the induction generator is getting much attention for its use with non conventional sources of energy. However, this machine suffers from variations in frequency and voltage with load. To overcome these problems, a complex control gear is required resulting in a costlier generator. Another type of machine which can be used as a self excited generator is reluctance machine which shares most of the advantages of the induction generator. It also has an additional merit of constant output frequency irrespective of the load or excitation capacitance variations.

Research in this direction was started in late 1990s using synchronous reluctance machine as a self excited generator. The scope of the reluctance generator in non-conventional energy application led to improvement on design and performance prediction of the SERG in early nineties. Initially the investigation had been made using conventional rotor pole i.e. salient pole and segmental. The performance of SERG was found unsatisfactory. **Abdel-Kader (1985)** developed an equivalent circuit for the reluctance generator in the same manner as the induction generator. The author had not taken care of saliency ratio; an essential parameter which decides the

performance of generator. **Rahim *et al.* (1990)** made a comparison between the steady state performance of induction and reluctance generators. In the same frame of induction machine, two types of rotor (salient and segmented) for reluctance generator were tested with same stator. Results had shown that reluctance generator had similar operating characteristics as induction generator in addition to the advantage of operating at a constant frequency, which is independent of load conditions. However the performance of reluctance generator could be enhanced by the use of segmental rotor.

Mohamadein et *al.* (1990) developed a steady state mathematical model based on Park's d-q axes transformation. They had shown that it was necessary for the machine to have a large d-axis reactance, whereas the q-axis reactance should be kept minimum to achieve good performance. **A.I. Aloah (1991)** used a direct method to find the capacitance requirement for a three phase self-excited reluctance generator under any load or speed. He derived the expression of load angle as well as minimum value of excitation capacitance and critical speed. **Rahman *et al* (1991)** suggested method for ac power generation from a constant speed drive using capacitor excited induction and reluctance machines. The proposed arrangement adopted one stator frame and two types of rotor, namely, salient pole and squirrel-cage rotor. A theoretical analysis has been by the authors by which the capacitor ratings required to achieve self-excitation for both reluctance and induction generators can be determined under

different load conditions. The stability limits of both generators are also investigated by developing the active-reactive power diagram for each generator. **A.I. Aloah (1992)** studied the effect of varying any one of three external parameters of speed excitation capacitance and load on the machine performance using the mathematical model developed by Mohamadein [35]. Furthermore, for successful self excitation and stable operation of the machine while varying one of the three external parameters it was found that the range of operation is bounded by minimum and maximum value for excitation capacitance, rotor speed and maximum value of load current. However, the reluctance generator can not operate beyond their limiting values. The computational results were verified by their corresponding experimental investigations. **T. F. Chan (1992)** presented a general method for analyzing the steady state performance of a three phase, self excited reluctance generator supplying an isolated inductive load. The author utilized piecewise linearization of quadrature axis air gap emf vs. direct axis magnetizing reactance curve. This enabled a direct computation of the minimum capacitance required to initiate self excitation for a given load impedance. Magnetic saturation is assumed to be confined to the direct axis represented by a direct axis magnetizing reactance. **I.Boldea *et al* (1993)** presented a reluctance generator of 1 kW rating with high performance: efficiency, power factor and power density. Single lamination/insulation-layer for the fabrication of axially laminated anisotropic rotor utilized by the author

led to high saliency ratio giving high performance. The steady state performance and maximum power conversion capability of reluctance generator was demonstrated by utilizing the model in rotor co-ordinates neglecting the core losses. The structure of a two pole ALA rotor reported by the author does not have capability to accommodate a shaft naturally. The shaft must be designed in such a way that a rotor can adopt it easily. **Wang *et al* (2000, 2001)** studied the performance of reluctance generator under unbalanced excitation capacitance in star connected mode. The authors presented an approach based on eignvalues and eignvalue sensitivity to determine minimum loading resistance of an isolated self-excited reluctance generator. **Hail and Rabinovici (2001)** presented new methods of finding the machine parameter measurement and the known conventional methods were compared. The new method permitted one to measure the L_d and L_q parameters without involving the stator winding resistance and leakage inductance by running the machine as reluctance generator. **Guha, S. and Kar, N.C. (2005)** presented a linearized model of saturated self excited synchronous reluctance generator considering the effect of saturation in both the direct and quadrature axes. The eignvalues of the state matrix of the linearized model has been derived to analyze the steady state stability of the system. The effect of other parameters such as excitation capacitance and load power factor has been investigated by using this model.

2.3 SCOPE OF THE PRESENT WORK:

The exhaustive literature survey presented in this chapter revealed that a good quantum of work has been done to improve the performance of synchronous reluctance machine by suitable design of rotor. The literature survey carried out on the subject of self excited reluctance generator indicates that it can be made commercially viable and an alternative for self excited induction generator. However, the following issues need further attention:

(i) There is a lack of experimental evidence of a practical four-pole axially laminated anisotropic rotor reluctance generator which is predicted to have better performance characteristics.

(ii) There is a need to develop a mathematical model of SRM to predict both steady state and transient state performance. The transient performance will help in determining starting transients and transients associated.

(iii) Attention is needed to improve the voltage regulation of self excited reluctance generator (SERG).

To meet the pressing problem of synchronous reluctance generator the present research work is intended to focus on following issues:

(i) To design and fabricate of 4-pole an axially laminated anisotropic prototype rotor for a synchronous reluctance machine.

(ii) To suggest a mathematical model for the machine to analyze both steady state and transient performance.

(iii) To verify predicted results using the model with experimental results obtained from tests conducted on the 4-pole SERG in the laboratory.

THEORY & MODELLING OF SYNCHRONOUS RELUCTANCE MACHINE

THEORY & MODELLING OF SYNCHRONOUS RELUCTANCE MACHINE

The reluctance machine has long been treated as a special case of a generalized synchronous machine. Perhaps it is the simplest and most economical electromagnetic structure of all rotating machines. Fast progress in power electronics, control techniques and advanced magnetic materials offers much potential for synchronous reluctance motor for applications that have traditionally been dominated by drives with D.C. or induction machines. Reluctance machine as a self excited reluctance generator attracted attention of few engineers in the last decade. A detailed study of self excited reluctance generator is essential as it has some inherent merits over self excited induction generator as an isolated power source. This chapter deals with theory of operation of synchronous reluctance machine and maximization of its saliency ratio. A mathematical model of synchronous reluctance machine has also been presented in this chapter.

3.1 PRINCIPLE OF OPERATION:

Electromechanical energy conversion involves the interchange of energy between an electrical system and a mechanical system through the medium of a coupling magnetic field. The process is essentially

reversible except for a small amount of energy that is lost as heat energy in electric machines. The coupling field is involved in establishing the electromagnetic torque as well as the reaction induced emf. Torque is produced in the machine because of the mutual action existing between the windings to bring about an alignment of their associated fields. As long as currents exist in each winding and the field pattern is proper, there exists a torque owing to this mutual coupling. However, there are machines in which it is possible to produce toque when only one part of the machine is excited. A force can exist whenever a flux is set up in a geometrical configuration characterized by a reluctance that varies with rotor position. A general expression for the instantaneous torque developed by a doubly excited electromechanical energy conversion device with salient pole rotor and stator represented in Fig.3.1 is given by

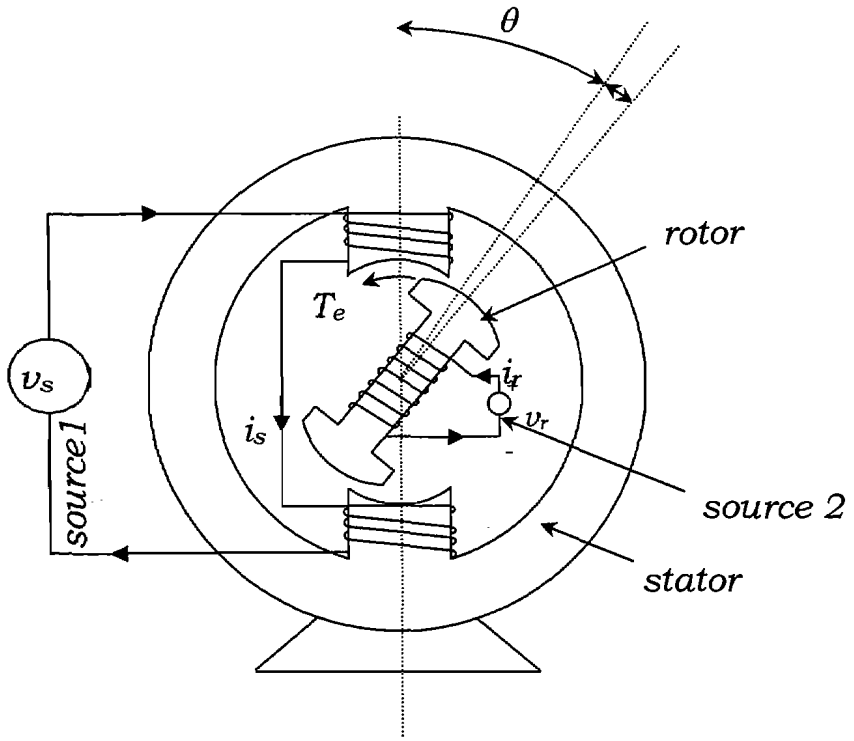

Fig. 3.1 Doubly excited electric machine with salient pole rotor and stator

$$T_t = \frac{1}{2} i_s^2 \frac{dL_s}{d\theta} + \frac{1}{2} i_r^2 \frac{dL_r}{d\theta} + i_s i_r \frac{dM_{sr}}{d\theta} \qquad \text{---------- (3.1)}$$

where,

i_s = instantaneous current in stator winding

i_r = instantaneous current in rotor winding

L_s = self inductance of stator winding

L_r = self inductance of rotor winding

M_{sr} = mutual inductance of between stator and rotor windings

θ = rotor displacement angle

A current i_r is assumed to flow in the rotor windings producing the air gap flux field. The current i_s is assumed to flow in the stator winding. This current may be direct, single phase alternating current, or the phase current of a polyphase system applied to polyphase stator winding. In the above expression the third term is dependent upon the currents in the rotor and stator windings and the rate of change of the mutual coupling between these windings with rotor displacement angle θ. It is usually called the electromagnetic torque of the energy conversion device. The other two terms represents the torque produced because of variation of reluctance experienced by the stator and rotor flux with rotor position. This is called the reluctance torque. In case stator has a cylindrical structure and its winding is excited only, with the rotor having salient poles as shown in Fig. 3.2, then the equation (3.1) reduces to

$$T_{ri} = \frac{1}{2} i_s^2 \frac{dL_s}{d\theta} \qquad \text{---------- (3.2)}$$

where

T_{ri} = instantaneous value of reluctance torque

L_s = self inductance of stator winding

$\theta = \omega_r t - \delta$ = rotor displacement angle at time t

ω_r = angular speed of rotor

δ = torque angle

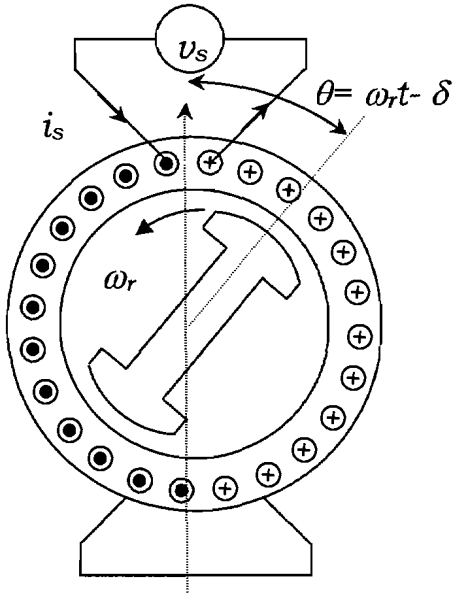

Fig. 3.2 singly excited reluctance machine

Therefore, as long as the reluctance of the magnetic circuit varies as viewed for different positions of the rotor, a torque due this reluctance variation exists. Inserting the general expression for the self inductance, $L_s = \frac{N_s^{\,2}}{\Re_s}$ into equation (3.2),

Where

N_s = no. of turns in stator winding

$\Re_s$ = reluctance experienced by the stator flux

One gets

$$T_{ri} = \frac{1}{2} i_s^2 \frac{dL_s}{d\theta} = \frac{1}{2} i_s^2 \frac{d}{d\theta} \frac{N_s^2}{\Re_s} = \frac{1}{2} (N_s i_s)^2 \frac{d}{d\theta} \frac{1}{\Re_s}$$

$$= -\frac{1}{2} \left(\frac{N_s i_s}{\Re_s} \right)^2 \frac{d\Re_s}{d\theta} = -\frac{1}{2} \phi^2 \frac{d\Re_s}{d\theta} \qquad \text{---------- (3.3)}$$

where ϕ = instantaneous flux produced by the stator mmf $N_s i_s$ acting in the path of reluctance $\Re_s$

When the rotor axis lies along stator field axis the reluctance seen by stator flux will be a minimum because the magnetic path consists of two small air gaps and a large amount of high permeability iron. This path is called the direct axis of the machine and leads to a minimum reluctance $\Re_d$. As the rotor axis is displaced towards $\theta = \Pi/2$, the reluctance seen by stator flux is a maximum because it now consists of two very large air gaps. The rotor alignment with respect to the stator-produced flux is now said to be in its quadrature axis. This is called as maximum value of reluctance $\Re_q$. As a result of the shaping of the pole pieces and the distributed nature of the stator winding, the reluctance variation $\Re_s$ is a cosinusodial function of θ. Since for each full revolution of the rotor structure there are two positions each of minimum and maximum reluctance, it follows that L_s is a double frequency function of θ. The complete variation of the reluctance is

depicted graphically in Fig.3.3. The analytical expression for this reluctance is given by

$$\Re_s = \frac{\Re_q + \Re_d}{2} - \frac{\Re_q - \Re_d}{2}\cos 2\theta \qquad \text{---------- (3.4)}$$

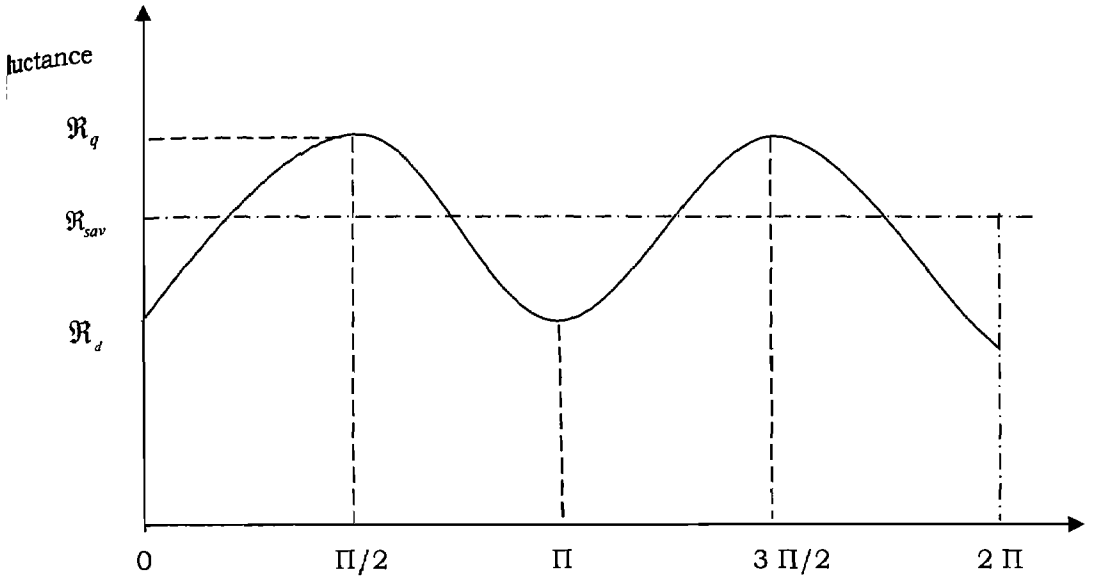

Fig. 3.3 Variation or reluctance with rotor position θ

If a sinusoidal voltage of rms value V is applied to the stator winding, then

$$\phi = \Phi \cos \omega t \qquad \text{---------- (3.5)}$$

Where, $\Phi = \frac{V}{\sqrt{2}\pi f N_s} = \frac{V}{4.44\ f N_s}$

$\omega = 2\pi f$ = angular frequency of supply voltage V

Moreover, from equation (3.4) we can write

$$\frac{d\Re_S}{d\theta} = \frac{d}{d\theta}\left(\frac{\Re_q + \Re_d}{2} - \frac{\Re_q - \Re_d}{2}\cos 2\theta\right)$$

$$= (\Re_q - \Re_d)\sin 2\theta$$

$$= (\Re_q - \Re_d)\sin 2(\omega_r t - \delta) \qquad \text{---------- (3.6)}$$

Upon substituting equations (3.5) and (3.6) in equation (3.3), then it results

$$T_{ri} = -\frac{1}{2}\Phi^2(\Re_q - \Re_d)\sin 2(\omega_r t - \delta)\cos^2 \omega t \qquad \text{---------- (3.7)}$$

But $\cos^2 \omega t = \frac{1}{2}(1 + \cos 2\omega t)$

Hence,

$$T_{ri} = -\frac{1}{4}\Phi^2(\Re_q - \Re_d)[\sin 2(\omega_r t - \delta) + \sin 2(\omega_r t - \delta)\cos 2\omega t] \qquad \text{---------- (3.8)}$$

Also,

$$\sin 2(\omega_r t - \delta)\cos 2\omega t = \frac{1}{2}\sin[2(\omega_r + \omega)t - 2\delta] + \frac{1}{2}\sin[2(\omega_r - \omega)t - 2\delta]$$

Accordingly

$$T_{ri} = -\frac{1}{4}\Phi^2(\Re_q - \Re_d)\{\sin 2(\omega_r t - \delta) + \frac{1}{2}\sin[2(\omega_r + \omega)t - 2\delta] + \frac{1}{2}\sin[2(\omega_r - \omega)t - 2\delta]\}$$

------- (3.9)

Equation (3.9) still represents the instantaneous value of the reluctance torque. To obtain the average value, we must integrate over one period of ωt. Thus

$$T_r = \text{average } T_{ri} = \frac{1}{2\Pi}\int_0^{2\Pi} T_{ri}\, d(\omega t) = \frac{1}{\Pi}\int_0^{\Pi} T_{ri}\, d(\omega t) \qquad \text{----------(3.10)}$$

From equations (3.9) and (3.10) one gets

$$T_r = \frac{1}{\Pi}\left\{-\frac{1}{4}\Phi^2(\Re_q - \Re_d)\left[\int_0^{\Pi}\sin(2\omega_r t - 2\delta)d(\omega t) + \frac{1}{2}\int_0^{\Pi}\sin[2(\omega_r + \omega)t - 2\delta]d(\omega t)\right.\right.$$
$$\left.\left. + \frac{1}{2}\int_0^{\Pi}\sin[2(\omega_r - \omega)t - 2\delta]d(\omega t)\ \right]\right\}$$

---------- (3.11)

Examination of the equation (3.11) reveals that the first integral term always yields a zero value because the first sine term within the bracket is always varying with time for one period of time. Moreover the second and the third integral terms also yield zero whenever $\omega \neq \omega_r$. If $\omega = \omega_r$, then the expression for the reluctance torque becomes

$$T_r = \frac{1}{\Pi}\left[-\frac{1}{4}\Phi^2(\Re_q - \Re_d)\int_0^{\Pi}\frac{1}{2}\sin(-2\delta)d(\omega t)\right]$$

This leads to

$$T_r = \frac{1}{8}\Phi^2(\Re_q - \Re_d)\sin 2\delta \qquad \text{---------- (3.12)}$$

Thus we see that the machine is capable of producing an average reluctance torque, but only when the angular speed of the rotor is equal to the angular frequency of the stator line current. Furthermore, this torque varies with an argument that is double the torque angle δ. In contrast, the electromagnetic torque has a fundamental variation with torque angle. It follows, therefore, that the maximum electromagnetic torque occurs at $\delta=\Pi/2$, whereas the maximum reluctance torque occurs at $\delta= \Pi/4$.

An alternate form of the average reluctance torque can be formed by expressing $\Re_d$ and $\Re_q$ in terms of their corresponding

reactances. Neglecting saturation in reluctance machine direct-axis reactance x_d and the quadrature-axis reactance x_q is defined as:

$$x_d \equiv \omega L_d = \omega \frac{N_s^{\,2}}{\Re_d}$$

$$x_q \equiv \omega L_q = \omega \frac{N_s^{\,2}}{\Re_q} \qquad \text{---------- (3.13)}$$

where ω is the angular frequency of the stator current and N_s denotes the stator winding turns. Inserting the values of $\Re_d$ and $\Re_q$ from equation (3.13) in above torque equation (3.12), we get

$$T_r = \frac{1}{4}\frac{V^2}{\omega}\frac{x_d - x_q}{x_d x_q}\sin 2\delta \qquad \text{---------- (3.14)}$$

It is interesting to note that for a machine with a uniform air gap x_d and x_q is equal, which causes the reluctance torque to disappear. From above expression it is obvious that difference between direct axis reactance and quadrature axis reactance or its ratio i.e. saliency ratio is most important parameter to decide the performance of synchronous reluctance machine (SRM). This in turn needs rotor geometrical optimization to maximize saliency ratio of SRM discussed in next section.

3.2 MAXIMIZATION OF THE SALIENCY RATIO:

Stator and its polyphase winding of synchronous reluctance machine are similar to that of a standard three phase induction

motor. Its rotor is the main component for design to maximize saliency ratio. It should present a variable magnetic reluctance along the air gap. The main classes of rotor design aimed at maximizing saliency ratio shown in Figs.3.4-3.7. The objective is to achieve a high L_d by providing essential flux guides to d-axis flux and low L_q by providing flux barrier to q-axis flux in all types of rotor.

The rotor of early reluctance motors employed simple salient poles construction, like a conventional salient pole synchronous machine with winding removed as shown in Fig.3.4. This geometry was used by Lee [45] in low speed reluctance motor. This rotor is obtained by removal of material from a conventional induction motor rotor, either by a milling operation after casting the cage, or by

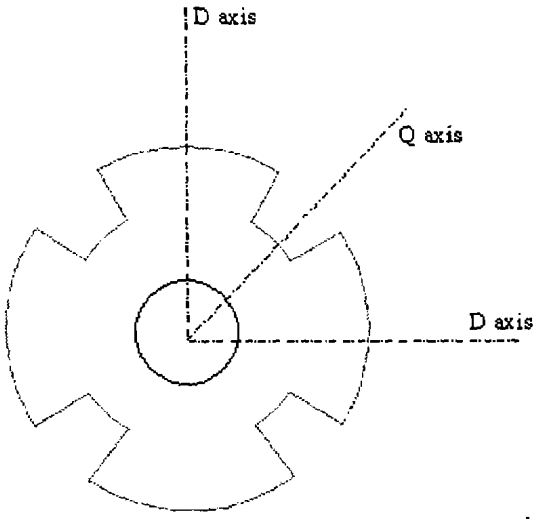

Fig.3.4 Salient pole rotor

punching before casting the cage. Rotor of this type has simple construction but the saliency ratio is less than two which is too small for competitive performance. Its power factor does not exceed 0.4. A

high saliency ratio could not be expected for this rotor configuration. These machines characterized by very low power factor and efficiency were larger than induction machines of corresponding rating. Its low efficiency and poor performance were inadmissible in motors of large output and seemed to justify the general opinion that the synchronous reluctance motor was inherently inferior to the other type of motors. Kostko [47] pointed out the essential limitation of the salient pole design that widening of the interpolar cutout to decrease the q-axis inductance, the pole arc being thereby narrowed, results in an unwanted reduction in L_d. So the multiple barrier or segmented arrangement is the natural way to make a synchronous reluctance machine because it involves no sacrifice of pole arc in d-axis.

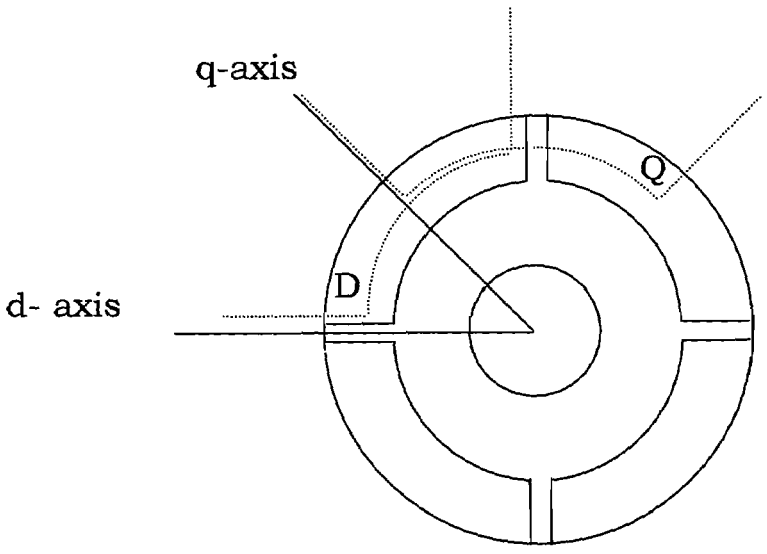

Fig.3.5 Segmental rotor

Saliency ratio of two or more than two is obtained by utilizing segmental rotor construction in synchronous reluctance motor to secure optimum performance. Lawrenson [44] utilized a segmental

rotor construction and presented the superiority of new reluctance machine over the conventional one having salient pole rotor. Gupta [42] presented improvements in reluctance motors with purely segmental rotors incorporating a shallow axial channel in the center of the air-gap face of each segment and filling this channel with conducting material. A reluctance machine with segmental rotor which can operate at better power factor in acceptable range (above 0.5 or 0.6), has a better pull out power than conventional reluctance machine of the same size. It is derived from a conventional salient pole machine by replacing the central (permeable) cylinder of the salient-pole rotor by a non-magnetic one. Its magnetic structure is shown in Fig.3.5 for a four pole synchronous reluctance machine. In the new form of rotor, the corresponding main flux paths are essentially circumferential whereas the main flux paths in a conventional machine are essentially radial. The magnetic-pole centers of a normal rotor coincide with the physical centre-lines of the poles whereas in the new rotor the magnetic-pole centre coincides with the centre of the non-magnetic spaces between the physical poles. It means that the direct and quadrature axes of the new machine are associated with the physical interpolar and polar axes, respectively, which is, of course, the reverse of the association for a conventional machine. Typical flux paths associated with the direct and quadrature axes reluctances, x_d and x_q, are marked, respectively, D and Q in Fig.3.5. The reluctance of these paths shows clearly the merit of the new

magnetic circuit. In short, ignoring the reluctance of the iron, the reluctance of the direct-axes paths is that of the air gap, while the reluctance of the quadrature axes is that of the air-gap in series with the very much larger reluctance of the interpolar space. It is thus to be expected that, even for large pole-arc/pole-pitch ratios, say 0.9 or 0.95, it should be possible to achieve large ratios of x_d/x_q and thus large output powers. The new segmental rotor reluctance motor gives significant improvement in its power factor, efficiency, and pullout power over conventional salient-pole rotor reluctance machine. The poor power factor and efficiency as compared with induction machines have continued to plague the widespread use of such machines.

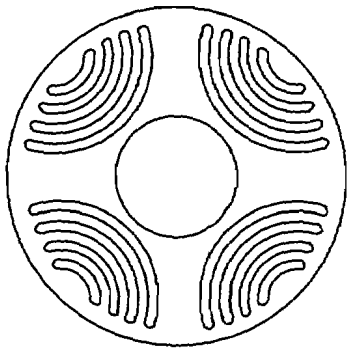

Fig.3.6 Rotor with multiple flux barriers

Saliency ratios of four or more have been achieved by using flux guided/axially laminated anisotropic rotor. Reluctance machine fitted with this type of rotor competes with an induction motor. The cost of such rotors will be drastically reduced when mass production takes place. In flux guided rotor the flux guides should ideally have the shape of the flux path. This will maximize the d-axis flux linkage and

thus, the value of x_d will be large. On the other hand, the flux barrier should be ideally perpendicular to the flux lines. This will ensure minimum q-axis flux linkage resulting in low value of x_q. Thus, the saliency ratio will be large. Typically the rating of the new machine with single flux barrier, with a pull out torque 140-160% of full load torque, is 75-85% of that of an induction motor of the same frame size. The starting torque and current of synchronous reluctance machine with flux barriers are comparable to those for a primitive reluctance motor of equal size. This led to a thought of using a rotor with multiple barriers as shown in Fig. (3.6) to maximize d-axis flux linkage and to minimize the q-axis flux. These requirements lead to multiple barrier rotors. By using higher number of barriers a large saliency ratio is achievable which can give sufficiently large operating power factor with reduced torque ripple. By using higher number of barriers a saliency ratio around nine is achievable but higher the number of barriers used resulting weaker and more pliable laminations. An optimum width is chosen to compromise between the widths for highest ratio and larger difference of inductances.

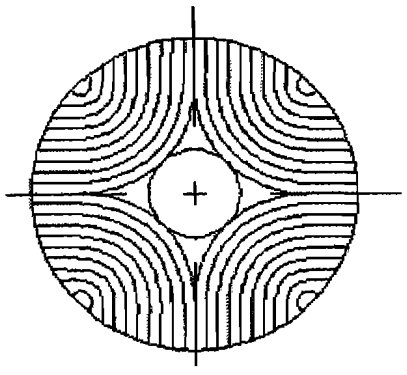

Fig.3.7 Axially laminated anisotropic rotor

Due to difficulty of constructing the multiple-barrier from a unitary lamination attention was given to replace the usual radial lamination by axial lamination of anisotropic material whose permeability was not only directional but also followed a pattern corresponding to the natural shape of the flux lines. The ideal rotor is one which is infinitely permeable along the flux lines and completely impermeable across it. Approximately this shape of rotor is obtained by fabricating axially laminated rotor of anisotropic magnetic material. Its laminations are shaped to follow the d-axis flux and flux barrier which inhibit the q-axis flux as shown in Fig. 3.8.

The basic structural requirements of the axially laminated anisotropic rotor shown in Fig.3.7 to provide a high saliency ratio are given below :

- Lamination layers must be of a good magnetic material with a favoured direction of orientation, such as grain oriented lamination used in transformer.
- Insulation layers must be made of a nonmagnetic and nonconducting material, such as paper lamination sheets for winding insulation.
- The rotor pole holder must be nonmagnetic and nonconducting such as phenolic linen. The holder must have adequate mechanical strength for machining and for the torque to or from the shaft.

- The bolts must be nonmagnetic to ensure the expected strong rotor magnetic anisotropy.

Another observation deserves to be emphasized that in an induction machine, the length of airgap length is not designed as small as mechanically possible since the zig-zag leakage flux, phase belt-leakage flux, and skew leakage flux, all cross the airgap and inversely proportional to the airgap length. If the airgap length is designed too small, these leakage fluxes will become significant and degrade the performance of the machine. For an ALA-rotor reluctance machine, airgap length may be designed as small as is mechanically feasible since the leakage fluxes in the machine, primarily consisting of the stator leakage and end-connection leakage fluxes, do not depend on the airgap length. However, the component in the leakage fluxes, dependent on the airgap, is almost absent in the ALA-rotor reluctance machine. The smaller airgap in an ALA-rotor reluctance machine will reduce the magnetizing current, resulting in a high power factor. In next chapter design of axially laminated anisotropic rotor for a synchronous reluctance has been presented. The studies of performance and maximum power conversion capabilities of the reluctance generator can be initiated by developing the mathematical model in rotor co-ordinates.

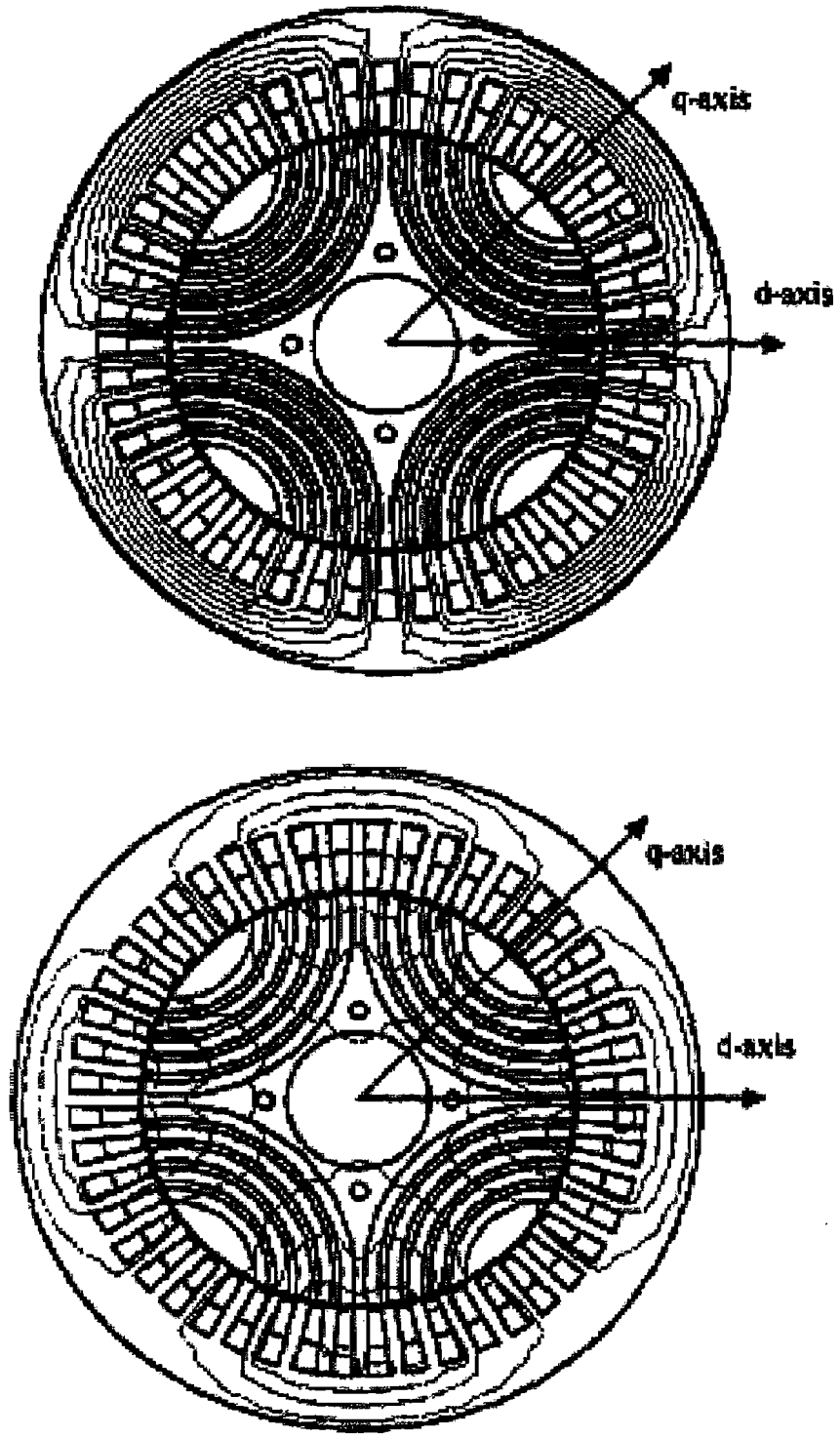

Fig.3.8 d and q- axis magnetic field distribution in SRM

3.3 MATHEMAICAL MODEL OF SRM:

The model should be able to represent the actual device as accurately as it is required for the purpose of analysis. There are two different approaches to the modeling of electrical machines, i.e., field theory and circuit theory.

The field theory approach is particularly difficult both in concept and mathematical development. It is mainly applied to design problems. The circuit approach being simple is chosen to represent the synchronous reluctance machine in the present work. There are two justifications for selecting this approach. The first is that the circuit theory can in fact be developed as a self-contained entity without reference to the internal phenomena. The second is a widespread in performance than in design aspect.

The original mathematical machine model is always obtained using basic physical laws and the original geometry of the machine. The voltage equations for the stator and the rotor of any rotating electrical machine are written in the original reference frame for the stator and the rotor.

It is possible to achieve a considerable simplification of the model by the use of a corresponding transformation in a new reference frame. The role of reference frame transformations in machine analysis is analogous to that of simple changes of reference axes in coordinate geometry. Apart from providing a unified approach to machine analysis, these transformations bring about simplifications

in the equations describing the machine. The physical interpretation to a reference transformation is the replacement of actual machine windings by equivalent fictitious windings, the axes of whose mmf are aligned with the newly defined axes of reference. The model is solved in its transformed form and the results are then transformed back to the original reference frame.

For synchronous reluctance machine with asymmetrical rotor structure, analysis can be simplified by referring machine variables to the rotor reference frame. The synchronous reluctance machine comprises three phase stator winding and a unique rotor geometrical structure with minimum and maximum reluctance in direct and quadrature axis. The three phase stator winding are magnetically coupled. The coupling is a function of rotor position and therefore the flux linking each winding is also a function of the rotor position. Hence the instantaneous terminal voltage of any winding takes the form,

$$v = ri + \frac{d\lambda}{dt} \qquad \text{----------} (3.15)$$

where r is the winding resistance, i is the current, and λ is the flux linkage.

The above equations are a set of differential equations describing the behavior of the machine. However their solution is complicated by the fact that the inductances are the function of rotor angle θ which in turn is a function of time. And hence, these are

differential equations with variable coefficients which are the function of time with the result, that their solution is quite complicated. This complication, however, can be avoided by transferring the three phase stator variables (*abc)* of the armature windings in two phase *(dq)* windings in rotor reference frame resulting a linear, time independent and power invariant transformation.

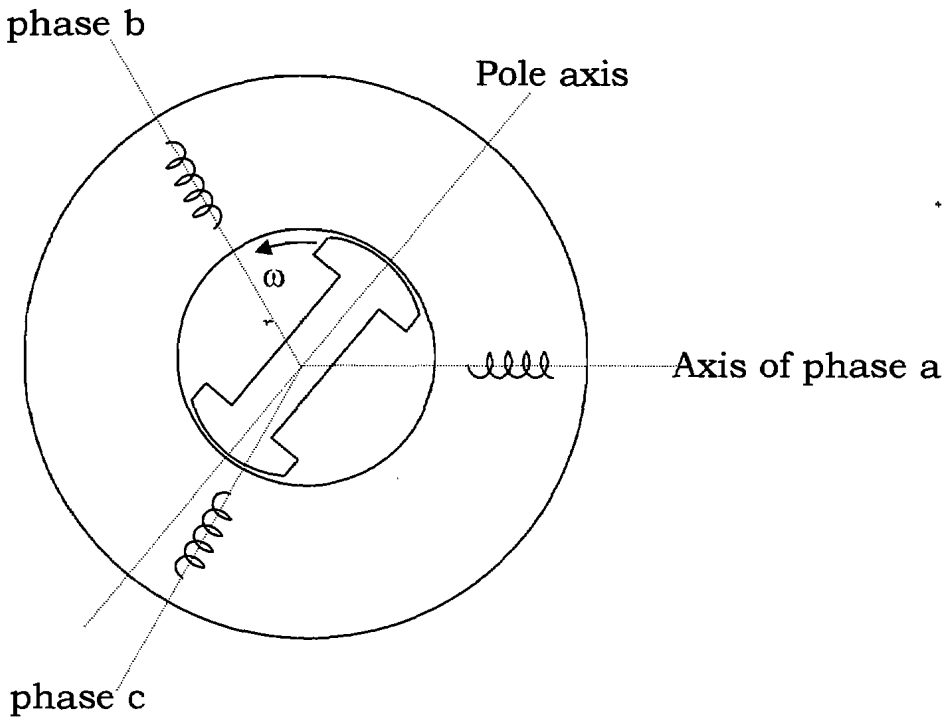

Fig.3.9 Two pole three phase armature winding with salient pole rotor

TRANSFORMATION FROM 3-PHASE WINDING (*abc*) TO 2-PHASE (*dq*) WINDING IN ROTOR REFERENCE FRAME:

A three phase stationary system (*abc*) is transformed to a two winding (*dq*) system moving with synchronous speed. The two windings carry dc current. The *dq* windings are placed on the rotor.

For three phase (*abc*) winding the reference frame is stator but in case of *dq* variables the reference frame is rotor rotating at synchronous speed with respect to stator.

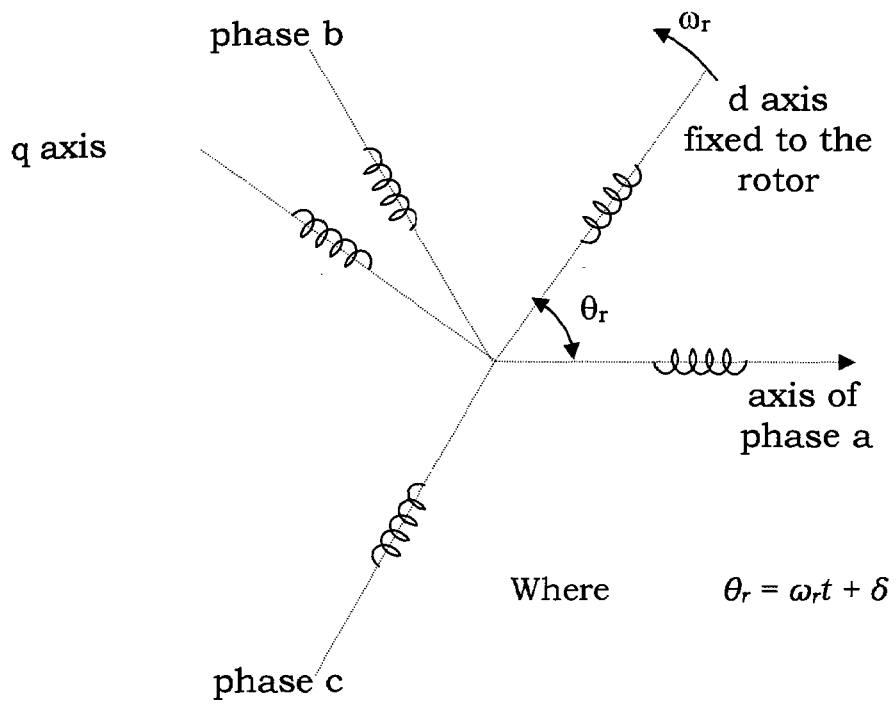

Fig.3.10 Transformation from three phase windings (*abc*) to two phase (*dqo*) windings in rotor reference frame

The transformation [27] is expressed as

$$[F_{dq0}] = \sqrt{\frac{3}{2}}[C][F_{abc}]$$

$$[F_{abc}] = \sqrt{\frac{2}{3}}[C][F_{dq0}]$$

---------- (3.16)

where C is the connecting matrix of Park transformation given by

$$[C] = \sqrt{\frac{2}{3}}\begin{bmatrix} \cos\theta_r & \cos(\theta_r - 120^0) & \cos(\theta_r + 120^0) \\ -\sin\theta_r & -\sin(\theta_r - 120^0) & -\sin(\theta_r + 120^0) \\ \frac{1}{\sqrt{2}} & \frac{1}{\sqrt{2}} & \frac{1}{2} \end{bmatrix}$$

$$[C] = \sqrt{\frac{2}{3}}\begin{bmatrix} \cos\theta_r & -\sin\theta_r & \frac{1}{\sqrt{2}} \\ \cos(\theta_r - 120^0) & -\sin(\theta_r - 120^0) & \frac{1}{\sqrt{2}} \\ \cos(\theta_r + 120^0) & -\sin(\theta_r + 120^0) & \frac{1}{\sqrt{2}} \end{bmatrix}$$

The *dqo* voltages can be expressed in terms of flux linkages. Consequently

$$\mathbf{v}_{dqo} = \mathbf{c}\mathbf{v}_{abc} \qquad \text{and} \qquad \mathbf{i}_{dqo} = \mathbf{c}\mathbf{i}_{abc}$$

where the voltage and current vectors are defined as,

$$\mathbf{i}_{dqo} = \begin{bmatrix} i_0 \\ i_d \\ i_q \end{bmatrix} \qquad \text{and} \qquad \mathbf{i}_{abc} = \begin{bmatrix} i_a \\ i_b \\ i_c \end{bmatrix}$$

$$\mathbf{v}_{dqo} = \begin{bmatrix} v_d \\ i_q \\ i_o \end{bmatrix} \qquad \text{and} \qquad \mathbf{v}_{abc} = \begin{bmatrix} v_a \\ v_b \\ v_c \end{bmatrix}$$

Furthermore if the transformation is unique, an inverse transformation exists, and the *abc* quantities can be calculated if the *dq*o quantities are known. In this case,

$$\mathbf{i}_{abc} = \mathbf{C}^{-1}\mathbf{i}_{dqo}$$

$$\mathbf{v}_{abc} = \mathbf{C}^{-1}\mathbf{v}_{dqo}$$

$$\lambda_{abc} = \mathbf{C}^{-1}\lambda_{dq0} \qquad \text{--------- (3.17)}$$

$\boldsymbol{C}$ is an orthogonal matrix and $\boldsymbol{C}^T\boldsymbol{C} = \boldsymbol{I}$. Since the inverse of a square matrix is unique, it is also true that $\boldsymbol{C}\boldsymbol{C}^T = \boldsymbol{I}$. This implies that $\boldsymbol{C}^{-1}=\boldsymbol{C}^T$. Consequently, $\boldsymbol{C}$ is power invariant and therefore the same power expression can be used in both the *abc* and *odq* frames of reference. It is easy to show that,

$$p = v_a i_a + v_b i_b + v_c i_c = v_0 i_0 + v_d i_d + v_q i_q \qquad \text{---------- (3.18)}$$

VOLTAGE EQUATION AND WINDING INDUCTANCE OF SRM

The following assumptions are made in obtaining the mathematical model of synchronous reluctance machine.

(i) Core loss is neglected in exciting branch.

(ii) All parameters of the machine are constant except that the d-axis magnetizing reactance X_{md} is affected by the magnetic saturation.

(iii) Space and time harmonic effect.

(iv) Machine is under three phase balanced operation

The voltage equations for each phase of 3-phase Synchronous reluctance motor as shown in Fig.3.9 are expressed as:

$$v_{as} = r_s i_{as} + \frac{d\lambda_{as}}{dt}$$

$$v_{bs} = r_s i_{bs} + \frac{d\lambda_{bs}}{dt}$$

$$v_{cs} = r_s i_{cs} + \frac{d\lambda_{cs}}{dt}$$

In matrix form, $$\mathbf{v}_{abcs} = \mathbf{r}_s \mathbf{i}_{abcs} + \frac{d\boldsymbol{\lambda}_{abcs}}{dt} \qquad \text{---------- (3.19)}$$

$$\mathbf{r}_s = \begin{bmatrix} r_s & 0 & 0 \\ 0 & r_s & 0 \\ 0 & 0 & r_s \end{bmatrix}$$

The flux linkage equations may be expressed as

$$\begin{aligned} \lambda_{as} &= L_{asas}\, i_{as} + L_{asbs}\, i_{bs} + L_{ascs}\, i_{cs} \\ \lambda_{bs} &= L_{bsas}\, i_{as} + L_{bsbs}\, i_{bs} + L_{bscs}\, i_{cs} \\ \lambda_{cs} &= L_{csas}\, i_{as} + L_{csbs}\, i_{bs} + L_{csc\,s}\, i_{cs} \end{aligned}$$

In matrix form, $$\boldsymbol{\lambda}_{abcs} = \mathbf{L}_s \mathbf{i}_{abcs}$$

$$\mathbf{L}_s = \begin{bmatrix} L_{ls} + L_A + L_B \cos 2\theta_r & -\frac{1}{2}L_A + L_B \cos 2\left(\theta_r - \frac{\Pi}{3}\right) & -\frac{1}{2}L_A + L_B \cos 2\left(\theta_r + \frac{\Pi}{3}\right) \\ -\frac{1}{2}L_A + L_B \cos 2\left(\theta_r - \frac{\Pi}{3}\right) & L_{ls} + L_A + L_B \cos 2\left(\theta_r - \frac{2}{3}\Pi\right) & -\frac{1}{2}L_A + L_B \cos 2(\theta_r + \Pi) \\ -\frac{1}{2}L_A + L_B \cos 2\left(\theta_r + \frac{\Pi}{3}\right) & -\frac{1}{2}L_A + L_B \cos 2(\theta_r + \Pi) & L_{ls} + L_A + L_B \cos 2\left(\theta_r + \frac{2}{3}\Pi\right) \end{bmatrix}$$

Where L_{ls} is the leakage inductance, L_A is a constant magnetizing inductance, and L_B is the amplitude of the sinusoidal varying magnetizing inductance.

For three phase synchronous reluctance machine, the stator magnetizing inductance is defined [27] as one and half times the magnetizing inductance of a two phase machine. The relation between phase inductances and *dq* inductances in rotor reference frame is given by

$$L_{mq} = \frac{3}{2}(L_A - L_B)$$

$$L_{md} = \frac{3}{2}(L_A + L_B) \qquad \text{---------- (3.20)}$$

The relation between inductance and d-q inductance in rotor reference frame is given by

$$L_d = L_{ls} + \frac{3}{2}(L_A + L_B)$$

$$L_q = L_{ls} + \frac{3}{2}(L_A - L_B) \qquad \text{---------- (3.21)}$$

MACHINE EQUATION IN ROTOR REFERENCE FRAME:

Transformation of stator variable (*abc*) in equation (3.19) of synchronous reluctance machine (SRM) to *dq* variables in rotor reference frame using above transformation yields

$$(\mathbf{C})^{-1}\mathbf{v}_{dqo} = \mathbf{r}_s(\mathbf{C})^{-1}\mathbf{i}_{dqo} + \frac{d}{dt}\left[(\mathbf{C})^{-1}\boldsymbol{\lambda}_{dq0}\right] \qquad \text{---------- (3.22)}$$

Premultiplying each side by $\mathbf{C}$ yields

$$\mathbf{v}_{dqo} = \mathbf{r}_s\mathbf{i}_{dqo} + \frac{d\boldsymbol{\lambda}_{dq0}}{dt} + \omega_r\boldsymbol{\lambda}_{dqo} \qquad \text{---------- (3.23)}$$

where,

$$\boldsymbol{\lambda}_{dq} = \begin{bmatrix} L_d & 0 \\ 0 & L_q \end{bmatrix}\begin{bmatrix} i_{ds} \\ i_{qs} \end{bmatrix}$$

$$\mathbf{v}_{ds} = r_s i_{ds} - \omega_r \lambda_{qs} + \frac{d\lambda_{qs}}{dt}$$

$$\mathbf{v}_{qs} = r_s i_{qs} + \omega_r \lambda_{ds} + \frac{d\lambda_{ds}}{dt} \qquad \text{---------- (3.24)}$$

The expression for electromagnetic torque is obtained by expressing i_{as}, i_{bs} and i_{cs} in terms of i_{qs} and i_{ds}

$$T_e = (polepairs)(L_d - L_q) i_{ds} i_{qs} \qquad \text{---------- (3.25)}$$

SRM AS SELF EXCITED RELUCTANCE GENERATOR:

The synchronous reluctance machine with static capacitance in shunt across its terminals in Fig.(3.11) will build up its voltage in a manner similar to the DC shunt generator and the self excited induction generator. Residual magnetism in the iron of the magnetic circuit sets up a small alternating voltage in the stator; this voltage applied to the capacitor causes a magnetizing current to flow in the stator winding. If the capacitance is of the proper value causing adequate flow of current through the winding so as to increase the flux existing in the air gap. An increase of air gap flux will result in a higher voltage which will result in a larger exciting drawn by the capacitance which in turn causes more air gap flux until the terminal voltage of the machine reaches its final build up value. This value is determined by the magnetizing curve of the machine and by the capacitive reactance of the connected capacitance.

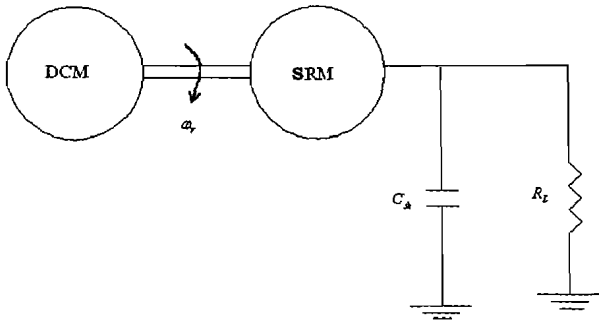

Fig.3.11 Single line diagram of self excited reluctance generator

Due to saliency of the reluctance generator, the gap flux is rotated at the same speed of rotor. Thus the frequency of the reluctance generator is directly proportional to the actual speed of the rotor without any slip as in the induction generator. The synchronous operation of reluctance generator leads to a high reduction in rotor iron losses than the induction generator.

3.5 PERFORMANCE ANALYSIS OF SERG

Using equation (3.24) of synchronous reluctance machine, the voltage equation in rotor reference frame for self excited reluctance generator is expressed as:

$$v_{ds} = -r_s i_{ds} - \omega_r \lambda_{qs} + \frac{d\lambda_{ds}}{dt}$$

$$v_{qs} = -r_s i_{ds} + \omega_r \lambda_{ds} + \frac{d\lambda_{qs}}{dt}$$

---------- (3.26)

The current equation of the excitation capacitor bank at no load is given by

$$\begin{bmatrix} i_{qs} \\ i_{ds} \end{bmatrix} = \begin{bmatrix} Cp & \omega_1 C \\ -\omega_1 C & Cp \end{bmatrix} \begin{bmatrix} v_{qs} \\ v_{ds} \end{bmatrix}$$

---------- (3.27)

The d-axis and q-axis operational equivalent circuit of SERG is shown in Figs.3.12 and 3.13 respectively by using equations (3.23) and (3.24).

Using above two equations 4x4 state matrix is obtained under no load condition. This is the final expression of SERG model given by

$$\frac{d}{dt}\begin{bmatrix} i_{ds}^r \\ i_{qs}^r \\ v_{ds}^r \\ v_{qs}^r \end{bmatrix} = \begin{bmatrix} \frac{-r_s}{L_d} & \frac{-\omega_r L_q}{L_d} & \frac{-1}{L_d} & 0 \\ \frac{\omega_r L_d}{L_q} & \frac{-r_s}{L_q} & 0 & \frac{-1}{L_q} \\ \frac{1}{C} & 0 & 0 & \omega_r \\ 0 & \frac{1}{C} & -\omega_r & 0 \end{bmatrix} \begin{bmatrix} i_{ds}^r \\ i_{qs}^r \\ v_{ds}^r \\ v_{qs}^r \end{bmatrix}$$

---------- (3.28)

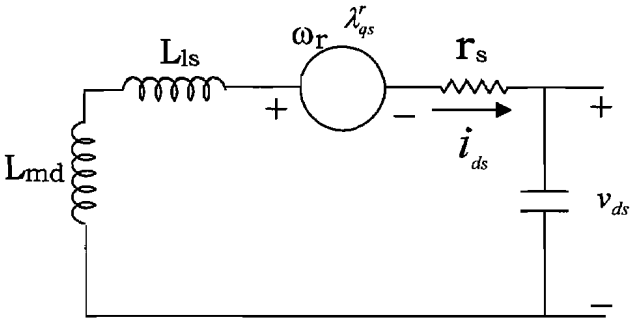

Fig.3.12 d-axis operational equivalent circuit of SERG

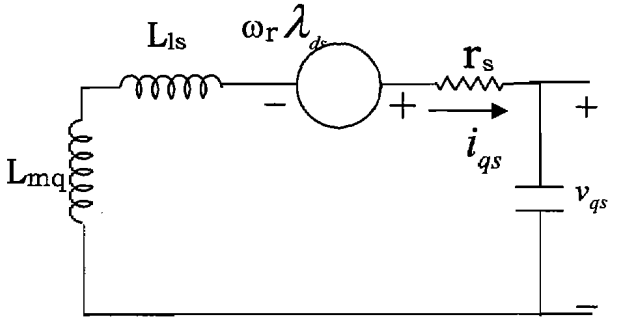

Fig.3.13 q-axis operational equivalent circuit of SERG

Under steady state and balanced conditions we have d/dt of the variables becomes zero and the machine phase voltage are equal. The equation (3.26) reduces to:

$$V_{ds} = -r_s i_{ds} - \omega_r \lambda_{qs}$$
$$V_{qs} = -r_s i_{qs} + \omega_r \lambda_{ds}$$

---------- (3.29)

Combining above two equations yields

$$\bar{E} = (r_s + jx)\bar{i} + \bar{V}$$

where, r_s and x are per phase armature resistance and leakage reactance in ohms respectively.

E is resultant air gap voltage given by $\bar{E} = jx_{dm}\bar{i}_{ds} - x_{qm}\bar{i}_{qs}$

and $\bar{V} = \bar{V}_d + j\bar{V}_q$

Thus the equivalent circuit model of the three phases self excited reluctance generator is shown in Fig. (3.14). The parallel branch across terminals a and b may be combined into an impedance $Z_{ab} = R_{ab} - X_{ab}$, Where,

$$R_{ab} = \frac{R_L X_C^2}{R_L^2 + (X_C - X_L)^2}$$
$$X_{ab} = \frac{X_C(R_L^2 + X_L^2 - X_C^2)}{R_L^2 + (X_C - X_L)^2}$$

The equivalent circuit can thus be reduced to Fig.3.15. Where

$$R_t = r_s + R_{ab}$$
$$X_t = X_{ab} - X$$
$$E = Z_t I$$
$$I^2 = I_d^2 + I_q^2$$
$$E^2 = (I_d X_{dm})^2 + (I_q X_{qm})^2$$

$$I_d^2 X_{dm} + I_q^2 X_{qm} = I^2 X_t$$

$$I_q^2 (Z_t^2 - X_{qm}^2) = I_d^2 (X_{dm}^2 - Z_t^2)$$

$$I_q^2(X_t - X_{qm}) = I_d^2(X_{dm} - X_t)$$

$$X_{dm}^2 - AX_{dm} - (Z_t^2 - AX_t) = 0$$

Where

$$A = \frac{Z_t^2 - X_{qm}^2}{X_t - X_{qm}}$$

it is assumed that $X_t \neq X_{mq}$

$$X_{md} = \frac{A \pm \sqrt{A^2 + 4(Z_t^2 - AX_t)}}{2}$$

$$V = IZ_{ab}$$

$$I_c = \frac{V}{X_C}$$

$$I_L = \frac{V}{Z_L}$$

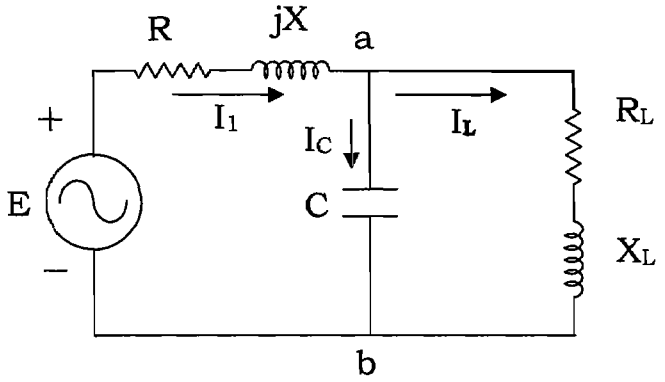

Fig.3.14 Equivalent circuit of SERG

To improve the voltage regulation of self excited reluctance generator short shunt compensation technique may be used. In this method a capacitance is connected in series with load as shown in Fig.3.16. The above derivation may be modified accordingly.

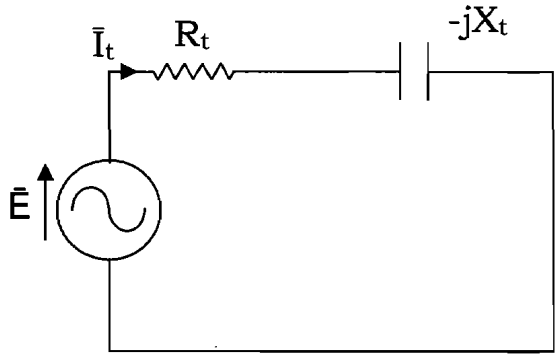

Fig.3.15 Reduced equivalent circuit of SERG

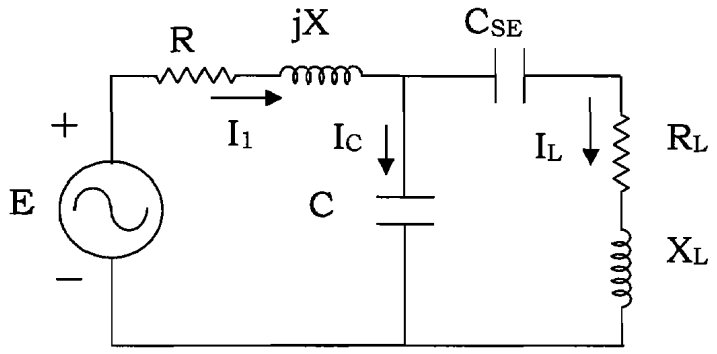

Fig.3.16 Equivalent circuit of SERG with short shunt compensation

To obtain steady state performance X_{md} can be calculated by evaluating R_t, X_t and A for given values of load impedance (R_L+jX_L), excitation capacitance (C_{sh}) and machine parameters. The corresponding air gap voltage E_q can be determined by experimentally obtained E_q/X_{md} characteristic at a given speed. Subsequently I_d, I_q and I are evaluated. Then load current I_L, excitation current (I_c), output power (P_{out}) efficiency. Various computed performance characteristics of SERG has been obtained by writing Matlab environment.

5 DIGITAL SOLUTION OF THE PERFORMANCE:

To simulate the voltage build up transient and steady state performance of self excited reluctance generator, the step by step solution is given below.

For Transient Response:

Runge-Kutta fourth order method is used to solve the set of four simultaneous nonlinear ordinary differential equations using machine model equation(3.28). The equations are given below.

$$\frac{d}{dt}i_{as} = -\frac{r_s i_{ds}}{L_d} - \frac{\omega_r L_w i_{ds}}{L_d} - \frac{i_{ds}}{L_d} \qquad \text{---------- (3.29)}$$

$$\frac{d}{dt}i = \frac{\omega_r L_d i_{qs}}{L_q} - \frac{r_s i_{qs}}{L} - \frac{i_{qs}}{L_d} \qquad \text{---------- (3.30)}$$

$$\frac{d}{dt}v_{ds} = \frac{1}{c}v_{ds} + \omega_r v_{ds} \qquad \text{---------- (3.31)}$$

$$\frac{d}{dt}v_{qs} = \frac{1}{c}v_{qs} - \omega_t v_{qs} \qquad \text{---------- (3.32)}$$

where $L_d = a_1.E_q^4 + a_2.E_q^3 + a_3.E_q^2 + a_4.E_q + a$

---------- (3.33)

Following steps have been followed:

STEP 1: Read the values of parameters; initialize the state variables; fix the step size Δt, and specify the final time t_f.

STEP 2: Set t = 0.

STEP 3: Calculate L_d using equation 1.5.

STEP 4: Calculate k_1, k_2, k_3, and k_4 for each state variable, i.e., i_{ds}^r, i_{qs}^r, v_{ds}^r, and v_{qs}^r.

STEP 5: Calculate Δi_{ds}^r, Δi_{qs}^r, Δv_{ds}^r, and Δv_{qs}^r.

STEP 6: Update $t = t + \Delta t$, $i_{ds}^r = i_{ds}^r + \Delta i_{ds}^r$, $i_{qs}^r = i_{qs}^r + \Delta i_{qs}^r$, $v_{ds}^r = v_{ds}^r + \Delta v_{ds}^r$, and $v_{qs}^r = v_{qs}^r + \Delta v_{qs}^r$.

STEP 7: If $t < t_f$, go to STEP 3, otherwise, go to STEP 8.

STEP 8: Plot the results and stop.

For Steady-State Response:

(a) For the Plot of V_L vs. C_{sh} at No Load

Following steps have been followed:

STEP 1: Read n, r_s, X, X_{qm}, and X_L.

STEP 2: Fix $R_L = \infty$ and Cse = ∞.

STEP 3: Set iteration count k = 1.

STEP 4: Initialize $C_{sh} = C_{sh}^1$.

STEP 5: Calculate Z_1, R_{ab}, X_{ab}, R_t, Z_t, A, and X_{dm}^k.

STEP 6: Calculate E_q^k corresponding to X_{dm}^k using the following equation:

$$E_q^k = \begin{cases} 0; & X_{dm}^k \le 90.0 \\ 534.0 - 0.8824\, X_{dm}^k; & 130 < X_{dm}^k \le 198 \\ 867.7 - 2564\, X_{dm}^k; & 198 < X_{dm}^k \le 237.0 \\ 2156 - 8.0 X_{dm}^k; & 237 < X_{dm}^k \le 247.0 \\ 11707 - 46.665\, X_{dm}^k; & 247 < X_{dm}^k \le 250.0 \\ 0; & X_{dm}^k > 250.0 \end{cases}$$

STEP 7: Calculate V_L^k.

STEP 8: If k < n, increase k by 1, increase C_{sh} by ΔC_{sh} (i.e., $C_{sh}^{k+1} = C_{sh}^k + \Delta C_{sh}$), and go to STEP 5; otherwise, go to STEP 9.

STEP 9: Plot V_L vs. C_{sh}.

STEP10: Stop.

(b) For Plots of V_L, P_{out}, and I_C with respect to I_L while R_L is varying, and C_{sh} and C_{se} are fixed

Following steps have been followed:

STEP 1: Read n, r_s, X, X_{qm}, and X_L.

STEP 2: Fix C_{sh} and C_{se}.

STEP 3: Set iteration count k = 1.

STEP 4: Initialize $R_L = R_L{}^1$.

STEP 5: Calculate Z_1, R_{ab}, X_{ab}, R_t, Z_t, A, and $X_{dm}{}^k$.

STEP 6: Calculate $E_q{}^k$ corresponding to $X_{dm}{}^k$ using the following equation:

STEP 7: Calculate $I_L{}^k$, $V_L{}^k$, $P_{out}{}^k$, and $I_C{}^k$.

$$E_q^{\,k} = \begin{cases} 0; & X_{dm}^{\,k} \le 90.0 \\ 534.0 - 0.8824\, X_{dm}^{\,k}; & 130 < X_{dm}^{\,k} \le 198 \\ 867.7 - 2564\, X_{dm}^{\,k}; & 198 < X_{dm}^{\,k} \le 237.0 \\ 2156 - 8.0 X_{dm}^{\,k}; & 237 < X_{dm}^{\,k} \le 247.0 \\ 11707 - 46.665\, X_{dm}^{\,k}; & 247 < X_{dm}^{\,k} \le 250.0 \\ 0; & X_{dm}^{\,k} > 250.0 \end{cases}$$

STEP 8: If k < n, increase k by 1, increase R_L by ΔR_L (i.e., $R_L{}^{k+1} = R_L{}^k + \Delta R_L$), and go to STEP 5; otherwise, go to STEP 9.

STEP 9: Plot V_L vs. I_L, P_{out} vs. I_L, and I_C vs. I_L.

STEP 10: Stop.

(c) For Plot of V_L, vs. I_L while C_{se} is varying, and R_L and C_{sh} are fixed

Following steps have been followed:

STEP 1: Read n, r_s, X, X_{qm}, and X_L.

STEP 2: Fix R_L and C_{sh}.

STEP 3: Set iteration count k = 1.

STEP 4: Initialize $C_{se} = C_{se}^1$.

STEP 5: Calculate Z_1, R_{ab}, X_{ab}, R_t, Z_t, A, and X_{dm}^k.

STEP 6: Calculate E_q^k corresponding to X_{dm}^k using the following equation:

$$E_q^k = \begin{cases} 0; & X_{dm}^k \le 90.0 \\ 534.0 - 0.8824\, X_{dm}^k; & 130 < X_{dm}^k \le 198 \\ 867.7 - 2564\, X_{dm}^k; & 198 < X_{dm}^k \le 237.0 \\ 2156 - 8.0\, X_{dm}^k; & 237 < X_{dm}^k \le 247.0 \\ 11707 - 46.665\, X_{dm}^k; & 247 < X_{dm}^k \le 250.0 \\ 0; & X_{dm}^k > 250.0 \end{cases}$$

STEP 7: Calculate I_L^k, and V_L^k.

STEP 8: If $k < n$, increase k by 1, increase R_L by ΔR_L (i.e., $C_{se}^{k+1} = C_{se}^k + \Delta C_{se}$), and go to STEP 5; otherwise, go to STEP 9.

STEP 9: Plot V_L vs. I_L.

STEP 10: Stop.

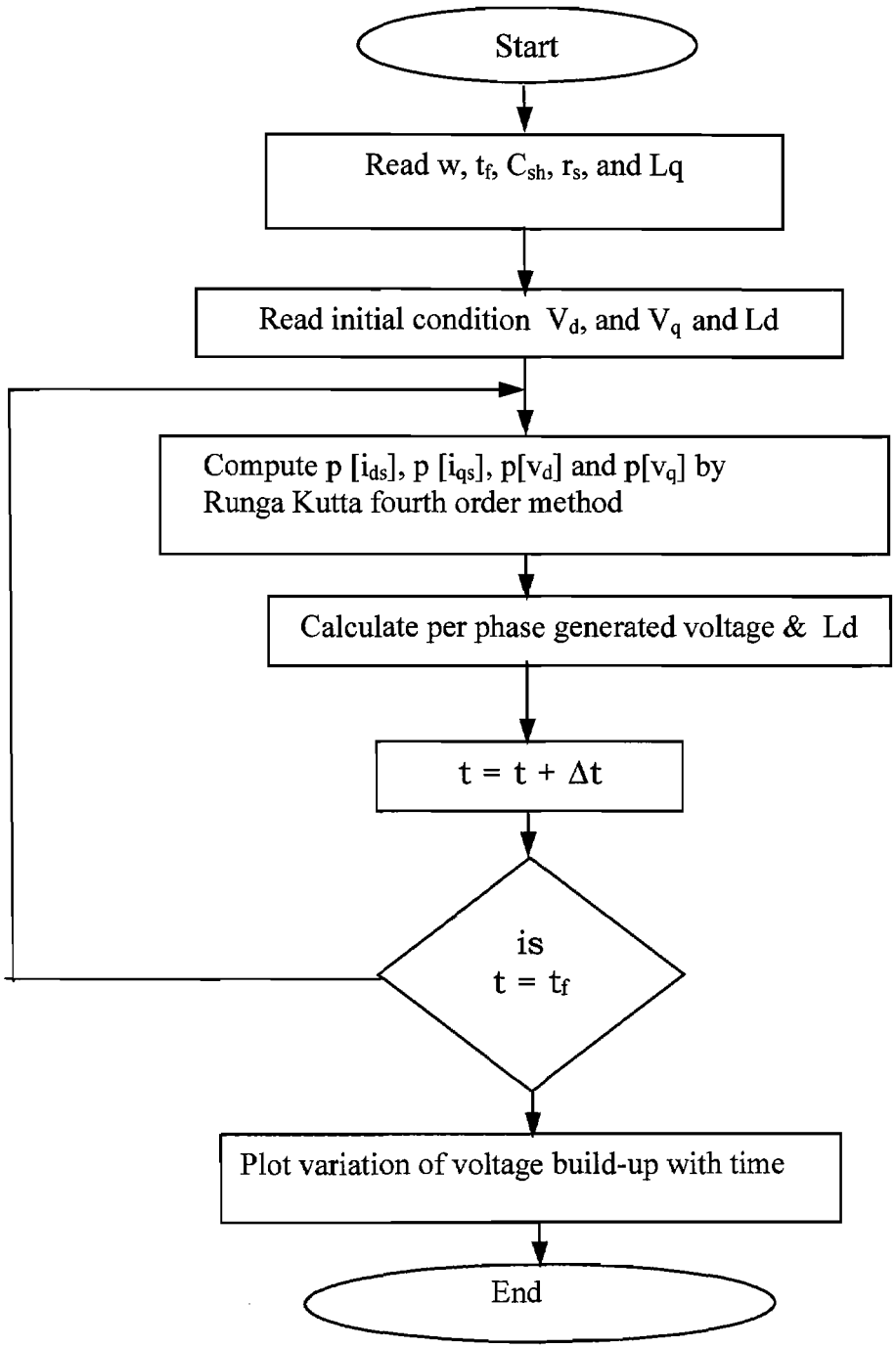

Fig.3.17 Flow chart for transient state analysis

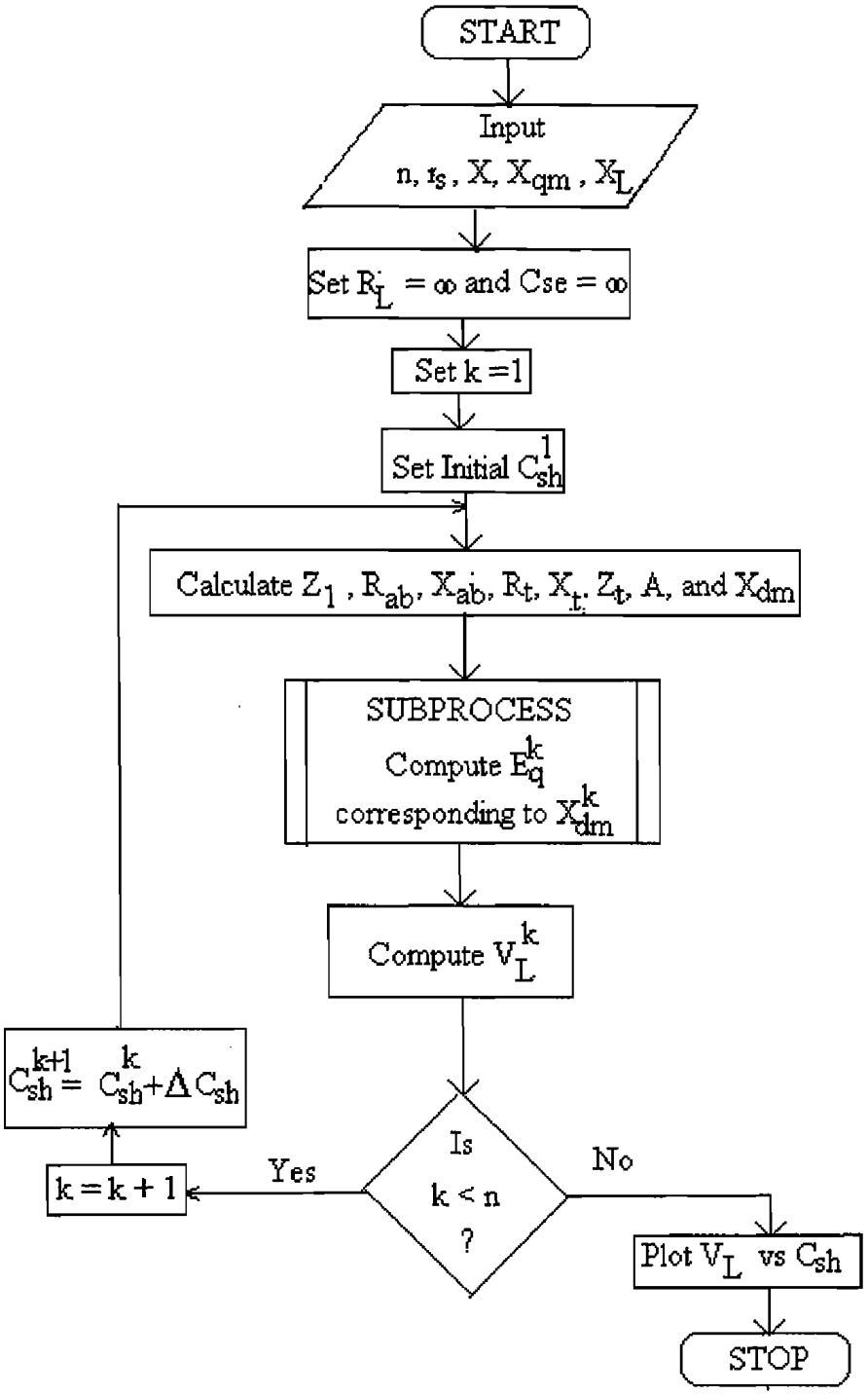

Fig.3.18 Flowchart for the Plot of V_L vs. C_{sh} at No Load

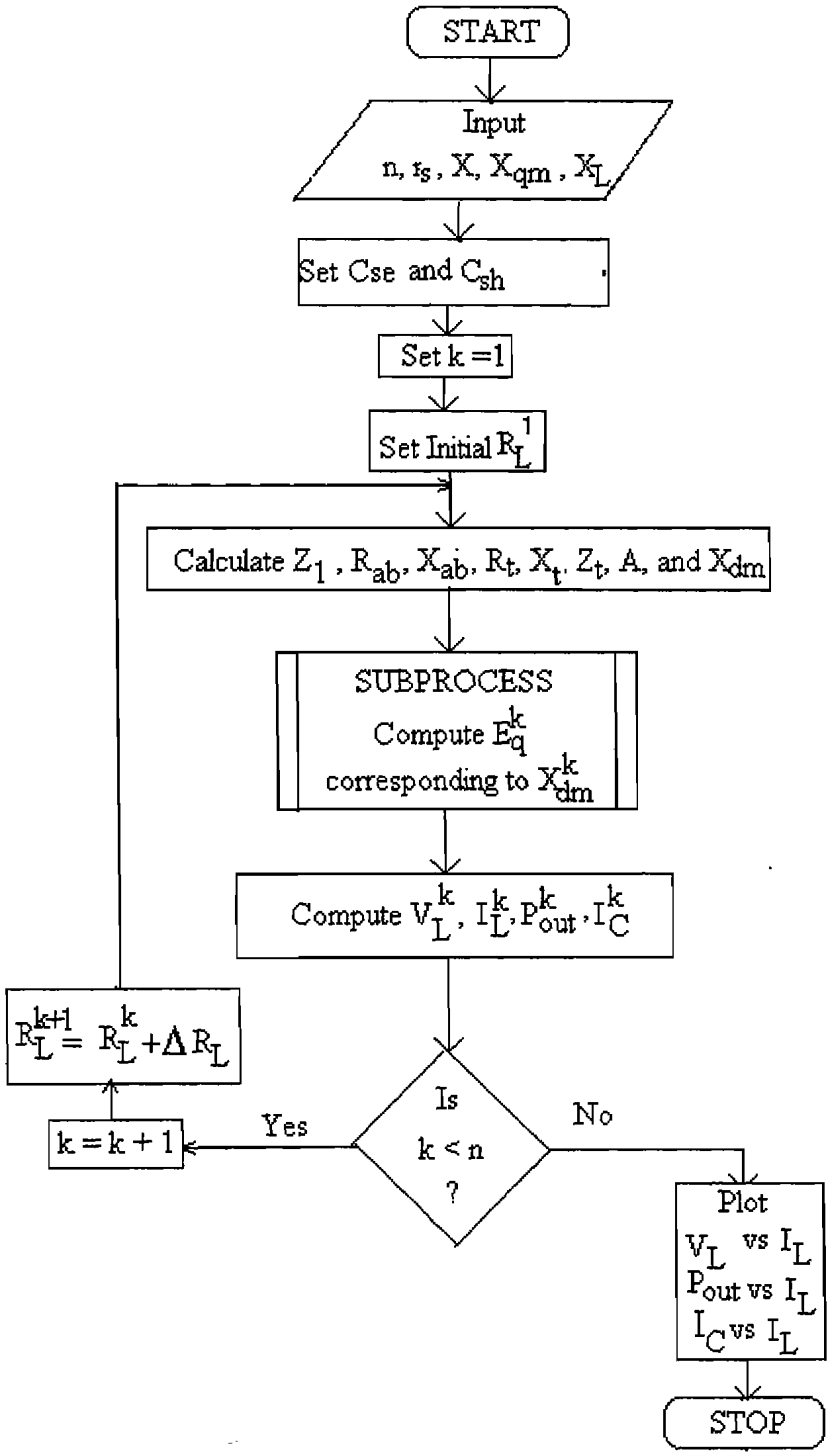

Fig.3.19 Flowchart for Plots of V_L, P_{out}, and I_C with respect to I_L

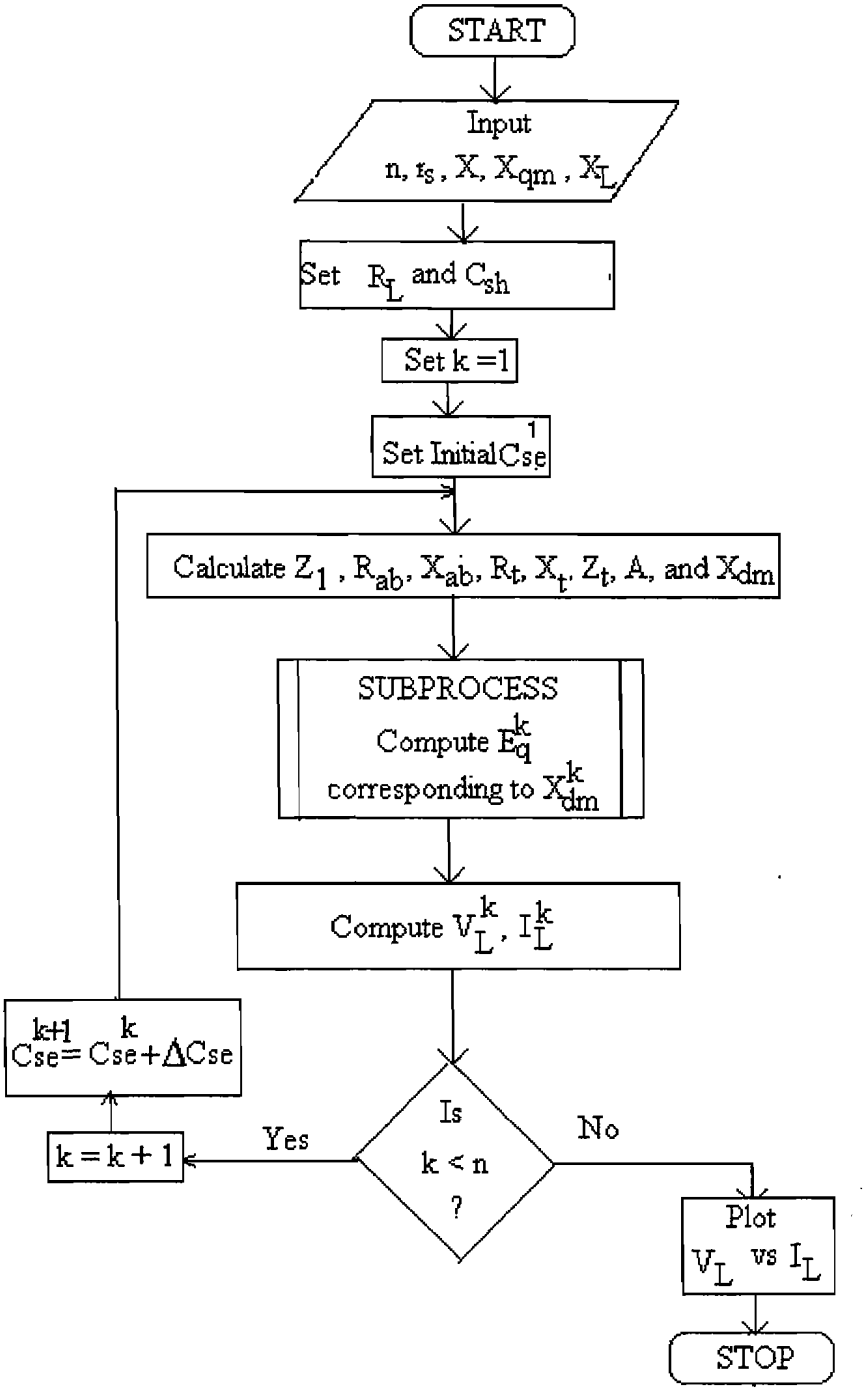

Fig.3.20 Flowchart for Plot of V_L, vs. I_L while C_{se} is varying

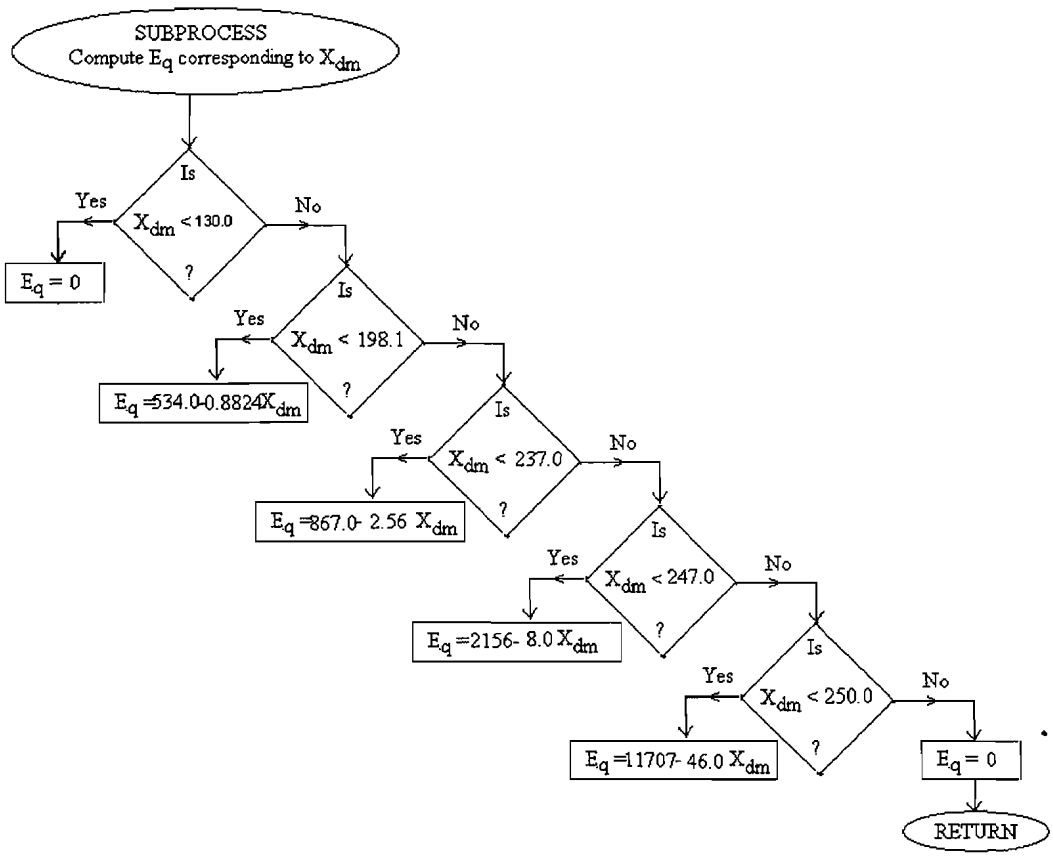

Fig.3.21 Flowchart for computation of Eq

DESIGN AND FABRICATION OF AXIALLY LAMINATED ANISOTROPIC ROTOR

Chapter -4

DESIGN AND FABRICATION OF AXIALLY LAMINATED ANISOTROPIC ROTOR

The performance of axially laminated anisotropic synchronous reluctance machine is very much dependent upon its saliency ratio. A simple calculation based on the ideal flux paths is used to estimate the theoretical limits of saliency ratio. A simple analytical method has been presented to determine the saliency ratio of axially laminated anisotropic rotor in terms of machine design parameters.

4.1 SIMPLE ESTIMATE OF MAXIMUM SALIENCY RATIO:

The ideal rotor is one which is infinitely permeable along the flux lines and completely impermeable across them. This would require a hypothetical anisotropic material whose permeability was not only directional but also followed a pattern corresponding to natural shape of the flux lines. Approximately this shape of rotor is obtained by fabricating axially laminated rotor of anisotropic magnetic material. The achievable saliency ratio (ξ) is limited by three factors given below:

(i) The q-axis permeance can not be zero and

(ii) The laminations are subjected to saturation in the axis.

(iii) If the laminations are too thick they can short circuit the stator slot opening. However, this factor has lesser importance.

Assume that the laminations and flux barriers are everywhere very thin and let t be the average ratio of flux barrier thickness to the combined thickness of lamination and flux barrier. Then *1/ (1-t)* is a measure of the flux concentration that occurs in the laminations owing to the loss of effective *d-* axis pole arc to the flux barriers. For a peak air gap flux density of 0.8T and a saturation density of around 1.7T, t must be limited to order of 0.5 [18]. Now the synchronous reactance x_d is inversely proportional to the airgap length g and x_q is inversely proportional to the sum of g and combined thickness of the flux barriers, which is of the order of tR, where R is the rotor radius. Therefore the saliency ratio is given approximately by,

$$\xi = \frac{x_d}{x_q} = \frac{(tR+g)}{g} = \frac{tR}{g} + 1 \qquad \text{-------- (4.1)}$$

With t=0.5 and R/g=typically 100, this indicates a maximum unsaturated saliency ratio of about 50 which is even larger than Kostko[47] prediction of 25. This simple theory explains the limitation due to finite q-axis permeance limiting factor (i) as discussed earlier but limitation due to the other two factors are more difficult to estimate. The unsaturated figure of 50 is a yardstick against which practical design of axially laminated anisotropic rotor can be evaluated. To evaluate the saliency ratio of axially laminated anisotropic (ALA) rotor accurately an analytical method has been presented in next section.

ESIGN OF ALA ROTOR:

A design for axially laminated anisotropic rotor is elaborated in this section. The structure consists of laminations of magnetic steel interleaved with non-magnetic material of approximately the same thickness, which is formed to make poles as shown in Fig. 4.1. Where ε is rotor position in mechanical radians and β is rotor angle in mechanical radians.

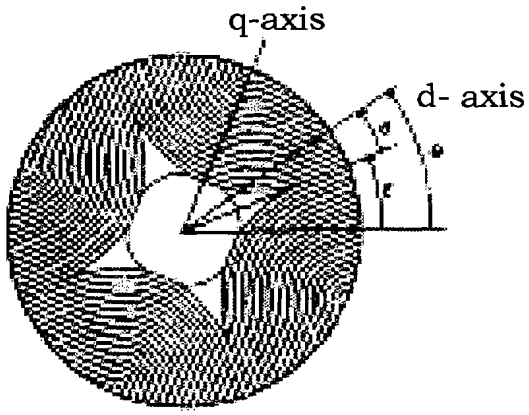

Fig.4.1 Direct and quadrature axis with rotor in arbitrary position

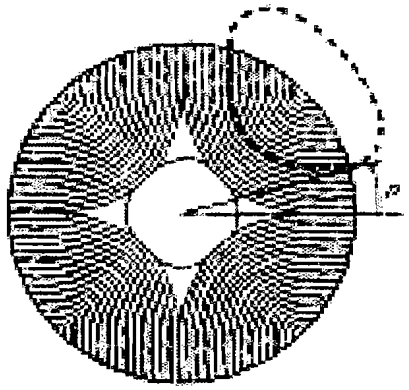

Fig.4.2 Flux path along laminations

The design allows low reluctance paths to flux from any point in the airgap parallel to the direct axis and high reluctance paths to flux parallel to the quadrature axis. Assuming the air /iron ratio in the rotor is approximately the same as the slot/tooth ratio in the stator, flux densities will be similar in both areas. Apart from the curved sections in the interior of the rotor, the laminations are straight and parallel to the direct axes. Thus, the greatest possible cross sections of iron and nonmagnetic material are obtained. Since the cross section of the iron is fixed by the air gap flux density, it allows maximum cross section of non magnetic material, which ensures the maximum reluctance in the quadrature axis and the minimum quadrature magnetizing inductance L_{mq}.

Assuming an ideal winding and phase 1 is stationed at θ=0, then the current density due to the three phase current is expressed as

$$i_d \sin(p\beta) - i_q \cos(p\beta) \qquad \text{-------- (4.2)}$$

Where p is the number of pole pairs.

The phase currents will set up two sets of fluxes in the airgap. The first will be the direct axis flux, which is computed from flux density B_d, which will be symmetrical about the direct axes. The second will be the quadrature axis flux, which is computed from flux density B_q and is symmetrical about the quadrature axes. Fig. 4.1 shows these axes for a four pole machine. Symmetry about the axes gives the following relationships:

$$B_d(\beta) = B_d(-\beta) = -B_d\left(\frac{\pi}{4} - \beta\right)$$
$$B_q(\beta) = -B_q(-\beta) = B_q\left(\frac{\pi}{4} - \beta\right). \qquad \text{--------- (4.3)}$$

The mmf equation may be written for the closed loop indicated in Fig. (4.2) assuming iron of infinite permeability.

$$\frac{N}{2}\int_{\varepsilon+\beta}^{\varepsilon+\frac{\pi}{4}-\beta} i_d \sin(p\theta - p\varepsilon) - i_q \cos(p\theta - p\varepsilon) d\theta$$
$$= \frac{g}{\mu_0}\left[B_d(\beta) + B_q(\beta) - B_d\left(\frac{\pi}{4} - \beta\right) - B_q\left(\frac{\pi}{p} - \beta\right)\right]$$
$$= \frac{2g}{\mu_0} B_d(\beta)$$

---------- (4.4)

In order to compute the flux crossing the laminations, it is necessary to consider conditions within the laminations. Both the laminations and the interleaved, nonmagnetic material are of uniform thickness t_t and t_a, respectively. Because of the assumed infinite permeability of the iron and the thickness of the nonmagnetic sections, flux density across each section will be uniform but need not to be the same in all sections. The mmf available to drive flux across the laminations depends on the circumferential section of airgap taken up by the laminations under consideration. Fig.(4.2) shows that a small circumferential section covers a section of laminations of depth. Of this depth, the fraction t_a/t_a+t_l is nonmagnetic. The flux density across this section is given by the mmf equation around the incremental flux path shown in Fig.4.1 that gives $\theta = \varepsilon + \beta$ and $d\theta = d\beta$ for any fixed rotor position. Then

$$\frac{N}{2}\left[i_d \sin(p\beta) - i_q \cos(p\beta)\right]d\beta$$

$$= \frac{g}{\mu_0}\left[B_d(\beta,\varepsilon) + B_q(\beta,\varepsilon) - B_d(\beta+d\beta,\varepsilon) - B_q(\beta+d\beta,\varepsilon)\right] + \frac{a}{\mu_0} B_a \cos(\beta) d\beta$$

---------- (4.5)

Where, N = Equivalent number of turns per phase.

A small section of rotor laminations reaching the rotor surface at angles β and $\pi/p - \beta$ covers a circumferential distance of $rd\beta$ at the air gap. It consists of two straight sections and one circular section. Its length s, is given by

$$S = \gamma_{arc.}\, \Gamma_c$$
$$= \frac{\pi^2 r(p-1)}{2p^2}\left(1 - \frac{2p\beta}{\pi}\right)$$

---------- (4.6)

Continuity of flux must be preserved in this volume, giving

$$S\left[\; B_a(\beta + d\beta) - B_a(\beta) \;\right] - r\left[B_d(\beta) + B_q(\beta) + B_d\left(\frac{\pi}{p} - \beta\right) + B_q\left(\frac{\pi}{p} - \beta\right)\right] d\beta = 0$$

---------- (4.7)

Solving two equations (4.3) and (4.5) gives the following expression (as described in Appendix-2,

$$B_q(\beta) = B_{q0} \sin(p\beta) \qquad \text{---------- (4.8)}$$

where $$B_{q0} = \frac{\pi^2 (p-1)\mu_0 N i_q}{16pa + 2\pi^2 p(p-1)g}$$

Flux density in the airgap is expressed as

$$B = B_{d0} \cos\left(p\theta - p\varepsilon\right) + B_{q0} \sin\left(p\theta - p\varepsilon\right)$$

---------- (4.9)

For single turn, centered on θ_1, the flux linkage is

$$\int_{\theta_1-\frac{\pi}{2p}}^{\theta_1+\frac{\pi}{2p}} BLr\,d\theta$$

$$= \frac{2Lr}{p}\left[B_{do}\cos(p\theta_1 - p\varepsilon) + B_{q0}\sin(p\theta - p\varepsilon)\right]$$

---------- (4.10)

Where L = Stack length and r = radius of the air gap.

The flux linkage for the phases obtained by multiplying the turns per phase in the above expression is given by

$$\lambda_{phase} = \frac{2}{3}L_{md}i_d\cos(\gamma - p\varepsilon) + L_{mq}i_q\sin(\gamma - p\varepsilon)$$

where,

$L_{md} = \dfrac{3\mu_0 N^2 Lr}{2p^2 g}$ = magnetizing inductance along d- axis

---------- (4.11)

$L_{mq} = \dfrac{3\pi^2(p-1)\mu_0 N^2 Lr}{16p^2 a + 2\pi^2 p^2 (p-1)g}$ = magnetizing inductance along d-axis

---------- (4.12)

$a = r\, t_a/(t_a + t_l)$ ----------(4.13)

and, γ is taken as 0, 2Π/3 and 4Π/3 for the first, second, and third phases respectively.

4.3 FABRICATION OF ALA ROTOR:

Steps for the fabrication of prototype axially laminated anisotropic synchronous reluctance rotor include:

- Selection of raw material.
- Processing of raw material.
- Finishing for getting cylindrical rotor.

Mild steel is utilized for fabrication of shaft of SERG. The selection is based on the criteria of both strength and economy. The selection of copper and aluminum might be a better option because of their magnetic properties, but due to difficulty of getting the material in proper dimensions and because of its relatively high cost, this is usually not preferable. The copper is diamagnetic ($\mu<1$) and aluminum is paramagnetic ($\mu>1$) while steel, iron are ferromagnetic ($\mu>>1$). The cold rolled grain oriented transformer lamination sheet steel (flux density 1.6 Wb/m^2) of 0.2 mm thickness has been used for the construction of rotor. For the insulation layer between laminations milo paper of thickness 0.25 mm was used. The nonmagnetic, nonconductive Bakelite was used as the rotor pole holder due to its good mechanical and thermal properties. Four bolts of 8.5 cm were used to firmly clamp lamination and insulation layers between pole holder and shaft. Eraldite and M-seal were used for primary fixing of lamination and insulation layers. Glass sleeves were used to isolate bolts from laminations.

First of all shaft of steel was fabricated according to the motor frame and ball bearing dimensions. Then semicircular slots on cylindrical shaft were prepared by milling operation for the lamination and insulation layer to be placed there. On these processed surfaces, two holes per pair of phases were bored between diagonally opposite faces. The clamping of lamination and insulation layers through bolts between pole holders through the holes bored on shaft is essential for

mechanical integrity of the rotor. The laminations were prepared in size of 7x11cm^2 and thickness 0.2 mm. The holes were made on laminations with the help of a punching machine. The milo insulation layer of same size and thickness (0.25 mm) was inserted alternately with the laminaions in formation of poles.

After the clamping of lamination and insulation layers tightly between the pole holders, heated eraldite solution was used thoroughly to paste the rotor, so that laminations and bakelite get additional support against cutting tool during machining and laminations do not get twisted or the pole holder may not get damaged. By machining the rotor on the Lathe machine the smooth cylindrical rotor of diameter 8 cm and length 11 cm was obtained. An air gap of 0.25 mm was obtained between rotor and stator surface.

The isometric view of fabricated axially laminated anisotropic rotor has been shown in Fig 4.3. Fig.4.4 shows shaft; fabricated for ALA rotor with front, side and isometric views. The sectional view of axially laminated anisotropic synchronous reluctance rotor with bolt, shaft, pole holder, laminations and insulation layers has been shown in Fig.4.5.

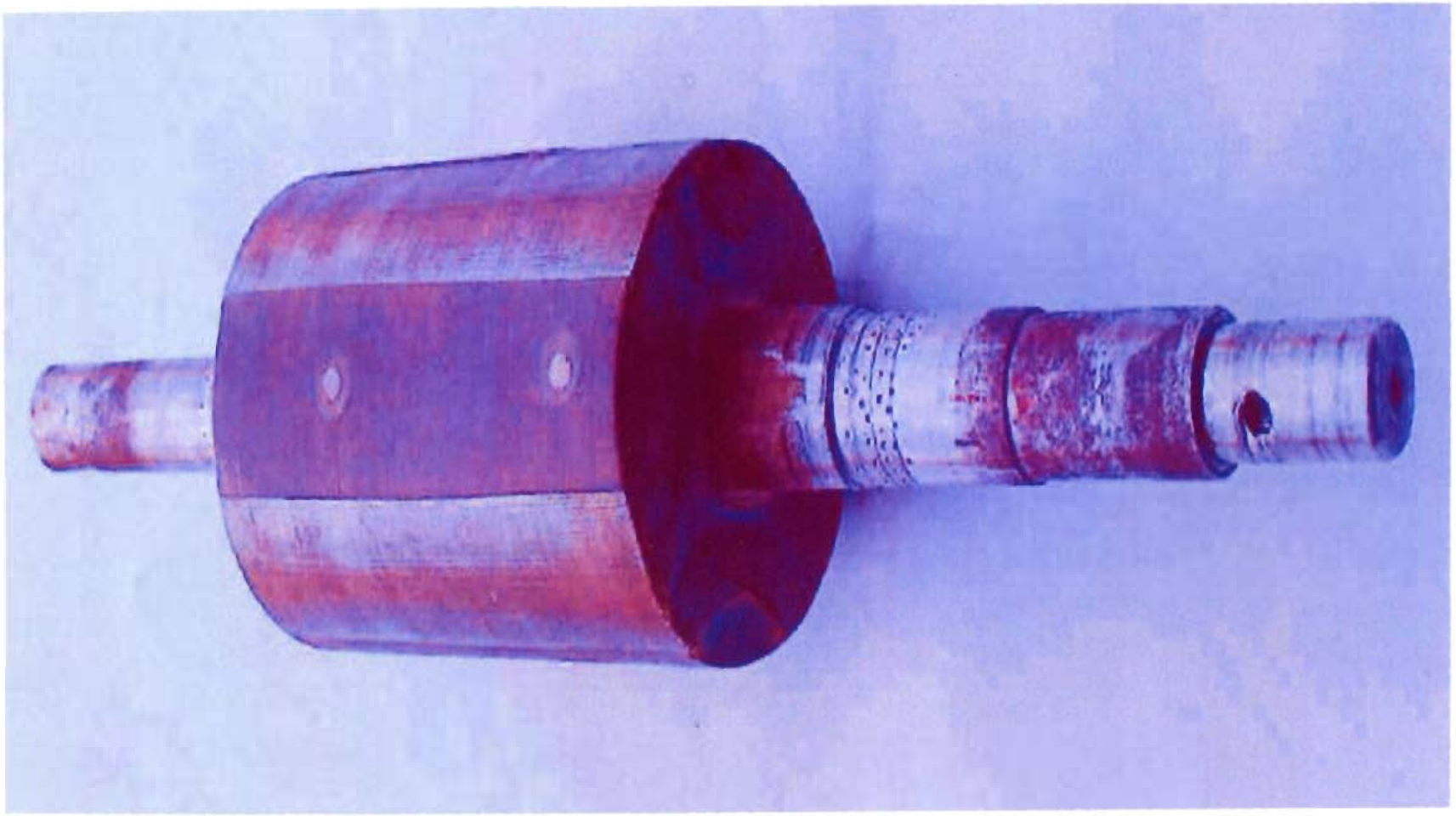

Fig.4.3 Fabricated 4-poles axially laminated anisotropic rotor

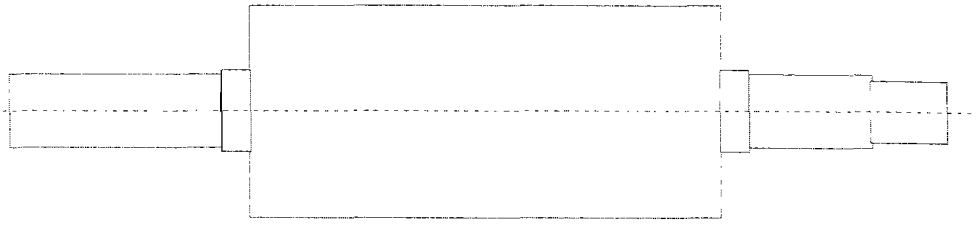

Front view

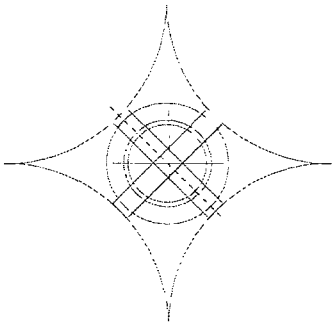

Side view

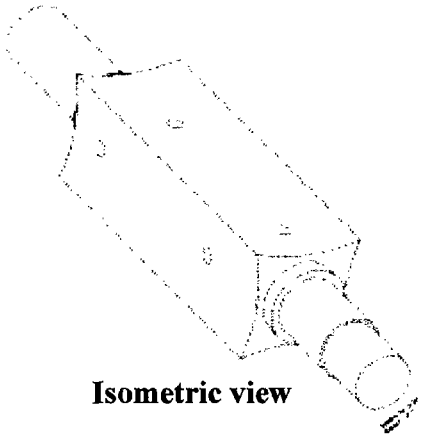

Isometric view

Fig.4.4 Fabricated rotor shaft

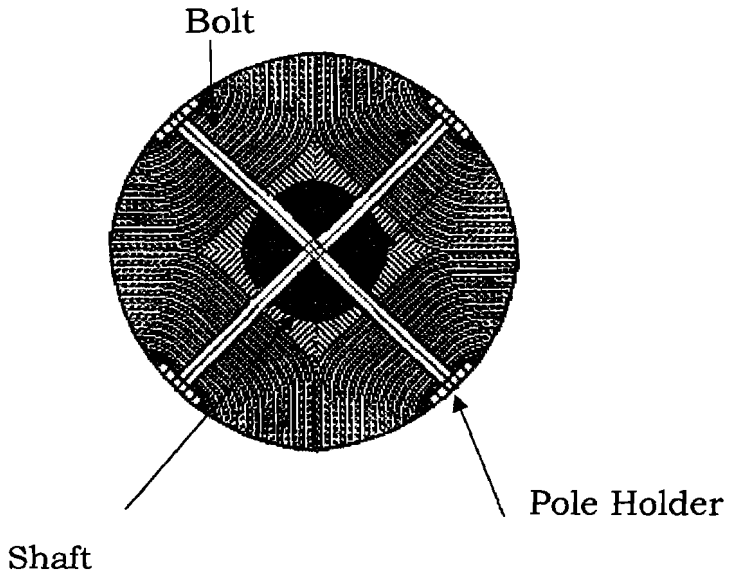

Fig.4.5 Sectional view of axially laminated anisotropic rotor

4.3 COMPARISON WITH INDUCTION MACHINE:

The Power available from a rotating electrical machine depends on the dimensions of the airgap, the airgap flux density, and the allowable stator current loading and speed. If the bore diameter is D m ,length of machine is L m, peak values of the last two quantities are B_m Wb/m^2 and ac_m A/m sinusoidally distributed and their peaks coincides, then the optimum power [33] is expressed as

$$P_{max} = \frac{1}{4}\pi^2 D^2 L \omega B_m ac_m \text{ Watts} \qquad \text{---------- (4.14)}$$

The peak values of airgap flux density and peak current loading in the reluctance machine is expressed by(Appendix-2)

$$B_m = \frac{8pL_d i_d}{3\pi NLD}\sqrt{1+\frac{L_q^2 i_q^2}{L_d^2 i_d^2}}$$

$$ac_m = \frac{Ni_q}{D}\sqrt{1+\frac{i_d^2}{i_q^2}} \qquad \text{---------- (4.15)}$$

The power in terms of machine parameters, current variable and maximum power for synchronous reluctance machine is given by combining (4.14) and(4.15)

$$P_{SRM} = P_{max}\frac{1-\frac{L_{mq}}{L_{md}}}{\sqrt{\left(1+\frac{i_d^2}{i_q^2}\right)\left(1+\frac{L_{mq}^2 i_q^2}{L_{md}^2 i_d^2}\right)}}$$

---------- (4.16)

In case of reluctance machine with ideal rotor, $L_{mq} \to 0$ and $L_{md} \to \infty$, then $P=P_{max}$, that is the limiting power is as high for this motor as for any motor with the same flux density and current loadings. An achievable ratio L_{mq}/L_{md} may be 0.05, and at full load, the ratio i_d/i_q should be no more than about 0.4 then

$P_{SRM}=0.88P_{max}$ ---------- (4.17)

By way of comparison, it is shown in the Appendix-3 that the torque available from the corresponding induction mahine is

$$P_{im} = P_{max}\sqrt{\frac{1-L_r^2/K^2L_m^2}{1+K^2+2L_r/L_m}} \qquad \text{---------- (4.18)}$$

where

L_r = Rotor leakage inductance

L_m = Magnetizing inductance (= L_{md})

K = Ratio of magnetizing current to load current.

In this case a realistic value for the ratio L_r / L_m may be 0.05 and at rated load, the value of K may be about 0.4, giving

$$P_{IM} = 0.88 P_{max} \qquad \text{---------- (4.19)}$$

From equations (4.17) and (4.19) it is clear that for the same frame power rating is same for both reluctance machine and induction machine. The saliency ratio suggested here is realistic. However, it appears that the reluctance machine may be capable of producing more power with an improved design of ALA rotor made up of materials having better anisotropic qualities.

4.4 EXPERIMENTAL SETUP & PARAMETER MEASURMENT:

To be able to judge the validity of the theoretical results obtained by the various performance equations outlined in the last chapter, number of experiments was conducted on the prototype synchronous reluctance machine developed in the laboratory. A standard stator frame of a three phase squirrel cage induction motor of ratings 1 KW 400/230 V, 50 Hz and 4-pole was employed for synchronous reluctance machine. The rotor of squirrel cage inductance motor was replaced by an axially laminated anisotropic rotor resulting an axially laminated anisotropic three phase synchronous reluctance machine. Its design and fabrication is already explained in sections 4.1 and 4.2. Basic data of this prototype has

been given in Appendix-1. The synchronous reluctance machine is driven by a DC shunt motor of 1kW, 240V. A three phase capacitor bank was connected to the reluctance machine terminals to obtain self excited generator action. Synchronous running test and ac standstill test has been conducted on the machine to measure the parameters of equivalent circuit. The tests are described below.

4.5.1 SYNCHRONOUS RUNNING TEST:

The machine inductances in the rotor reference frame, L_d and L_q are nonlinear function of direct axis current I_d and the quadrature axis current, I_q, respectively. The nonlinearity is mostly due to magnetic saturation. The magnetic saturation occurs mainly in direct axis. Therefore L_q can be assumed to be a constant. Moreover the quadrature axis current, I_q does not contribute to the magnetic saturation in the *d*-axis direction.

This test can be performed on the prototype synchronous reluctance machine (SRM) by running it at synchronous speed with the help of a dc shunt motor (1KW, 240V). Prototype SRM is connected to the power supply through a 3-phase autotransformer (3-phase, 50Hz, 400V, 3KVA) at the rated line voltage. The supply voltage is then gradually increased through auto transformer in steps of 20 volts. The supply current at each step was recorded by a digital ammeter. On no load the pole axes are practically coincident with the

direct axis. At synchronous running no load condition the direct and quadrature axis currents are [38]:

$$I_q = 0$$
$$I_d = I_{nl} = V/\sqrt{(X_d^2 + r_s^2)} \qquad \text{---------- (4.20)}$$

where V is the supply voltage and r_s is the stator resistance per phase.

The equation (4.20) provides a method to measure X_d,

$$X_d = \sqrt{((V / I_{nl}) - r_s^2)} \cong V / I_{nl} \qquad \text{---------- (4.21)}$$

where I_{nl} is the no load current.

4.5.2 AC STANDSTILL TEST:

The machine parameter consists of its self inductances, the mutual inductances, the stator winding resistances and the core loses. The stator winding resistance was measured by dc voltmeter-ammeter method. The resistance increases slightly with temperature rise. In the present work it is assumed that the core losses can be neglected without causing significant error in computation of the parameter. If the inductances vary sinusoidally with rotor position, they can be expressed as

$$L_{aa} = L_{sl} + L_{s2}\cos(2\theta)$$
$$L_{bb} = L_{sl} + L_{s2}\cos(2\theta + 2\pi/3)$$
$$L_{cc} = L_{sl} + L_{s2}\cos(2\theta - 2\pi/3)$$

$$L_{ab} = -L_{s0}/2 + L_{s2}\cos(2\theta - 2\pi/3)$$
$$L_{bc} = -L_{s0}/2 + L_{s2}\cos(2\theta) \qquad \text{---------- (4.22)}$$
$$L_{ca} = -L_{s0}/2 + L_{s2}\cos(2\theta + 2\pi/3)$$

Where L_{sl} is leakage inductance, L_{s0} is a constant magnetizing inductance and L_{s2} is the amplitude of the sinusoidally varying magnetizing inductance.

The relation between inductances in equation and the dq inductance in rotor reference frame is given by

$$L_d = L_{sl} + \frac{3}{2}(L_{s0} + L_{s2})$$
$$L_q = L_{sl} + \frac{3}{2}(L_{s0} - L_{s2}) \qquad \text{---------- (4.23)}$$

The inductances can be measured by a simple method. A single frequency voltage is applied at one of the phases. The supplied current and the voltage at the terminals of another phase are measured. The ratio of the voltage to the current is the mutual impedance between the two phases. L_{s0} and L_{s2} can be calculated from the measured values of mutual inductances at two different rotor angles [3]. The angle $\theta = 30^0$ and $\theta = -30^0$ (electrical angles) should preferably be selected, because it corresponds to extreme mutual inductances that can be easily recognized. If RMS measurements are carried out without phase differences consideration, the two extreme values will appear as two maximum values and the sign of one of them must be inverted.

To measure the leakage inductances, an AC single frequency test can be performed to measure the self inductance of one of the phases. If the rotor is aligned with that phase, $(L_{s0}+L_{s2})$ should be subtracted from the self inductance value to obtain the leakage inductance. Once the leakage inductance and the magnetizing inductance are determined, the direct and quadrature axis inductances can be calculated. These measurements are more difficult in the presence of magnetic saturation. However, the magnetic saturation is less important in the operation of the variable reluctance machine as a motor.

The ac stator winding resistance is determined by dc voltmeter-ammeter method and the ac resistance is by multiplying it with a factor of 1.2. From equation (4.22) and (4.23) the leakage reactance, saliency ratio, direct and quadrature axis inductance can be evaluated.

RESULT AND DISCUSSION

Chapter -5

RESULTS AND DISCUSSION

This chapter is devoted to results of tests conducted on the prototype synchronous reluctance machine fitted with axially laminated anisotropic rotor and acting as a self excited synchronous reluctance generator. Design and fabrication of axially laminated anisotropic rotor has been presented in last chapter. Enough information of steady state performance as well as transient like voltage build-up process exists for an axially laminated anisotropic rotor self excited reluctance generator is not available. Therefore, it is very important to simulate the steady state performance and voltage build-up process for the prototype self excited reluctance generator. Experimental results have been compared with digitally simulated results. Voltage regulation improvement using short shunt compensation has also been presented. For simulation of performance, parameters of the synchronous reluctance machine have been determined by laboratory tests as explained in previous chapter. Flowcharts for steady state performance and voltage build-up have already been given in last chapter 3 (Figs 3.17 and 3.21).

To determine the leakage inductance, saliency ratio, direct and quadrature axis inductance of the 3-phase, 50 Hz, 4 pole, 400 V, 1 Kw reluctance machine, ac standstill test has been conducted as explained in section 4.5.2. The experimental data has been given in

Table 5.1 presented at the end of this chapter. The calculated values of these parameters have been shown in Table 5.2 presented at the end of this chapter. The computed values of direct axis, quadrature axis inductance and its saliency ratio are 0.793H, 0.190H and 4.174 respectively, neglecting saturation.

It is essential to know the magnetization curve of self excited reluctance generator (SERG) to simulate its performance. The nature of magnetization curve and value of excitation capacitance determine the generated emf in case of self excited ac generators.

5.1 MAGNETIZATION CURVE OF SERG:

Magnetization curve at synchronous speed is obtained by

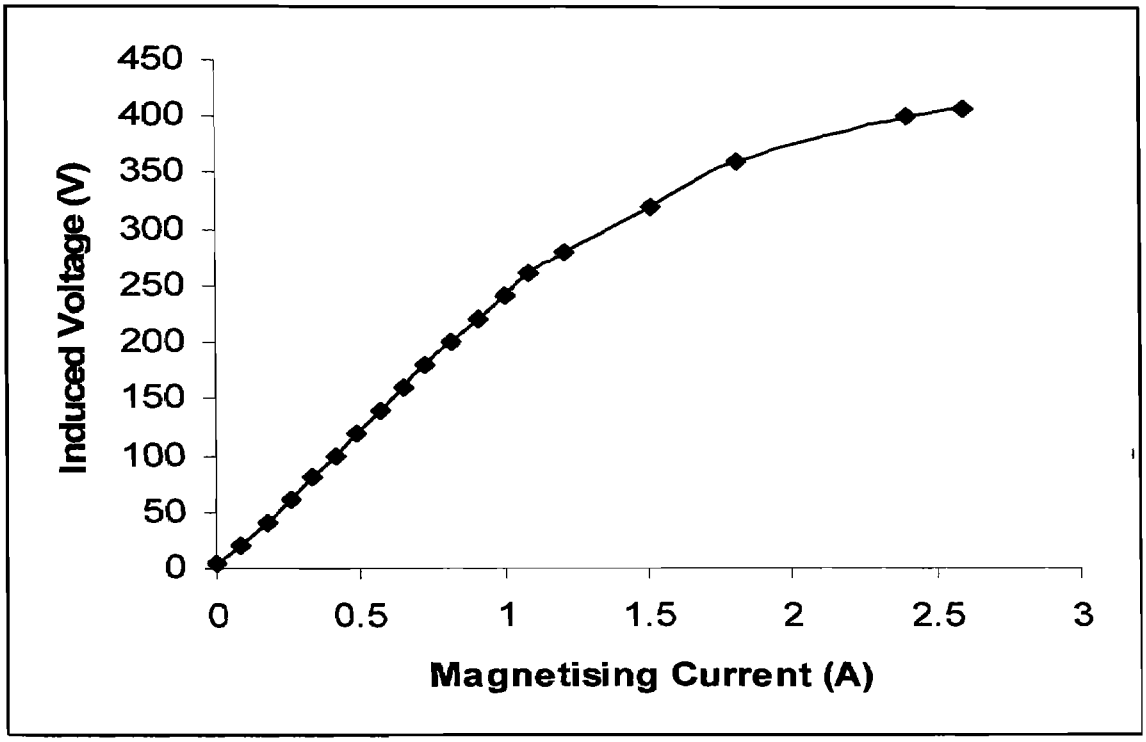

Fig.5.1 Magnetization curve of self excited reluctance generator

performing synchronous running test as explained in section 4.5.1. The data of this test has been given in Table 5.1 presented at the end of this chapter. Magnetization curve (induced voltage vs magnetizing current) has been shown in Fig.5.1. Under this operating condition the input current is assumed equal to direct axis current I_d.

It will be more appropriate to draw E_q versus X_{md} curve, X_{md} for any n^{th} experimental point will be given by,

$$x_{md}/_n = \frac{E_q/_n}{Id/_n}$$

The resulting curve is shown in Fig.5.2.

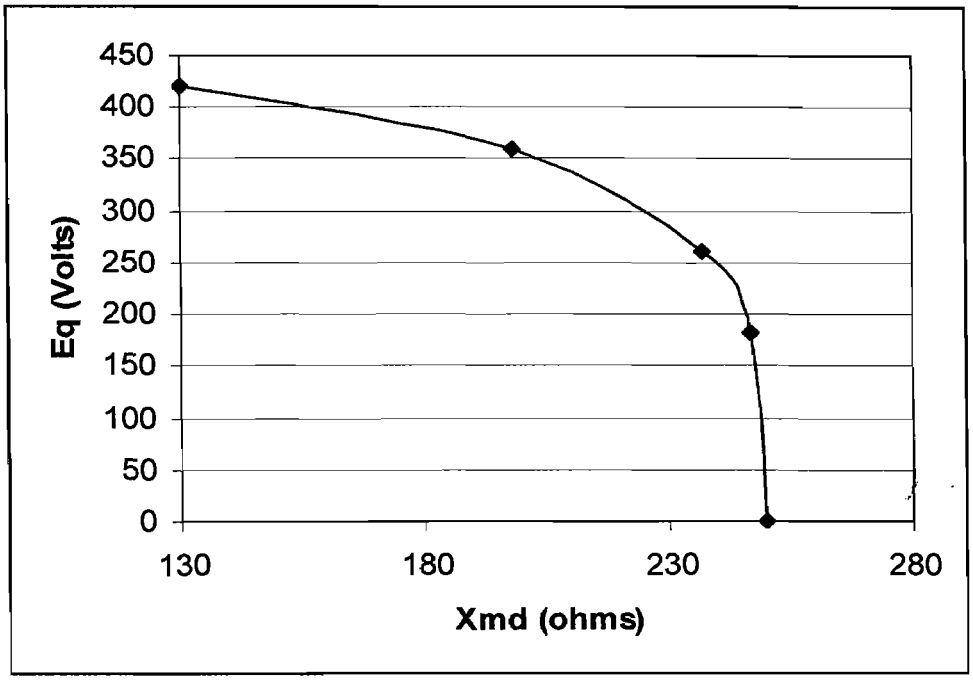

Fig 5.2 Induced voltage vs magnetizing reactance of SERG

The E_q versus X_{md} curve has been linearized using Excel program into five zones. The linear equation describing E_q in terms of X_{md}, for the five zones E_q are given by

$$E_q = \begin{cases} 534.7 - 0.8824\,X_{dm} & 130 < X_{dm} < 198 \\ 867.7 - 2564\,X_{dm} & 198 < X_{dm} < 237 \\ 2156 - 8X_{dm} & 237 < X_{dm} < 247 \\ 11707 - 46.665\,X_{dm} & 247 < X_{dm} < 250 \\ 0 & 250 < X_{dm} \end{cases}$$

5.2 EFFECT OF MAGNETIZING INDUCTANCE ON SELF EXCITATION:

In case of self-excited reluctance generator the variation of magnetizing inductance is the guiding factor for determining the dynamics of voltage build up and stabilization. If the unsaturated value of L_d is considered for determining the onset of self excitation, there will be an error. Using Fig.5.2, the magnetizing inductance L_d ($L_d = X_{md}/\omega$) versus E_q relation may be expressed using best curve fit method (curxpert software). The relation is expressed by fourth order polynomial given by

$$L_d = a_1.E_q^{\,4} + a_2.E_q^{\,3} + a_3.E_q^{\,2} + a_4.E_q + a$$

where a_1, a_2, a_3, a_4 and a are constants and E_q is the per phase voltage induced in stator winding of SERG. The values of the constants as obtained from computed results are:

$a_1 = -0.504759\times10^{-11}$; $a_2 = 04.28127\times10^{-8}$; $a_3 = -1.66997\times10^{-5}$;

$a_4 = 0.00284$; $a = 0.61852$;

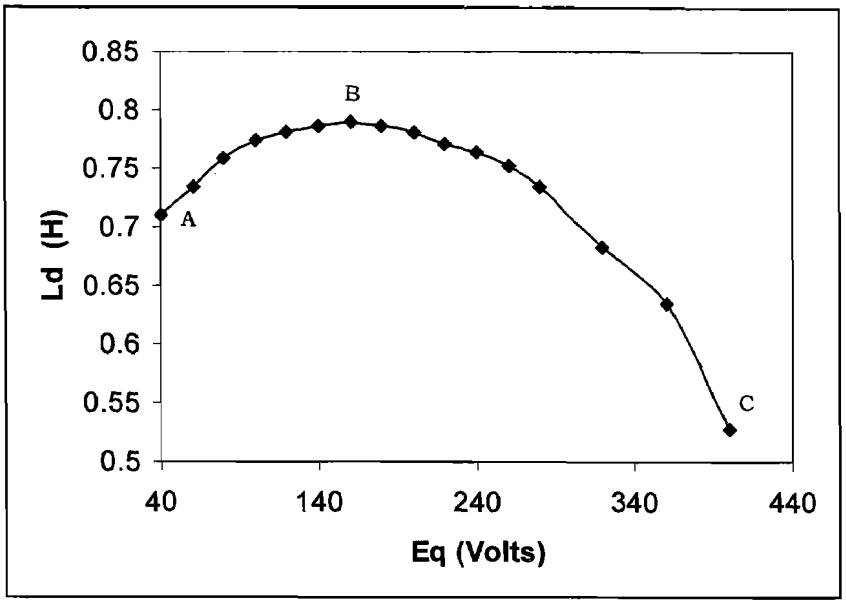

Fig.5.3 Induced emf vs. magnetizing inductance of SERG

Referring the Fig.5.3, L_d starts from a smaller value then increases to reach its peak value and finally starts to drop. At the start of self excitation point A, where the voltage is close to zero, L_d is close to 0.71H. Once self excitation starts the generated voltage will grow and then L_d also increases up to point B. Beyond point B, up to point C, L_d starts to decrease while the voltage continues to grow until it reaches its steady state value. Between point A and B is the unstable region. If the SERG starts to generate in this region, a small decrease in speed will cause a decrease in voltage and will bring a decrease in L_d which in turn decreases the voltage and finally the voltage will collapse to zero. The region between B and C is the stable region.

5.3 SIMULATION OF SERG GENERATED VOLTAGE:

Matlab environment has been used to predict the generated volage under no load condition of a three phase self excited reluctance generator rotating at a constant speed (1500rpm). Its stator terminals have been connected with appropriate capacitors bank. Once the voltage reaches its steady state value, load can be connected across the capacitors. The simulation was carried out by solving the set of first order differential equations for SERG as given in equation (3.28). Step by step solution of this model expressed in set of differential equation has already been shown in flowchart of section 3.5. The experimental and simulated transients volt-time characteristics of the machine during build up are shown in Fig.5.3 for an excitation capacitance 20μF. Fig.5.4 shows the corresponding characteristics for an excitation capacitance of 29μF.

5.4 STEADY STATE PERFORMANCE:

The prototype self excited reluctance generator was driven by a DC shunt motor (1kW, 230V) in laboratory. The terminals of the test machine were connected to a bank of three phase capacitors (400V 50Hz, 5 kVA in delta mode). The reluctance machine will build up the voltage for a given capacitance if the rotor speed reaches a critical speed, very similar to self excited induction generator. The no load generated voltage waveforms has been recorded for two values of

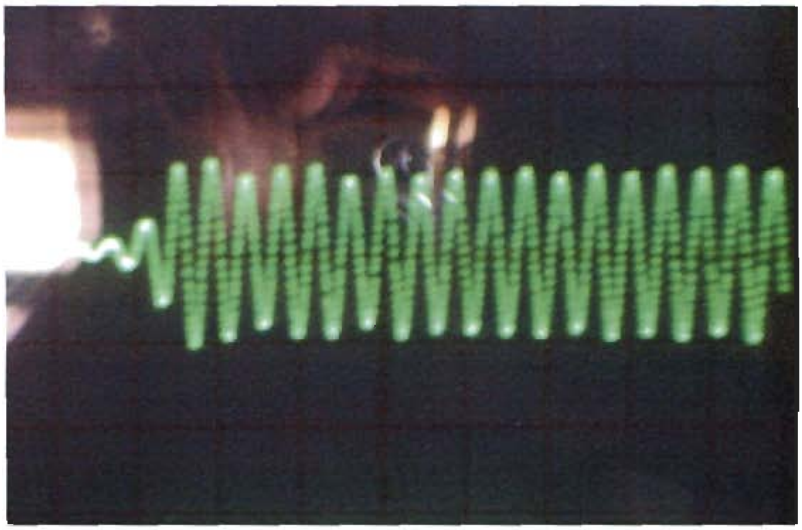

5V/DIV, X10 PROBE, POT.RATIO 1/10, 50 ms/div

(a)

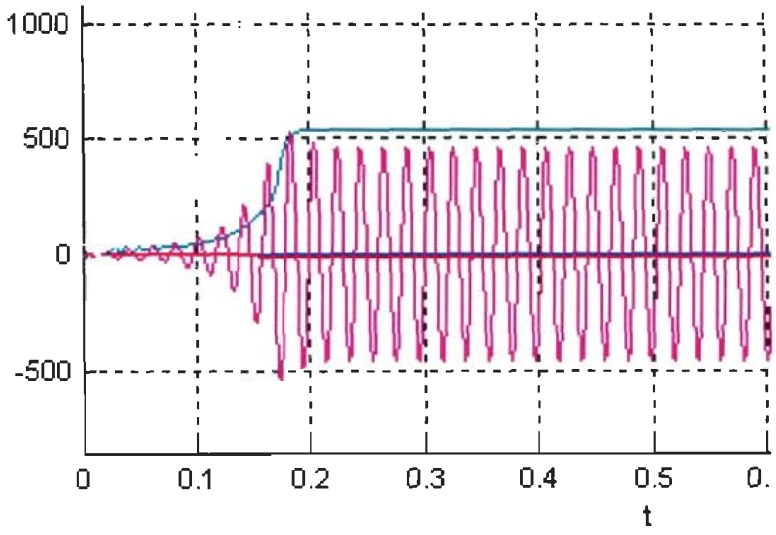

(b)

Fig.5.3 Transient responses of voltage build up at 1500 rpm and Csh= 20μF

(a) ---Experimental

(b) ---Simulated

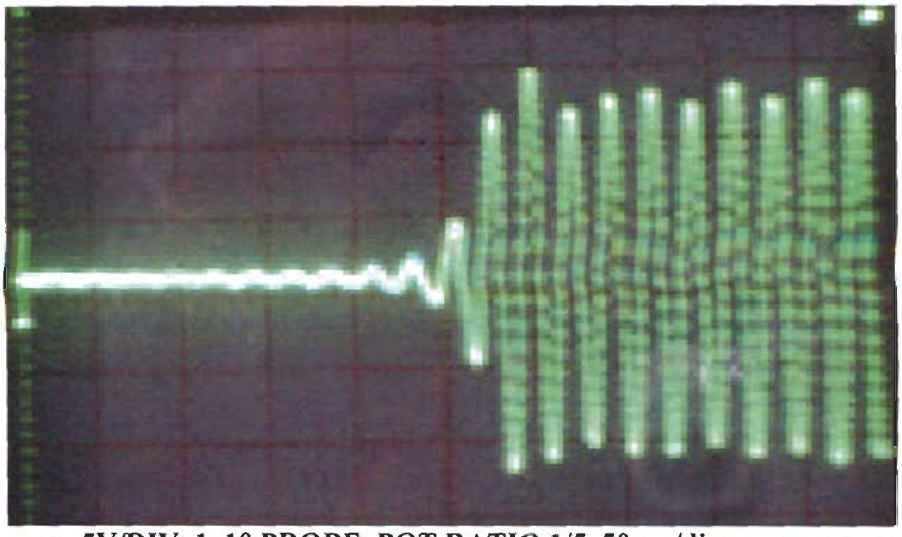

5V/DIV, 1x10 PROBE, POT.RATIO 1/5, 50 ms/div

(a)

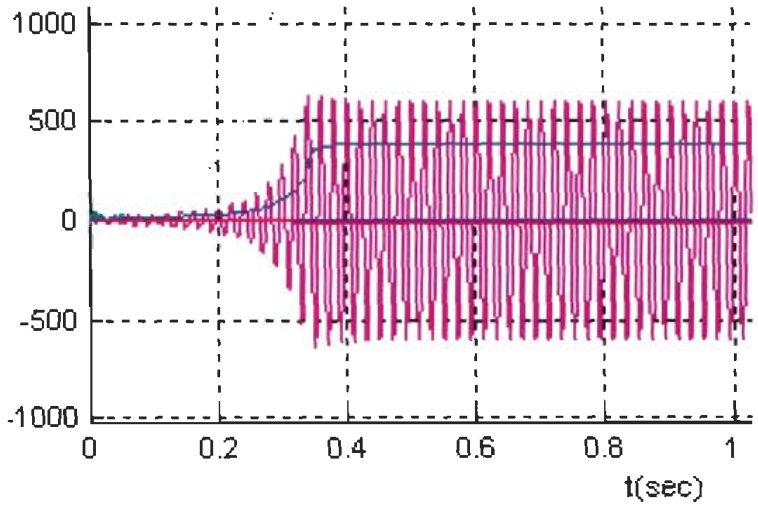

(b)

Fig.5.4 Transient responses of voltage build up at 1500 rpm and Csh= 29μF

(a)---Experimental

(b)---Simulated

capacitors i.e. 20 and 29 μFs at two different rotor speed 1200rpm and 1500rpm as shown in Figs. (5.5) and (5.6). At 1500rpm peak voltages were found to be 500V and 575V for 20 and 29 μFs respectively as shown in Figs. 5.5 & 5.6. When primemover speed was decreased to 1200rpm the recorded voltage reduced linearly in agreement with theoretical operation as shown in Figs. 5.7 & 5.8. The generated voltage waveform clearly indicated that the large harmonic content produced by the salient and segmental rotor especially the third harmonic [25] was appreciably reduced in case of axially laminated anisotropic rotor self excited synchronous reluctance generator.

The computed and experimental variation of no load terminal V_o voltage with shunt excitation capacitance C_{sh} is shown in Fig.5.9 at 1500rpm. It has been observed that voltage build up is not possible for a value of below C_{sh} 13μF.

Performance results have been also recorded for different excitation capacitances and load conditions. A three phase delta connected lamp load has been used to load the self excited reluctance generator for unity power factor variable load. The data has been given in Table5.4 and 5.5 presented at the end of this chapter . The final results have been shown in figures (5.9) to (5.14). It has been observed that the induced voltage increases with excitation capacitance. The terminal voltage drops with increased load current.

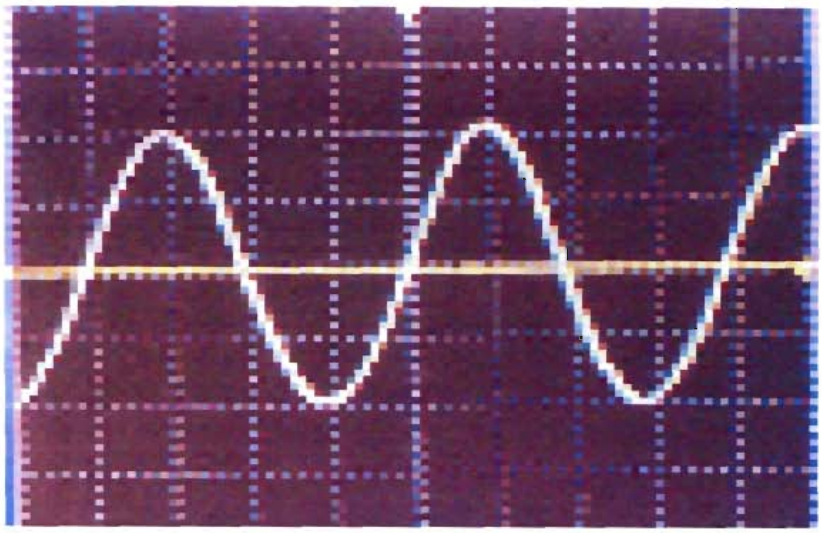

50v/div, 50ms/div, Pot. Ratio 1/5

Fig.5.5 Waveform of no load terminal voltage at 1500 rpm & C sh=20μF

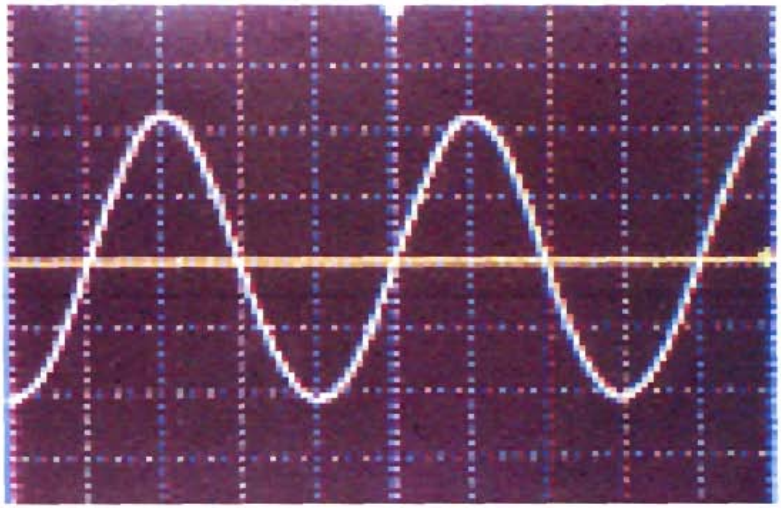

50v/div,50ms/div,Pot. Ratio 1/5

Fig.5.6 Waveform of no load terminal voltage at 1500 rpm and Csh=29μF

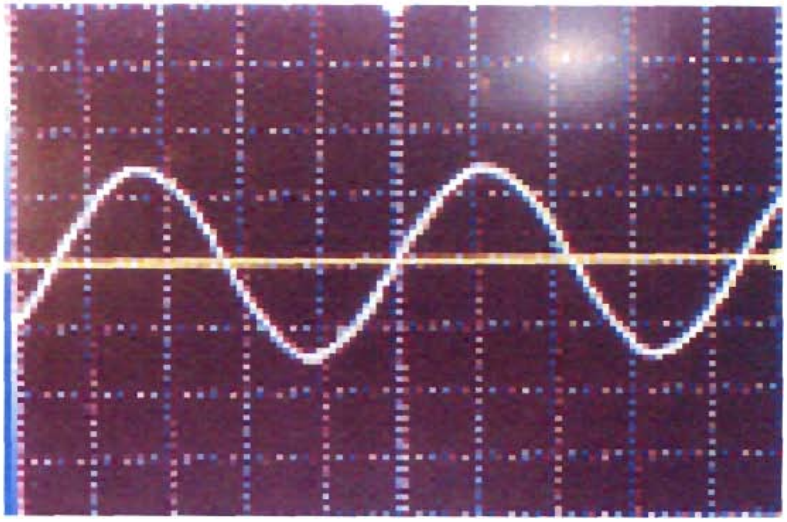

50v/div, 50ms/div, Pot. Ratio 1/5

Fig.5.7 Waveform of no load terminal voltage at 1200 rpm and Csh= 20μF

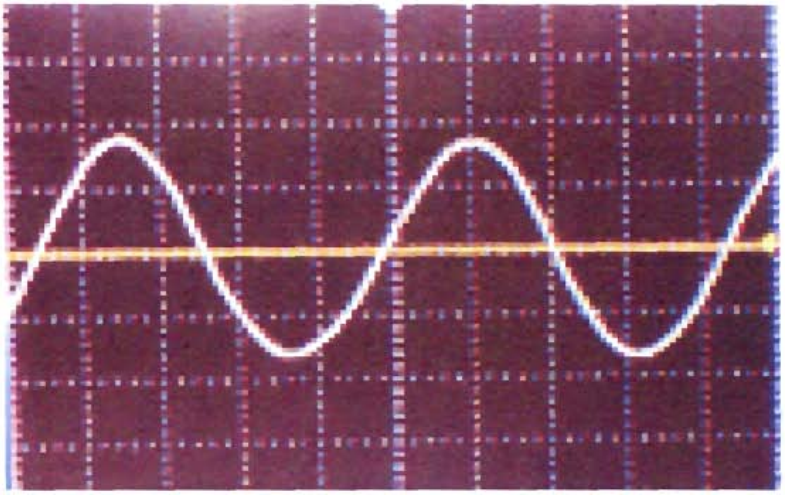

50v/div, 50ms/div, Pot. Ratio 1/5

Fig.5.8 Waveform of no load terminal voltage at 1200 rpm and Csh=29μF

The load characteristic collapses in a similar way to that of the DC shunt generator. The reason is simple: the fixed excitation capacitance is unable to provide sufficient magnetization above a certain loading. The generator currents are reduced (as an overload protection) when the SERG is short circuited (Fig.5.10). The output power can be increased at higher capacitance as observed in Fig.5.12. A close agreement between computational and experimental result has been found.

To overcome the problem of poor voltage regulation in case of self excited reluctance generator, inclusion of additional series capacitance to provide additional VAR with load is an attractive option. When the axially laminated anisotropic rotor SERG is operating under no load condition, there will not be any current through the series capacitor (C_{se}), and only the shunt capacitor (C_{sh}) will be effective in the circuit as shown in Fig.3.16. But when loaded, both shunt and series capacitors will be effective. Hence proper value of these element can be chosen by first studying the variation of of no load terminal voltage with C_{sh}. The variation of no load terminal voltage with shunt capacitance is shown in Fig.5.9 at 1500rpm. As a first approximation, a value 20μF for C_{sh} corresponding to no load terminal voltage equal to rated value has been considered. Fig.5.14 depicts the variation of full load voltage regulation with series capacitance obtained both experimentally and computationally. It reveals that there is a distinct

minimum value of voltage regulation for a certain value of Cse. This is the best value as far as the full load voltage regulation is concerned. The effect of Cse on load voltage is shown in Fig.5.13. It is observed that there is a rise in the terminal voltage with load which requires a protection against excessive overvoltage.

On the contrary rapid fall in the terminal voltage of SERG automatically provides a protection against overloading or short circuit. Further, a close agreement between computed and experimented results can be found.

It has been observed that the results obtained in case of voltage build-up process and steady state performance clearly indicating an alternative for self excited induction generator to supply electrical energy to remote and hilly region harnessing micro/small hydro potential.

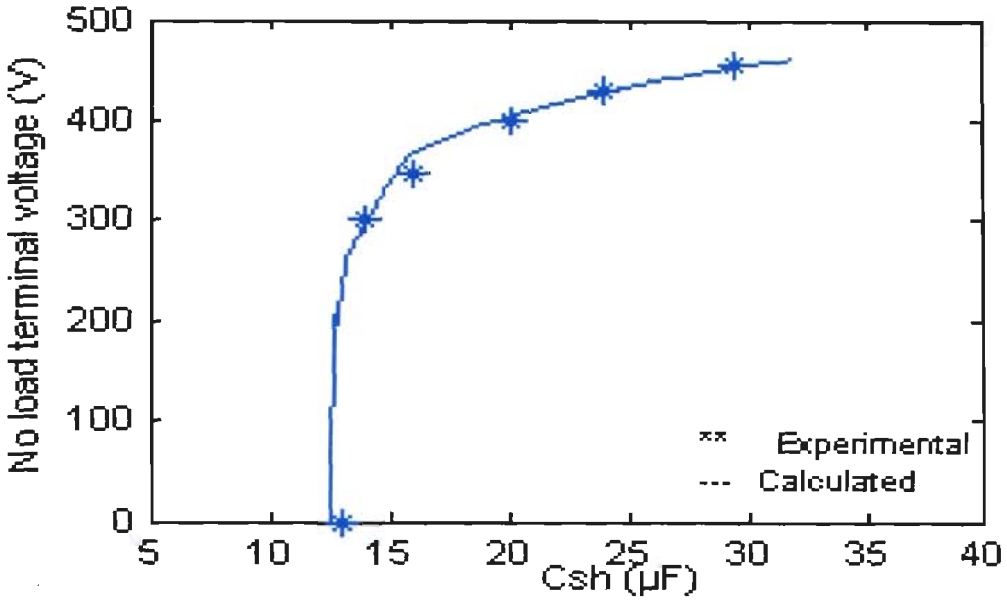

Fig.5.9 No load voltage vs excitation capacitance

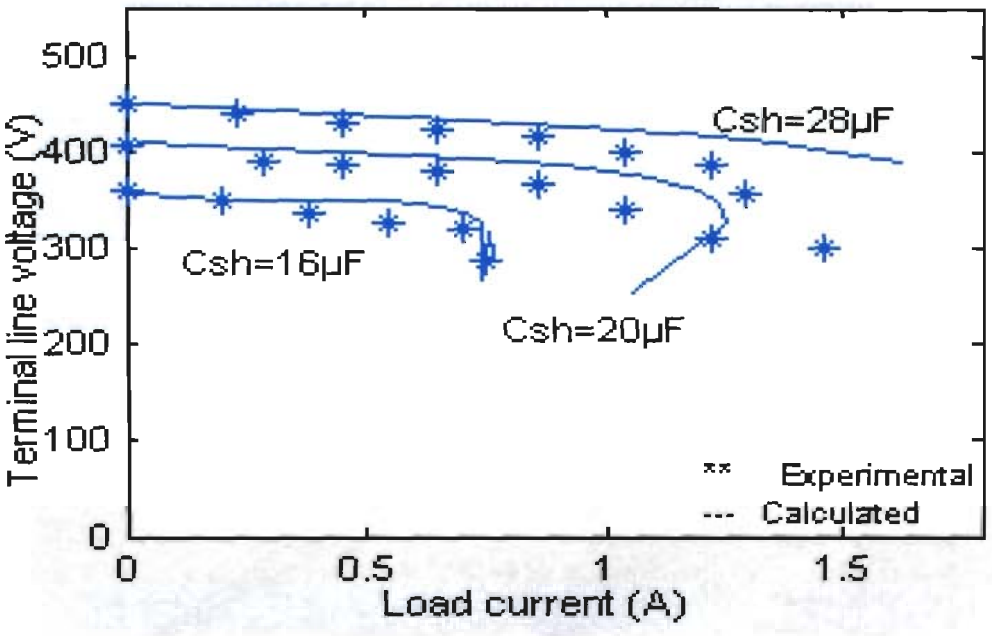

Fig.5.10 External characteristics of SERG

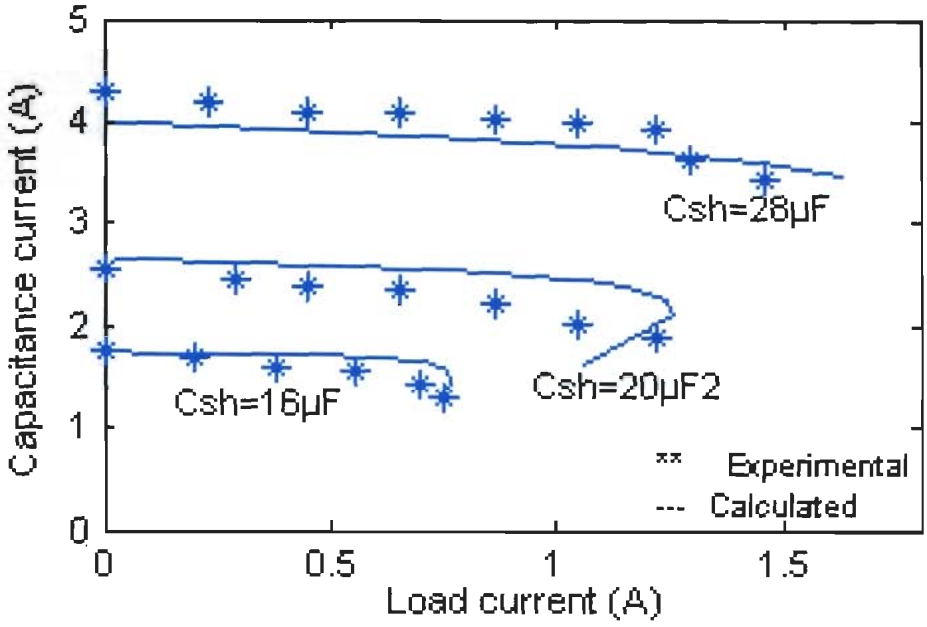

Fig.5.11 Capacitance current versus load current

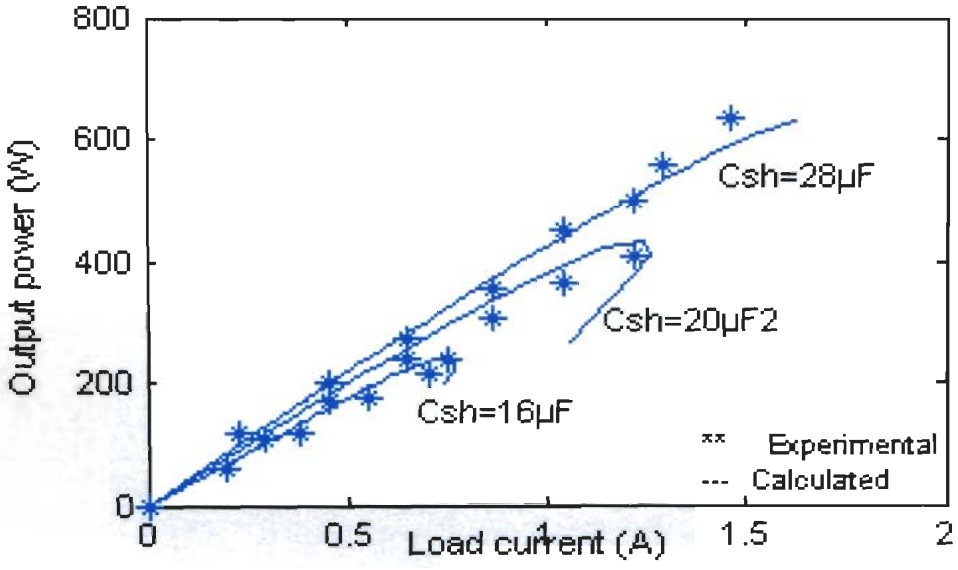

Fig.5.12 Output power versus load current

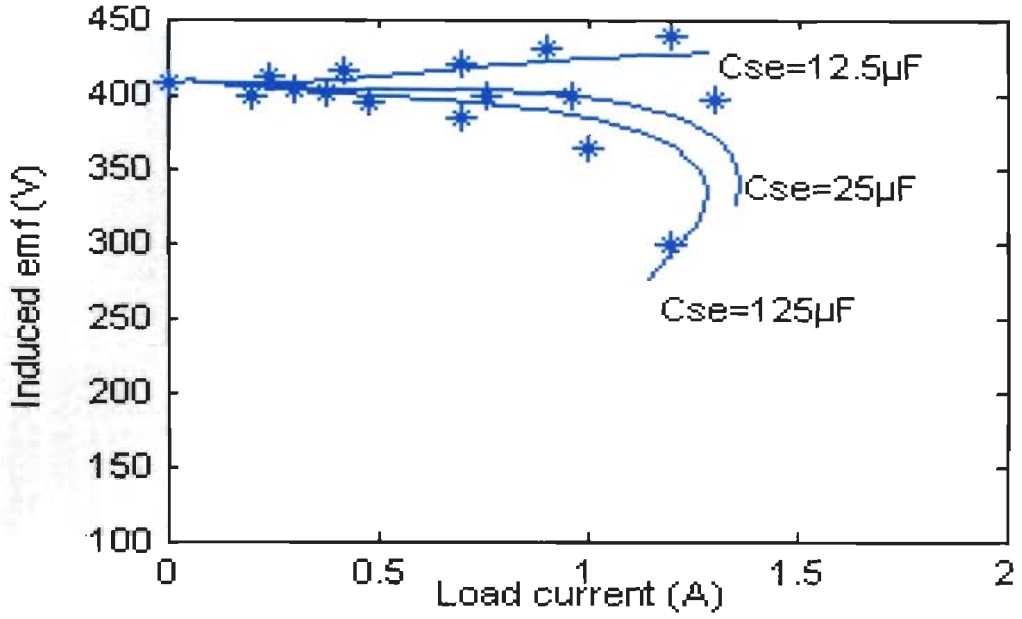

Fig.5.13 External characteristics with various C_{SE}

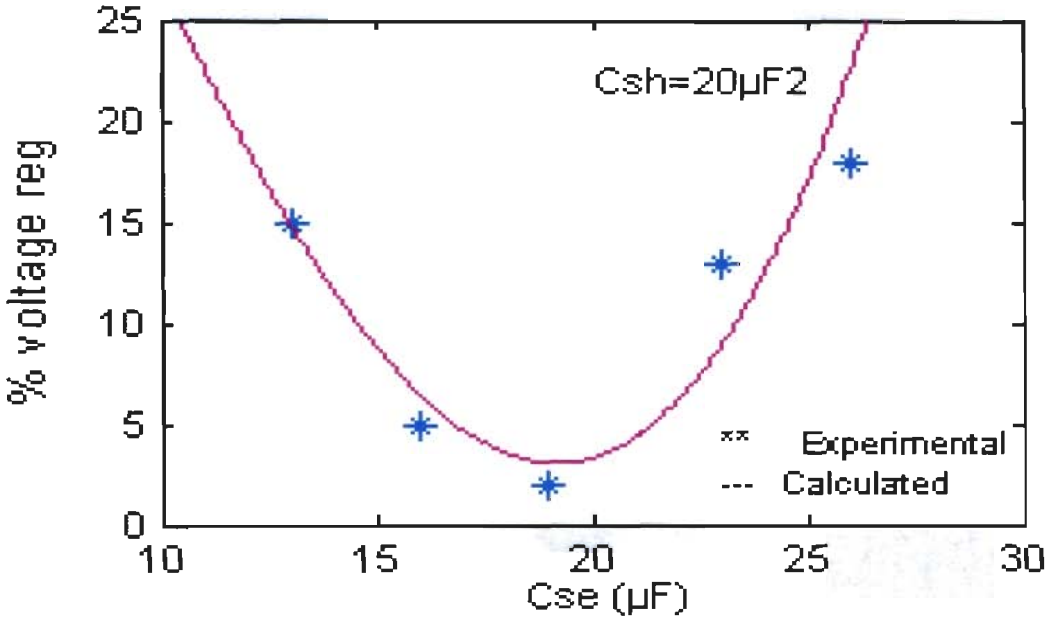

Fig.5.14 Percent voltage regulation with various C_{SE}

Synchronous Running Test:

Table (5.1)

Line voltage, V	Line current, A	Phase current, A	Direct Axis Reactance, ohm	Direct Axis Inductance, mH
40	0.31	0.179	222.874	0.710
60	0.45	0.260	230.343	0.734
80	0.58	0.335	238.326	0.759
100	0.71	0.410	243.385	0.775
120	0.85	0.491	243.960	0.777
140	0.98	0.566	246.878	0.786
160	1.13	0.652	244.683	0.779
180	1.26	0.727	246.878	0.786
200	1.41	0.814	245.119	0.781
220	1.57	0.906	242.139	0.771
240	1.73	0.999	239.710	0.763
260	1.89	1.091	237.693	0.757
280	2.1	1.212	230.343	0.734
320	2.61	1.507	211.711	0.674
360	3.13	1.807	198.523	0.632
400	4.16	2.402	165.719	0.528

Table (5.2)

Single phase ac stand still test for prototype synchronous reluctance machine

Applied voltage V	At electrical angle θ = 0°		At electrical angle θ = 90°		At electrical angle θ = 30°			At electrical angle θ = -30°		
	Minimum current A	Self inductance mH	Maximum current A	Self inductance mH	Minimum induced voltage V	Current A	Mutual inductance mH	Maximum induced voltage V	Current A	Mutual Inductance mH
20	0.11	0.579	0.49	0.130	0.49	0.16	0.010	14.8	0.17	0.277
40	0.23	0.554	0.98	0.130	1.01	0.33	0.010	29.9	0.33	0.289
60	0.34	0.562	1.47	0.130	1.51	0.50	0.010	44.2	0.48	0.293
80	0.44	0.579	1.95	0.131	2.03	0.64	0.010	60.0	0.63	0.303
100	0.54	0.590	2.39	0.133	2.47	0.78	0.010	75.9	0.79	0.306
120	0.67	0.570	2.94	0.130	2.89	0.91	0.010	90.7	0.95	0.304
140	0.78	0.572	3.22	0.138	3.16	1.01	0.010	103.7	1.09	0.303
160	0.89	0.573	3.72	0.137	3.35	1.09	0.010	122.7	1.31	0.298
180	1.01	0.568	4.3	0.133	3.60	1.12	0.010	134.0	1.44	0.296
200	1.13	0.564	4.75	0.134	3.73	1.20	0.010	147.5	1.62	0.290

Table (5.3)

Computed values of leakage inductance, saliency ratio, direct and quadrature axis inductance

Applied voltage, V	Ls2	Ls0	Lsl(1)	Lsl(2)	Llavg	Ld	Lq	Saliency ratio	Ld-Lq
20	0.178	0.198	0.203	0.149	0.176	0.740	0.205	3.804	0.535
40	0.186	0.205	0.163	0.149	0.156	0.743	0.185	4.009	0.558
60	0.189	0.208	0.165	0.149	0.157	0.753	0.186	4.054	0.567
80	0.195	0.216	0.168	0.151	0.159	0.776	0.190	4.092	0.586
100	0.197	0.217	0.175	0.153	0.164	0.786	0.195	4.143	0.592
120	0.196	0.216	0.158	0.150	0.154	0.772	0.185	4.285	0.588
140	0.195	0.215	0.161	0.158	0.160	0.776	0.190	4.099	0.586
160	0.192	0.212	0.168	0.157	0.162	0.769	0.192	4.009	0.577
180	0.191	0.211	0.166	0.154	0.160	0.763	0.190	4.005	0.572
200	0.187	0.207	0.170	0.154	0.162	0.752	0.192	3.919	0.560
Average value						0.783	0.191	4.176	0.572

Table (5.4)

No Load Test at 1500 rpm:

C_{sh} (μF)	13	16	20	24	29
No Load voltage (Volt)	0	348	400	430	455

Table (5.5)

Load Test at C_{sh} = 16μF

Output power, watts	Capacitive current, A	Load current, A	Load Voltage, volts
0	1.75	0	360
60	1.70	0.2	348
120	1.60	0.38	336
174	1.55	0.55	327
214	1.44	0.7	319
240	1.30	0.75	285

Table (5.6)

Load Test at C_{sh} = 20µF

Output power, watts	Capacitive current, A	Load current, A	Load Voltage, volts
0	2.55	0	405
110	2.46	0.29	390
170	2.38	0.45	385
238	2.35	0.65	378
304	2.22	0.86	365
364	2.02	1.04	340
406	1.88	1.22	310

Table (5.7)

Load Test at C_{sh} = 28.5µF

Output power, watts	Capacitive current, A	Load current, A	Load Voltage, volts
0	0.179	0	455
120	0.260	0.23	440
200	0.335	0.45	430
274	0.410	0.65	422
356	0.491	0.86	416
450	0.566	1.04	398
500	0.652	1.22	385
555	0.727	1.29	355
658	0.814	1.49	300

Table (5.8)

Terminal voltage at C_{sh} = 20μF

125 μF		24 μF		12.5 μF	
V1	IL1	V2	IL2	V3	IL3
407	0	407	0	407	0
400	0.2	404	0.3	412	0.24
395	0.48	402	0.38	415	0.42
384	0.7	400	0.76	420	0.7
363	1.0	399	0..96	430	0.9
300	1.2	397	1.3	438	1.2

SUMMARY AND CONCLUSION

Chapter -6

SUMMARY & CONCLUSION

For supply of electrical energy to local loads in hilly and remote areas utilizing small hydro power reserves, it will be necessary to have a standalone self exited ac generator. For a long time research workers toyed with the idea of utilizing an induction generator for this purpose. Synchronous reluctance generator appears to be a better option from the point of view of constancy of frequency, enhanced maximum power and better voltage regulation.

The present work has successfully demonstrated that a self excited three phase synchronous reluctance generator having axially laminated anisotropic rotor can replace the self excited induction generator. Therefore it may be possible to use such a generator to supply local loads using a low range hydro turbine at the small water reservoirs.

The moot point of designing a reluctance generator is the saliency ratio. Higher is the saliency ratio more will be the maximum power developed. Ideally a saliency ratio tending to infinity will give a maximum power which is equal to the optimum power that can be developed by the rotating electrical machine. To that end the use of axially laminated anisotropic rotor will be important.

In the present thesis a 3 phase, 4 pole, 50 Hz, 400 Volt & 1Kw synchronous reluctance machine having axially laminated anisotropic

rotor, has been designed and fabricated. The prototype machine has a saliency ratio of 4.2 as obtained from the test result. The machine has been used as a self excited generator by using a bank of three phase, delta connected, 5 KVA static capacitors.

The thesis has suggested a mathematical model for analyzing both steady state and transient performance. Park transformation has been used to obtain the equivalent circuits in the direct and quadrature axis. Saturation has been considered in the direct axis only. The axis parameters have been determined by simple laboratory test.

No load test and load test have been performed on the prototype machine in the laboratory. The no load test yields the voltage build up transient and steady state voltage reached for two values of shunt connected excitation capacitor. The transients have been recorded by Tektronix make [model no. TDS 2024] digital storage oscilloscope. Numerical analysis using Matlab environment has been carried out to get the computed transient characteristics. The experimental result and computed result compare favorably.

The external characteristic of the machine has been determined from load test for three values of the excitation capacitor. Computed characteristics match closely with those obtained experimentally. It has been found that like a dc shunt generator the output voltage beyond a certain load current collapses. This critical value is dependent on the magnitude of the excitation capacitance, increasing with the increase of capacitance. It has been found that

there is a critical value of excitation capacitance below which the voltage build up is not possible. Therefore, the maximum power output increases with the increase of excitation capacitance. However needless to mention that there will be a limit to the power output because of excessive capacitive current to be fed by the generator winding as indicated by the shunt excitation current vs load current characteristics.

The output voltage waveshape as recorded by the oscilloscope was almost sinusoidal containing negligible harmonics, particularly third harmonic. In literature [25] it has been reported that the reluctance generator having salient and segmental rotor structure developed voltages having much higher harmonic content.

The voltage regulation of the machine needs special attention. For the prototype machine experimental and computer results have indicated a voltage regulation in the range of 5% to 25% at full load. Better regulation is obtained with a higher value of excitation capacitance and conversely a poor voltage regulation results with a lower value of excitation capacitance. Voltage regulation can be further improved by inserting series capacitance in series with the load. However an optimum value of capacitor has to be chosen so that the output voltage remains within tolerable limits for both full load and lightly loaded conditions.

The frequency of generated voltage of the prototype reluctance generator running at a constant speed is independent of the load. For an induction generator the frequency varies with load requiring a

complicated and costly control circuit to overcome this problem. As there is no rotor winding rotor copper losses are absent in a reluctance machine, which is an advantage over an induction generator.

The findings of the present thesis indicate that the self excited reluctance generator having axially laminated anisotropic rotor will be a better choice as a standalone generator as compared to a self excited induction generator.

Further research work needs to be carried to include harmonics and saturation in quadrature axis in the mathematical model. Improvement of voltage regulation by series compensation and determining an optimum compensation should get a closer look.

REFERENCES

REFERENCES

1. **Guha, Souvik and Kar, N.C. 2005.** A linearized model of saturated self-excited synchronous reluctance generator, *Electrical and Computer Engineering, Canadian Conference,* May1-4, pp.333-336.

2. **D. Seyoum, C. Grantham, F. Rahman and M. Nagrial 2002.** An insight into the dynamics of loaded and free running isolated self-excited induction generator, IEE Conference on Power Electronics, Machines and Drives, Publication No.487, pp.580-585.

3. **Ben-Hail N. and Rabinovici R. 2001**. Three phase autonomous reluctance generator, *IEE Proc-Electric Power Application.* Vol.148 (5), pp. 438-442.

4. **Li Wang and L. Wang 2001.** Minimum loading resistance and its effects on performance of an isolated self-excited reluctance generator**,** *IEE Proc-Generation Transmission and Distribution,* Vol.148(3), pp.251-256.

5. **Li Wang and Yung-Shan Wang 2000.** Steady-state performance of a self-excited reluctance generator under unbalanced excitation capacitors, *IEEE Trans. on Energy Conversion,*

6. **Li Wang and Jian-Yi Su 1999.** Dynamic performance of an isolated self-excited induction generator under various loading conditions, *IEEE Trans. on Energy Conversion*, Vol. 14(1), pp.

7. **Chabu I. E., Silva V. C. and Foggia A. 1999.** A new design technique based on a suitable choice of rotor geometrical parameters to maximize torque and power factor in synchronous

reluctance motor. *IEEE Trans. on Energy Conversion.* Vol. pp. 599-609.

8. **Jovanovic, M. G. and Betz, R. E. 1999.** Off-line testing of synchronous reluctance machines. *IEEE Transaction on energy conversion.* Vol.14 (3), pp.264-269.

9. **I. E. Chabu, V.C. Silva, A. Foggia, J.R. Cardoso, and S.I. Nabeta 1999.** A new design technique based on a suitable choice of rotor geometrical parameters to maximize torque and power factor in synchronous reluctance motors: Part-1, *IEEE Transaction on Energy Conversion.* Vol.14 (3), pp.599-604.

10. **Li Wang and Yung-Shan Wang 1998.** Characteristics of a self excited reluctance generator as affected by sudden connection of an induction motor load, *IEEE Trans. on Energy Conversion*, pp. 605-609.

11. **D. Miljavec and P. Jereb 1996.** Can be synchronous reluctance motor compared with induction motor? *IEEE Trans. on Energy Conversion*, pp.317-321.

12. **Hippner M. and Harley R. G. 1996.** Design aspects of axially laminated synchronous reluctance motors. *IEEE Trans. on Energy Conversion*, pp.173-177.

13. **L. Shridhar, Bhim Singh, C.S.Jha, B.P.Singh and S.S.Murthy 1995.** Selection of capacitors for the regulated short shunt self excited induction generator" *IEEE Trans. on Energy Conversion*, Vol. 10(1), pp. 10-17.

14. **L. Shridhar, Bhim Singh and C.S.Jha 1995.** Transient performances of the self regulated short shunt self excited

Induction Generator, *IEEE Trans. on Energy Conversion*, Vol. 10(2), pp.261-267.

15. **Lipo T. A. and Matsuo T. 1994.** Rotor design optimization of synchronous reluctance machine, *IEEE Transaction on Energy Conversion.* Vol. 9 (2), pp.359-365.

16. **M. J. Kamper and A. F. Volschenk 1994.** Effect of rotor dimensions and cross magnetization on $L_{d\ and}$ L_q inductances of reluctance synchronous machines with cageless flux barrier rotor, *IEE Proc-Electric Power Application.* Vol.141 (4), pp. 213-220.

17. **Boldea I., Nasar A. S. and Fu Z. X. 1994.** Performance evaluation of axially laminated anisotropic (ALA) rotor reluctance synchronous reluctance motors, *IEEE Trans. on Industry Applications.* Vol. 30(4), pp. 977-985.

18. **Staton D. A., Miller T. J. E. and Wood S. E. 1993.** Maximizing the saliency ratio of the synchronous reluctance motor, *IEEE Proceedings-B.* Vol.140 (4), pp.249-259.

19. **Boldea I., Fu Z. X. and Nasar S. A. 1993.** High-performance reluctance generator, *IEE Proceedings-B*, Vol.140 (2), pp. 124-130.

20. **Don Platt 1992.** Reluctance motor with strong rotor anisotropy, *IEEE Trans. on Industry Applications,* Vol. 28(3), pp.652-658.

21. **Chan T.F. 1992.** Steady-state analysis of a three phase self-excited reluctance generator, *IEEE Trans. on Energy Conversion,* Vol. 7(1), pp.223-229.

22. **Alolah A.L. 1992.** Steady-state operating limits of three phase self-excited reluctance generator, *IEE Proceedings-C*, Vol. 139(3), pp.261-268.

23. **A.I. Aloah 1991.** Capacitance requirement for three phase self-excited reluctance generator" IEE Proceedings-C, Vol.138 (3), pp.193-198.

24. **Boldea I. and Nasar S. A. 1991.** Emerging electric machines with axially laminated anisotropic rotors: A review, *Electric Machines and Power Systems,* Vol.19, pp.673-703.

25. **Y.H.A. Rahim, A.L. Mohamadien and A.S. Al Khalaf 1990.** Comparison between the steady-state performance of self excited reluctance and induction generators, *IEEE Trans. on Energy Conversions*, Vol. 5(3), pp.519-525.

26. **P.C.Sen 1989.** Principle of Electrical Machines and Power electronics, *Wiley International Edition, John Wiley & Sons.*

27. **Paul C. Krause and Oleg. Wasynczuk 1989.** Electromechanical Motion Device, *International Edition, McGraw-Hill Book Company.*

28. **C. Grantham, D. Sutanto and B. Mismail 1989.** Steady state and transient analysis of self excited induction generators, *IEE Proceedings- B*, Vol.136 (2), pp.61-67.

29. **Nagrial M.H. and RAHMAN M.A. 1988.**Operation and characteristics of self-excited reluctance generator, Record of *IEEE-IAS Annual meeting,* Part 1, pp.55-58.

30. **Boldea I. and S.A.Nasar 1986.** Electric Machine Dynamics *MACMILLAN PUBLISHING COMPANY*, New York

31. **F.E. Abdel-Kader 1985.**The reluctance machine as a self-excited generator, *Electric Machines and Power Systems*, Vol. 10, pp.141-148.

32. **A.E. Fitzgarald, Kingsley and Umans 1985.** Electric machinery, 4th Edition, *McGraw-Hill.*

33. **Say, M.G. 1983**. *The Performance and Design of Alternating Current Machines,* M/s Pitman. London

34. **Klingshirn E. A. 1978.** DC standstill torque used to measure L_d of reluctance and synchronous machines, *IEEE Transactions on Power apparatus and systems,* Vol. 97 (5) pp.1862-1868.

35. **Rao, S. C. 1976.** Dynamic performance of reluctance motors with magnetically anisotropic rotors. *IEEE Transactions on Power apparatus and systems.* 95(4).

36. **Cruickshank A. J. O. Anderson A. F. and Menzies R. W. 1971.** Theory and performance of reluctance motors with axially laminated anisotropic rotors. *IEE Proceedings*, Vol.118 (7), pp.887-893.

37. **Honsinger, V. B. 1971.** The inductances L_d and L_q of reluctance machines. *IEEE Transactions on Power Apparatus and Systems,* Vol.90 (1), pp.298-304.

38. **Honsinger V. B. 1971.** Steady-state performance of reluctance machines, *IEEE Trans. on Power Apparatus and Systems,* Vol .90(1). pp. 305-315.

39. **Menzies R. W. 1971.** Theory and operation of reluctance motors with magnetically anisotropic rotors: Part-1 Analysis, *IEEE Summer Meeting.* pp. 35-41.

40. **Menzies R. W., R.M. Mathur and H.W. Lee 1971.** Theory and operation of reluctance motors with magnetically anisotropic rotors, *IEEE Summer Meeting.* pp.42-45.

41. **V. Del Toro 1968.** Electromechanical Devices for Energy conversion and control system, Prentice *Hall Inc.*

42. **P.J. Lawrenson and S.K. Gupta 1967.** Developments in the performance and theory of segmental-rotor reluctance motors, *IEEE Proceedings*, Vol.114 (5), pp.645-653.

43. **Lipo T. A. and Krause P.C. 1967.** Stability analysis of a reluctance synchronous machine, *IEEE Trans. on Power Apparatus Systems,* Vol. 86, pp.825-834

44. **Lawernson P. J. and Agu L. A. 1964.** Theory and performance of polyphase reluctance machines, *IEEE Proceeding,* Vol.111 (8), pp.1435-1445.

45. **Lee, C.H. 1960**. Theory and design of a very slow speed reluctance motor, *AIEE Transactions.* pp. 1683-1688.

46. **Wagner, C.F. 1939.** Self Excitation of Induction Motors, *AIEE Transactions (Electrical Engineering),* Vol. 58, Feb., pp. 47-51.

47. **Kostko, J.K. 1923.** Polyphase reaction synchronous motors, *Journal of American Inst. Elect. Eng.* pp. 1162-1168.

APPENDIX -1

PROTOTYPE SYNCHRONOUS RELUCTANCE MACHINE

Stator:

Number of poles: 4,

Rated voltage: 400 V,

Stack length: 108mm

Inner diameter: 82.54 mm,

Type of winding: 3-phase double layer ac armature

Rotor:

Air gap: 0.25mm,

Number of steel lamination per pole: 20

Steel lamination: CRGO steel 0.3mm,

Flux barrier: paper 0.3mm thick

Parameters of SERG:

Stator resistance r_s=16.5 Ω

Stator direct axis inductance = 0.783H

Stator quadrature direct axis inductance = 0.191H

APPENDIX -2

Direct-axis and quadrature axis magnetizing inductance:

Fig. 4.1 shows direct and quadrature axes for a four pole machine. Symmetry about the axes gives the following relationships:

$$B_d(\beta) = B_d(-\beta) = -B_d\left(\frac{\pi}{p} - \beta\right)$$
$$B_q(\beta) = -B_q(-\beta) = B_q\left(\frac{\pi}{p} - \beta\right). \qquad \text{--------- (A1)}$$

Assuming iron of infinite permeability the mmf equation for the closed loop shown in Fig. (4.2) is given by

$$\frac{N}{2}\int_{\varepsilon+\beta}^{\varepsilon+\frac{\pi}{4}-\beta} i_d \sin(p\theta - p\varepsilon) - i_q \cos(p\theta - p\varepsilon)\, d\theta$$
$$= \frac{g}{\mu_0}\left[B_d(\beta) + B_q(\beta) - B_d\left(\frac{\pi}{4} - \beta\right) - B_q\left(\frac{\pi}{p} - \beta\right)\right].$$

--------- (A2)

Therefore,

$$-\frac{Ni_d}{2p}\left[\cos(p\theta - p\varepsilon)\right]_{\varepsilon+\beta}^{\varepsilon+\pi/p-\beta} - \frac{Ni_q}{2p}\left[\sin(p\vartheta - p\varepsilon)\right]_{\varepsilon+\beta}^{\varepsilon+\pi/p-\beta}$$
$$= \frac{g}{\mu_0}\left[B_d(\beta) + B_q(\beta) - B_d\left(\frac{\pi}{4} - \beta\right) - B_q\left(\frac{\pi}{p} - \beta\right)\right]$$
$$= \frac{2g}{\mu_0} B_d(\beta)$$

$$\frac{Ni_d}{p}\cos p\beta = \frac{2g}{\mu_0} B_d(\beta) \qquad \text{---------- (A3)}$$

Equation (A3) is given as

$$B_d(\beta, \varepsilon) = B_{d0}\cos(p\beta) \qquad \text{--------- (A4)}$$

Where, $B_{d0} = \frac{\mu_0 N}{2pg} i_d$

Fig.4.1 shows that a small circumferential section $rd\beta$ covers a section of laminations of depth $rcos(\beta)d\beta$. Of this depth, the fraction t_a/t_a+t_1 is nonmagnetic. The flux density across this section is given by the mmf equation around the incremental flux path shown in Fig.4.1 that provides.

$$\theta = \varepsilon + \beta \quad \text{and} \quad d\theta = d\beta$$

For any fixed rotor position. Then

$$\frac{N}{2}\left[i_d \sin(p\beta) - i_q \cos(p\beta)\right]d\beta$$

$$= \frac{g}{\mu_0}\left[B_d(\beta,\varepsilon) + B_q(\beta,\varepsilon) - B_d(\beta + d\beta,\varepsilon) - B_q(\beta + d\beta,\varepsilon)\right] + \frac{a}{\mu_0} B_a \cos(\beta)\, d\beta$$

---------- (A4)

The terms in B_d and B_q simplify to $-(\partial B_d/\partial\beta)d\beta$ and $-(\partial B_q/\partial\beta)d\beta$, the first of which can be evaluated using equation(A2). Equation (A4) may then be simplified to give

$$aB_a \cos(\beta) - g\frac{\partial B_q}{\partial \beta} - \frac{\mu_0 N}{2} COS(p\beta) i_q = 0$$

---------- (A5)

A small section of rotor laminations reaching the rotor surface at angles β and $\pi/p - \beta$ and covering a circumferential distance of $rd\beta$

at the air gap. It consists of two straight sections and one circular section represented by s. Its length may be approximated by an arc of radius given by

$$\Upsilon_{arc} = \frac{\pi r}{2p}\left(1 - \frac{2p\beta}{\pi}\right) \qquad \text{---------- (A5)}$$

and the circumscribing angle is given by

$$\mathcal{T}_c = \pi\left(1 - \frac{1}{p}\right) \qquad \text{---------- (A6)}$$

Using equations (A5) and (A6) the value of s is given by

$$S = \frac{\pi^2 r(p-1)}{2p^2}\left(1 - \frac{2p\beta}{\pi}\right)$$

---------- (A7)

Continuity of flux must be preserved in this volume, giving

$$S[B_a(\beta + d\beta) - B_a(\beta)] - r\left[B_d(\beta) + B_q(\beta) + B_d\left(\frac{\pi}{p} - \beta\right) + B_q\left(\frac{\pi}{p} - \beta\right)\right]d\beta = 0$$

---------- (A8)

Using equation (A1) the equation (A8) is given by

$$S\frac{\partial B_a}{\partial \beta} - 2rB_q(\beta) = 0$$

---------- (A9)

Solving equations (A5) - (A8) gives

$$B_q(\beta) = B_{q0}\sin(p\beta) \qquad \text{--------- (A10)}$$

Where, $$B_{qo} = \frac{\pi^2(p-1)\mu_0 N i_q}{16pa + 2\pi^2 p(p-1)g}$$

Flux density in the airgap is expressed as

$$B = B_{d0}\cos(p\theta - p\varepsilon) + B_{q0}\sin(p\theta - p\varepsilon)$$

-------- (A11)

For single turn, centered on θ_1, the flux linkage is

$$\int_{\theta_1-\frac{\pi}{2p}}^{\theta_1+\frac{\pi}{2p}} BLr\,d\theta$$

$$= \frac{2Lr}{p}\left[B_{do}\cos(p\theta_1 - p\varepsilon) + B_{q0}\sin(p\theta - p\varepsilon)\right]$$

---------- (A12)

where L = Stack length and r = radius of the air gap.

The density of the turns is $0.5N\cos(p\theta_1-\gamma)$ turns per radians, where γ takes on the values 0, $2\Pi/3$ and $4\Pi/3$ for the first, second, and third phases, respectively. After integrating over the whole airgap, the flux linkage for the three phases are found to be

$$\lambda_{phase} = \frac{2}{3} L_{md} i_d \cos(\gamma - p\varepsilon) + L_{mq} i_q \sin(\gamma - p\varepsilon) \qquad \text{--------- (A13)}$$

The magnetizing inductances in direct and quadrature axes in above expression are given by

$$L_{md} = \frac{3\mu_0 N^2 Lr}{8p^2 g} \qquad \text{---------- (A14)}$$

$$L_{mq} = \frac{3\pi^3 (p-1)\mu_0 N^2 Lr}{64\, p^2 a + 8\pi^2 p^2 (p-1) g} \qquad \text{---------- (A15)}$$

Where, $a = r\, t_a / (t_a + t_l)$

APPENDIX-3

Power developed by an induction machine

For a three phase winding with balanced sinusoidal currents, the peak current loading is

$$\alpha_{pk} = \frac{3N}{4r} i_{pk} \qquad \text{---------- (A16)}$$

Where i_{pk} is the peak value of phase current. The rms current is given by

$$i_{rms} = \frac{2\sqrt{2}r}{3N} \alpha_{pk} \qquad \text{---------- (A17)}$$

If the air gap flux density is setup by balance magnetizing current then its peak value is given by

$$B_{pk} = \frac{3\mu_0 N}{2pg} i_{mpk} \qquad \text{---------- (A18)}$$

The rms magnetizing current is

$$i_{mRMS} = \frac{2\sqrt{2}pg}{3\mu_0 N} B_{pk} \qquad \text{---------- (A19)}$$

The air gap voltage is

$$E_g = j\omega . \frac{3\pi\mu_0 N^2 rL}{8p^2 g} l_m \qquad \text{---------- (A20)}$$

We have $j\omega L_m I_m = (R + j\omega L_r) I_r \qquad$ ---------- (A21)

Say,

$$K = \frac{|\mathrm{Im}|}{|Ir|}$$ ---------- (A22)

Then,

$$R^2 = \omega^2\left(K^2 L_m{}^2 - L_r{}^2\right)$$ ---------- (A23)

$$|I_s| = |I_r|\sqrt{1 + K^2 + 2L_r / L_m}$$ ---------- (A24)

and,

$$|E_s| = |E_g|\sqrt{1 - L_r{}^2 / \left(K^2 L_m{}^2\right)}$$ ---------- (A25)

Rated power is

$$\frac{T\omega}{p} = 3|E_r||I_r|\,.$$ ---------- (A26)

Using equation (A16), (A19), (A20), (A24), (A25) and (A26) the expression of power developed in term of peak current loading, peak magnetic loading, stack length, bore diameter, magnetizing inductance and rotor leakage inductance is given by

$$P_{im} = \pi r^2 L B_{pk} \alpha_{pk} \sqrt{\frac{1 - L_r^2 / K^2 L_m^2}{1 + K^2 + 2L_r / L_m}}$$ ---------- (A27)

Vita

The author, Ajay Srivastava was born on 17th May 1967 at Gorakhpur district of Uttar Pradesh. He passed his High school and Intermediate examination with Ist division in the year 1982 and 1984 from Uttar Pradesh Board, Allahabad. He completed his B.E. degree in Electrical Engineering with Ist division from M.M.M. Engineering College, University of Gorakhpur in the year 1988. In July 1991 he joined as Assistant Professor in Electrical Engineering department, College of Technology, Pantnagar. He completed his M.Tech. Degree in Electrical Energy System in the Department of Electrical Engineering, college of Technology, Pantnagar in the year 1999.